M-Pos215 **PHARMACOLOGICAL SENSITIVITIES OF LARGE AND SMALL CONDUCTANCE Ca^{2+}-ACTIVATED K^+ CHANNELS IN GH_3 CELLS.** Daniel G. Lang and Aileen K. Ritchie. U.T.M.B., Galveston, Texas 77550.

We have previously demonstrated the coexistence of two types of Ca^{2+}-activated K^+ channels in GH_3 clonal anterior pituitary cells: BK channels which have a large unitary conductance (250 to 300 pS in symmetrical 150 mM KCl), a low sensitivity to internal Ca^{2+} at negative membrane potentials, and a strong voltage dependency of the open probability; and SK channels which have a small unitary conductance (9 to 14 pS), a high sensitivity to internal Ca^{2+} at negative membrane potentials, and a relatively weak voltage dependency of the open probability (Lang and Ritchie, Neurosci. Abs. 12: 560, 1986 and Pflugers Archiv, in press). The properties of the SK channels in GH_3 cells are similar to those seen in rat myotubes (Blatz and Magleby, Nature 323: 718-720, 1986). We have investigated the sensitivities of the BK and SK channels to both external TEA and apamin in excised, outside-out patches at room temperature. The pipette solution contained (in mM) 150 KCl, 10 HEPES, 0.5 $MgCl_2$, pH 7.20, and 5 μM added Ca^{2+} for BK channels or 1 μM free Ca^{2+} (buffered with 2 mM EGTA) for SK channels. The bath solution contained (in mM) 75 KCl, 75-X NaCl, X TEA-Cl, 10 HEPES, 5 4-AP, 2 $MgCl_2$, pH 7.30. Apamin (500 nM) inhibited SK channel openings (n = 6) but had no effect on BK channels. TEA caused a reduction of single channel current of both BK (n = 7) and SK (n = 3) channels. At holding potentials of -50 mV for the BK channels and -60 mV for the SK channels, the dose response curves could be fit by a one to one drug receptor occupancy with half maximal inhibition occurring at about 0.2 mM for the BK channels and 3 mM for the SK channels. The block by external TEA was not strongly voltage dependent for either channel (δ < 0.2). Supported by DK 33898 and the Muscular Dystrophy Association.

M-Pos216 **ACTION OF 12-HYDROPEROXY EICOSATETRA ENOIC ACID (12-HPETE) ON THE S-K^+ CHANNEL IN CELL-FREE PATCHES FROM APLYSIA SENSORY NEURONS.** F. Belardetti, M. Rosolowsky and W. Campbell. Department of Pharmacology, University of Texas Health Science at Dallas.

The release and transformation of arachidonate to 12-HPETE stimulated by the inhibitory neurotransmitter FMRFamide in Aplysia mechanosensory neurons (SN) increase the probability of opening (Popen) of the S-K^+ channel, producing a slow inhibition of transmitter release. In whole Aplysia nervous systems 12-HPETE is re-arranged (Piomelli et al., Soc. Neurosci. Abstr., 1987) to hepoxilins that are finally hydrated to trioxilins. Is 12-HPETE the terminal metabolite in SNs directly acting on the channel? To begin to test this hypothesis, cell-attached patches containing S-K^+ channels were obtained from SNs maintained in culture. Pressure application of 12-HPETE (1.6 μM in sea water, (SW), from ethanol stock solution dried and resuspended) on the cell body produced a reversible two-fold increase of the average patch current through an increase of Popen. Control application of SW plus dried ethanol was totally ineffective. Next, inside-out patches containing S-K^+ channels were obtained, a preparation presumably lacking the enzymes needed for the transformation of 12-HPETE. The cytoplasmic side of the patch was bathed with a solution including 2 mM EGTA, 0.96 mM Ca^{++}, 496 mM K^+-aspartate, 20 mM HEPES, pH 7.3. Under these conditions, pressure application in the bath of 12-HPETE (1.6 μM) did not alter the average current and Popen, supporting the hypothesis that the transformation of 12-HPETE is required for the modulation of the S-channel.

M-Pos217 DIRECT EFFECT OF FORSKOLIN ON VOLTAGE-GATED K^+ CHANNELS IN PC12 CELLS. T. Hoshi, S. S. Garber, and R. W. Aldrich. Dept. of Neurobiology, Stanford University, Stanford CA, 94305-5401.

Forskolin (FSK), a diterpene activator of adenylate cyclase, has been used to study the modulation of ion channels by the cAMP-second messenger system. We have studied the effects of FSK on voltage-gated K^+ channels in pheochromocytoma cells using the patch-clamp method. Externally-applied FSK decreases the amplitude of the whole-cell K^+ currents by drastically accelerating the time course of inactivation in a concentration-dependent manner (1-120 μM). This effect of FSK is distinct from that of externally applied phosphodiesterase inhibitors (IBMX, theophylline) in the presence of dbcAMP in the bath and ATP in the pipette on the whole-cell K^+ currents. The decrease in the current is not voltage-dependent. FSK does not affect the dependence of the current on the holding voltage, nor is its effect use-dependent. Single channel recordings in the outside-out configuration show that bath-applied FSK (12-120 μM) affects a class of voltage-gated K^+ channel, primarily responsible for the whole-cell K^+ currents. FSK reduces the peak probability of the channel being open and accelerates the inactivation of the ensemble averages. Single channel amplitude is not markedly affected. FSK decreases the mean open duration (e. g., 20 ms to 3.8 ms at +20 mV (120 μM FSK)) in a concentration-dependent manner. The average number of openings per depolarizing pulse also decreases at least 10-fold (at 120 μM FSK). Steady-state probability of the channel being open is negligible and independent of the presence of FSK. The channels are available to open after a few seconds of hyperpolarization (-70 mV to -100 mV). The median first latency is not affected. In the whole-cell and outside-out configurations, the FSK effect is immediate and reversible, though reversibility is not always complete. FSK is much less effective on the inside-out patches and is ineffective, when applied to the bath, in cell-attached configurations. The carrier, ethanol, has no effect.

The most obvious interpretation of these results is that FSK has a direct effect these K^+ channels without involving the cAMP-dependent protein kinase. Other more complicated interpretations such as those involving membrane-bound enzyme systems cannot be excluded. (Supported by the U.S. PHS grant NS23294 and a Searle Scholars Program/Chicago Community Trust grant to R. W. A., NIH postdoctoral fellowship to T. H., and NIH postdoctoral training grant to S. S. G.).

M-Pos218 GLUCOSE REDUCES BOTH ATP-BLOCKABLE AND CA-ACTIVATED K-CHANNEL ACTIVITY IN CELL-ATTACHED PATCHES FROM RAT PANCREATIC B-CELLS IN CULTURE

Atwater,I., Li,M.X., Rojas,E. & Stutzin,A. (Intr. by D.Gilbert) NIH, Bethesda, MD.

The unique ability of the B-cell to respond to varying concentrations of glucose depends on the metabolic modulation of K-channels. We have studied an ATP-blockable K-channel ,K(ATP), and a Ca-activated K-channel, K(Ca). We have observed that outward currents through K(ATP) are smaller with pipet K=5mM than with pipet K=140 mM and much smaller than inward currents (pipet K=140mM). Average conductance in cell attached patches is 12 pS for outward currents (pipet K=5mM) and 55 pS for inward currents (pipet K=140mM). Opening frequency is reduced and less sensitive to glucose than for inward currents. Outward currents through K(Ca) (pipet K=5mM) were also smaller than inward or outward currents measured with pipet K=140mM. Average conductance of K(Ca) is 71 pS in cell attached patches (pipet K=5mM), or 107 pS (pipet K=10-20mM), or 200-250 pS (pipet K=140mM). Furthermore, opening frequency was decreased by glucose in 12, unchanged in 8 and stimulated in 2 out of 22 cells. Experiments conducted under such physiological conditions as exposing the membrane patch to external Na and measuring outward K currents, indicate that the two K channel conductances are smaller than previously reported: K(ATP), is an inward rectifier and K(Ca) conductance is reduced by low external K. These studies further indicate that glucose increases cell Ca buffering and that both K channels are involved in glucose sensing in the pancreatic B-cell.

M-Pos219 PERTUSSIS-TOXIN RESISTANT G PROTEINS MEDIATE NEURONAL EXCITATION BY SUBSTANCE P.

Y. Nakajima, S. Nakajima and M. Inoue, Department of Biological Sciences, Purdue University, West Lafayette, IN 47907.

Substance P excites neurons by suppressing the inward rectification channels. We have investigated whether the substance P receptor interacts with inward rectification channels through a guanine nucleotide-binding (G) protein by using dissociated cultured neurons from the nucleus basalis and locus coeruleus of newborn rats. Intracellular application of GTPγS (100 μM) and GppNHp (350 μM), hydrolysis-resistant GTP analogues which irreversibly stimulate G proteins, maintained the action of substance P without recovery. Pretreatment with pertussis toxin (500 ng/ml, 15 to 22 hours) did not significantly alter the effectiveness of substance P. Intracellular application of cyclic AMP (100 μM) and 3-isobutyl-1-methylxanthine (IBMX) (1 mM) or 9-(tetrahydro-2-furyl) adenine (SQ 22,536) (100 μM), an inhibitor of adenylate cyclase, did not influence the action of substance P. We conclude that inhibition of the inward rectification channels by substance P is mediated through a G protein. However, neither adenylate cyclase nor cyclic AMP is involved. Since the action of substance P is resistant to pertussis toxin, this G protein is distinct from the inhibitory G proteins (Gi or Go), which are inactivated by pertussis toxin. (Supported by a NIH grant AG06093 and by an Alzheimer's Disease and Related Disorders Association Grant).

M-Pos220 IDENTIFICATION AND CHARACTERIZATION OF FOUR MODES OF ACTIVITY OF THE LARGE CONDUCTANCE CALCIUM ACTIVATED POTASSIUM CHANNEL IN CULTURED SKELETAL MUSCLE.

O. B. McManus and K. L. Magleby, Department of Physiology and Biophysics, University of Miami School of Medicine, Miami Florida 33101.

Currents through single calcium activated potassium channels were recorded with the patch clamp technique and the durations of open and closed intervals measured. Four separate modes of activity were identified based on abrupt changes in the mean open interval duration: normal mode, which included 96% of the intervals; intermediate open mode with 3.2% of the intervals; brief open mode with 0.5% of the intervals; and buzz mode with 0.1% of the intervals. The mean open interval durations were decreased to 61% of normal during the intermediate open mode, 12% of normal during the brief open mode, and 2.6% of normal during the buzz mode. Most mode transitions were observed from the normal mode to one of the other modes and then back to normal. Sojourns in the normal, intermediate open, brief open, and buzz modes lasted from 5-1000, 1.5-150, 1-7, and 0.01-1 s, respectively. Comparison of the distributions of open and closed interval durations in the various modes suggested that the channel enters a fewer number of kinetic states in the intermediate open, brief open, and buzz modes than in the normal mode. The time constants of the components of the open and closed interval durations during the intermediate and brief open modes suggested that activity in these modes may occur within a subset of states entered during normal activity. Supported by grants from the National Institutes of Health and the Muscular Dystrophy Association.

M-Pos221 **DOPAMINE HYPERPOLARIZES NORMAL LACTOTROPHS OF THE RAT PITUITARY GLAND BY INCREASING A POTASSIUM CONDUCTANCE.** Karen A. Gregerson and Gerry S. Oxford. Department of Physiology, University of North Carolina, Chapel Hill, NC 27514, and Department of Pediatrics, University of Maryland, Baltimore, MD 21201.

Transmembrane electrical activity in normal rat lactotrophs was examined during application of dopamine (DA), a physiological inhibitor of prolactin secretion. Prolactin-secreting cells, derived from anterior pituitaries of proestrous female rats, were identified for subsequent electrophysiological studies using the reverse hemolytic plaque assay. Using patch recording techniques, we measured membrane potential, action potentials, and currents through single potassium channels in response to DA. Brief application of 4μM DA (+0.5mM ascorbate) elicited a rapidly developing long-lasting hyperpolarization associated with an increase in membrane conductance. In cells exhibiting spontaneous Ca^{++}-dependent action potentials, the hyperpolarization was accompanied by cessation of spiking activity which reinitiated at the control rate following recovery of the resting membrane potential. Application of ascorbate alone had no effect. The selective D2 dopamine receptor agonist, RU24213, elicited a response similar to DA itself. This response could be blocked by DA receptor antagonists, sulpiride or (+)butaclamol, but not the inactive (-)butaclamol isomer. The DA-induced hyperpolarization occurred in either normal (150mM) or reduced (10mM) extracellular Cl^-, and exhibited a reversal potential coincident with the equilibrium potential of K^+, indicating that an increase in P_K rather than P_{Cl} underlies the DA response of the rat lactotroph membrane. During on-cell patch recordings with either low (5mM) or high (140mM) K^+ in the pipette, increased single K channel activity was observed when DA was applied to the extrapatch membrane. This suggests that dopamine induces activity of K^+ selective ion channels in rat lactotrophs via a second messenger. The subsequent hyperpolarization and loss of Ca^{++}-dependent excitation is likely a primary mechanism of dopaminergic inhibition of prolactin secretion. (Supported by NIH grant NS18788).

M-Pos222 **WHOLE-CELL K CURRENTS IN SINGLE SMOOTH MUSCLE CELLS ISOLATED FROM RABBIT PORTAL VEIN.** Normand Leblanc and Joseph R. Hume, Department of Physiology, University of Nevada, Reno, NV 89557.

Smooth muscle cells (SMC) were isolated from rabbit portal vein using collagenase. SMC were relaxed and exhibited a mean resting membrane potential of -47.9 mV. Whole-cell voltage clamp experiments were carried out using suction micropipettes without internal dialysis or patch pipettes with internal dialysis. Two types of outward current could be consistently identified: time-dependent and time-independent components. A third component with transient kinetics was also recorded in about 50% of the cells. External application of TEA (0.5 to 10 mM) blocked all three components. Perfusion with nominally Ca free solution reduced the time-independent current completely whereas the time-dependent was barely affected. Transient outward rhythmic current oscillations were occasionally observed in some cells. This type of activity was enhanced in high external Ca (5.4 mM), and reduced in Ca free solution or ryanodine (10 uM) suggesting involvement of spontaneous release of Ca from the SR (Benham and Bolton, J. Physiol. 381: 1986). These results are consistent with the existence of at least three distinct K channels recently described in cell-attached and membrane excised patches from the same preparation (Inoue et al., Pflugers Arch. 405: 1985; 406: 1986).
Supported by HL 30143 and AHA.

M-Pos223 MODULATION OF TWO K^+ CURRENTS IN MYOMETRIAL CELLS BY NOREPINEPHRINE (NE) AND THE HORMONAL STATUS OF THE RAT. L. Toro, E. Stefani and S.D. Erulkar.* Dept. Fisiologia, Biofisica y Neurociencias CINVESTAV-IPN. Apdo. Postal 14-740, México; Dept. Physiology and Molecular Biophysics, Baylor College of Medicine, Houston, Texas 77030; *Dept. Pharmacology & Mahoney Institute of Neuroscience, University of Pennsylvania, Philadelphia, PA 19104.

Two K^+ currents (I_{K1} and I_{K2}), with different kinetics and modulation, were observed in primary cultured myometrial cells (1-5 day old). Single cells were patched clamped using the whole cell configuration. External medium was Krebs solution. Electrode solution contained K^+ as the main cation. From a holding potential of -90 mV, the characteristics of I_K were as follows: a) I_{K1}: time to steady-state, $\tau = 3 \pm 1$ ms ($\pm$ S.D., n = 4); time constant of the rising phase, $\tau_{on} = 0.66 \pm 0.3$ ms (n = 4); activation potential, $V_a = -73 \pm 5$ mV (n = 4); and b) I_{K2}: $t = 27.5 \pm 3$ ms (n = 6), $\tau_{on} = 5 \pm 0.3$ ms (n = 5) and $V_a = -70 \pm 15$ mV (n = 4). NE (1 μM) potentiated I_{K1}. Maximum slope conductance ratio, G_{NE}/G was 4 ± 1 (n = 4). In contrast, I_{K2} was diminished. $G_{NE}/G = 0.6 \pm 0.1$ (n = 4); sometimes, the addition of NE diminished I_{K2} to an extent that inward currents became apparent. The relative proportion of I_{K1} to I_{K2} is related to the hormonal status of the rat. I_{K1} is predominant in animals at estrus, while I_{K2} prevails in animals at diestrus. In conclusion, the various responses of intact uterus to NE during the estral cycle, can obey to the differential mode of modulation of K^+ currents described above. Supported by grants NS12211, 5 RO1AR, AM3508503 (NIH).

M-Pos224 TEMPERATURE-DEPENDENT CONDUCTANCE OF A CANINE CARDIAC SARCOPLASMIC RETICULUM K^+ CHANNEL

Win K. Shen, Joseph A. Hill, Jr., Randall L. Rasmusson, Harold C. Strauss (Intr. by Sidney A. Simon). Duke University Medical Center, Durham, NC

Conduction properties of the canine cardiac SR-K channel have recently been characterized in planar lipid bilayers. The overall permeation process can be expressed as a symmetrical 3-barrier, 2-well model according to Eyring rate theory. To confirm the theoretically estimated barrier height, which was chosen to be 6.58 Kcal/mol to correspond to measured conductances (J. Hill, Ph.D. Thesis, 1987), we studied the effect of temperature on conductance (γ) under symmetrically saturated [KOAc] (500 mM). Results:

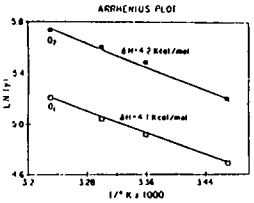

γ(pS)/Temp(K^o)	289	298	304	310
O1	116±11	138±13	156±12	184±3
O2	184±10	242±8	271±6	307±8
O1/O2(%)	63 (n=4)	57 (n=6)	58 (n=6)	60 (n=5)

O2=open state; O1=substate.

The Arrhenius plot (ln(γ) vs $1/K^o$) shows that the apparent activation enthalpies (ΔH) are 4.2±1.0 Kcal/mol (n=6) and 4.1±0.6 Kcal/mol (n=6) for O1 and O2, respectively. We conclude that: 1) SR-K channel conductance is weakly (Q_{10}=1.3) temperature-dependent, as one might expect from the high channel permeability for K^+. 2) ΔH agrees qualitatively with the estimated barrier height. 3) The equal ΔH values for O1 and O2 states suggest that the two states share a common conducting pathway with the same energy profile, therefore suggesting that O1 may be a consequence of the filtering bandwidth. (Supported by NIH Grants HL-19216 and 17670)

M-Pos225 GATING KINETICS OF A CANINE CARDIAC SARCOPLASMIC RETICULUM POTASSIUM (SR-K) CHANNEL

Win K. Shen, Randall L. Rasmusson, Harold C. Strauss. (Intr. by Jacob J. Blum) Duke University Medical Center.

Reconstituted canine cardiac SR-K channel in planar lipid bilayer system demonstrates at least three distinct states: closed state (C), open state (O2) and subconducting state (O1). All three states communicate freely with one another, implying a cyclic gating scheme (model 1). To obtain an adequate number of transitions, we studied gating kinetics at 37°C and made the following observations: 1) The mean dwell time of C ($\bar{\tau}_C$) is voltage-dependent while $\bar{\tau}_{O1}$ and $\bar{\tau}_{O2}$ are voltage-insensitive (table). 2) O2 dwell time probability distribution can be well fit with a single exponential function; C dwell time probability distribution appears to be biexponential. These data have led us to consider the minimal four-state gating schemes as shown in model 2 or 3.

Holding Voltage	Dwell Time (ms) C	O2	O1
-50 mV	2095	903	174
-30 mV	1216	1021	223
20 mV	232	749	179
40 mV	148	1217	326

Model 1 Model 2 Model 3

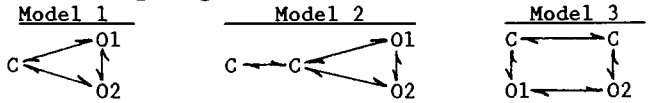

To further differentiate model 2 from model 3, we examined two conditional probabilities: a) At -50mV holding potential, the mean life time of all C which go to O1 ($\bar{\tau}_{C\to O1}$=1890±65 ms) is significantly different from the mean life time of all C which go to O2 ($\bar{\tau}_{C\to O2}$=2662±41 ms) ($p<0.01$); b) The ratio between the probability of C→O1 and the probability of C→O2 ($P_{C\to O1}/P_{C\to O2}$) is strongly voltage dependent. These observations are consistent with the model 3 gating scheme.

M-Pos226 POTASSIUM AND CALCIUM CONDUCTANCES OF Y-1 ADRENOCORTICAL CELLS. L. Tabares and J. López-Barneo. Departamento de Fisiología, Facultad de Medicina, Univ. de Sevilla, Spain.

Ionic currents have been recorded in a transformed line of murine adrenocortical cells which are excitable and secrete steroid hormones in response to ACTH. Experiments were done using the whole-cell variant of the patch-clamp technique. With 10 mM external Ca^{2+} and 140 mM K^+ internally, two types of voltage-dependent currents were observed. Depolarization to -20 mV, from a HP of -70 mV, elicited a small inward Ca^{2+} current with a peak amplitude of 100-150 pA. Larger depolarizations produced outward K^+ currents that masked the inward current component. The Ca^{2+} current was blocked by external Cd^{2+} and the K^+ current by TEA^+ or the replacement of internal K^+ by Cs^+. Activation threshold of the Ca^{2+} current was -60 mV and the peak of the I/V plot was near -20 mV. The inward current activated slowly and inactivated in less than 50 ms with test pulses larger than 40 mV. Half steady-state inactivation occurred at -65 mV. The amplitude of this current did not appreciably change when external Ca^{2+} was replaced by Ba^{2+}. The K^+ current was dependent on the internal Ca^{2+} concentration; it decreased in amplitude as Ca^{2+} was buffered with EGTA and almost totally disappeared with 10 mM internal EGTA (estimated Ca^{2+} concentration $< 10^{-10}$ M). This indicates that most of the K^+ current in Y-1 cells is Ca^{2+}-dependent. The Ca^{2+}-activated K^+ current appears to be also regulated by internal Mg^{2+} and H^+. Removal of Mg^{2+} reduced the amplitude of the current and at an internal Ca^{2+} concentration of 10^{-8} M lowering pH from 7.6 to 6 decreased by half the current amplitude, leaving the activation kinetics unaltered. This suggests that H^+ ions compete for the site normally occupied by Ca^{2+} and thus at low pH fewer channels open at a given membrane voltage. pH sensitivity was steeper in the range 6.8-7.4 which is near the physiological value.

M-Pos227 CHARYBDOTOXIN INHIBITS REGULATORY VOLUME DECREASE AND MITOGEN- OR Ca^{2+} IONOPHORE-INDUCED HYPERPOLARIZATION IN LYMPHOCYTES. S. Grinstein, J.D. Smith and C. Miller. Division of Cell Biology, The Hospital for Sick Children, Toronto, Canada and Department of Biochemistry, Brandeis University, Boston, MA, U.S.A.

The existence and role of Ca^{2+}-activated K^+ channels in lymphocytes is uncertain. Whereas their presence is suggested by indirect isotopic or spectroscopic methods, they have not been detectable by patch clamping. To assess the presence of Ca^{2+}-activated K^+ channels, we measured membrane potential in suspensions of rat thymic lymphocytes using bis-oxonol. The resting potential of approximately -50 mV underwent a marked hyperpolarization when the intracellular $[Ca^{2+}]$ was increased by addition of 50 nM ionomycin. This hyperpolarization was completely blocked by 10-30 nM charybdotoxin (CTX), a component of scorpion venom which selectively blocks Ca^{2+}-activated K^+ channels in other cells. CTX did not significantly affect the resting potential of thymocytes, suggesting that other pathways are responsible for the K^+ selectivity of the resting membrane. The mitogenic lectin concanavalin A increased cytoplasmic free $[Ca^{2+}]$ and hyperpolarized the membrane potential. This hyperpolarization was also eliminated by CTX, unmasking a moderate depolarization.

Osmotically swollen human peripheral blood lymphocytes regain near normal volume by losing KCl and osmotically obliged water. This regulatory volume decrease (RVD) is believed to occur through independent conductive K^+ and Cl^- channels. CTX was found to inhibit RVD suggesting that similar channels underlie the Ca^{2+}- and volume-induced changes in K^+ permeability in T lymphocytes.

M-Pos228 SINGLE CHANNEL ACTIVITY IN MEMBRANE VESICLES FROM MYOMETRIAL CELLS INCORPORATED INTO LIPID BILAYERS. L. Toro, H. Valdivia, R. Coronado, J.S. Smith and E. Stefani. Dept. Fisiologia, Biofisica y Neurociencias. CINVESTAV-IPN. Apdo. Postal 14-740. Mexico, D.F. and Dept. Physiology and Molecular Biophysics. Baylor College of Medicine. Houston, TX 77030

Ca^{2+}, Ca^{2+}-activated K^+ and Cl^- channels were recorded in membrane vesicles isolated from the uterus of Wistar rats (200 g) at different hormonal stages. Channels were incorporated into planar bilayers formed from equimolar mixtures of phosphatidylethanolamine and phosphatidylserine in decane. Ca^{2+}-activated K^+ channels were observed in membranes from animals at estrus and diestrus phases, banding at the 25-30% sucrose interface. They had a strong voltage and Ca^{2+} dependence (open probability, Po, was 0.01 and 1 at -20 and 0 mV respectively with 100 μM Ca^{2+} cis; Po=0.9 at 0 mV with 50 μM Ca^{2+}), similar to the behavior of the corresponding skeletal muscle channel. Unitary conductance was 305 pS in 250 mM external/50 mM internal KCl, with a reversal potential of 37 mV. Channels were charybdotoxin (CTX) sensitive. 10 to 50 nM CTX added to the external side (opposite side of Ca^{2+} activation) shortened the fraction of open time of the channel. Calcium channels were recorded using membranes of rats at diestrus, banding at the 30-35% sucrose interface. Channels with a conductance of 20 pS were observed at 0 mV in 100 mM Ba^{2+} external, 50 mM NaCl both sides. Cl^- channels were observed in membrane vesicles from animals at estrus, banding at the 25-30% sucrose interface. These channels were voltage-independent and had a unitary conductance of 64 pS in 250 mM external/50 mM internal KCl. In conclusion uterine smooth muscle has reconstitutible Ca^{2+}, Ca^{2+}-activated K^+ and Cl^- channels which may be involved in the discharge and control of spike activity in the whole muscle, regulating the contractile function of the uterus. Supported by NIH grants.

M-Pos229 FOUR VOLTAGE-DEPENDENT POTASSIUM CURRENTS IN ADULT HIPPOCAMPAL PYRAMIDAL CELLS (HPCs) Johan F. Storm, Dept. of Neurobiology & Behavior, SUNY, Stony Brook, NY 11794.

Previous studies have demonstrated 3 voltage-dependent Ca-independent K currents in HPCs: (1) I_M [Halliwell & Adams, 1982]; (2) I_A [Gustafsson & al. 1982; Segal & al. 1984; Zbicz & Weight 1985]; (3) I_K [Segal & Barker 1984]. However, "I_A" has shown quite different kinetics and sensitivity to 4-aminopyridine (4-AP) in slices (slow and sensitive) vs. cell cultures (fast and less sensitive). In addition, I_K has not been well characterized in adult HPCs. The present data suggest that there are two 4-AP-sensitive currents, one corresponding to the fast current seen in cultures (I_A), and another (here called I_D) which is slower and more sensitive to 4-AP.

CA1 pyramidal cells in slices from rats were voltage clamped with a single microelectrode (16-35MΩ) at 26-30°C. I_A activated within 7ms, at potentials positive to -50mV, and inactivated with a time-constant (τ_1) of 14-25ms, over the range -90 to -40mV. I_D differed from I_A in three respects: (1) more negative ranges of activation (-65 to -30mV) and inactivation (-120 to -60mV); (2) slower kinetics (activation within 25ms; inactivation: 1-20s); and (3) higher sensitivity to 4-AP (blocked by ~30μM, vs. ~2mM for I_A). Both I_A and I_D may participate in spike repolarization, and I_D can delay for up to 10s the discharge in response to depolarizing current [Storm, Biophys. J. 49:369a].

I_K activated positive to -40mV (τ_a=20-30ms at -25mV), and inactivated slowly between -100 and -40mV. I_K was blocked by 10-20mM tetraethylammonium (TEA), unlike I_A and I_D. I_M was substantially blocked by 5mM TEA, but I_M and I_K were far less sensitive to 4-AP than I_D. Indirect evidence suggests that I_K (but not I_M) also contributes to repolarization of the action potential. I_D may explain the effects of small doses of 4-AP on excitability and synaptic efficacy. [Grant NS18579].

M-Pos230 BARIUM BLOCK OF OUTWARD AND INWARD CURRENT IN MONOCYTE-DERIVED MACROPHAGES STIMULATES RESPIRATORY BURST ACTIVITY. B. Jow, J.M. Zeller, and D.J. Nelson. The University of Chicago, Dept. of Neurology, Chicago, Ill. 60637.

The ability to initiate a respiratory burst, and thereby generate reactive oxygen species is central to the cytotoxic properties of phagocytes. Activation of the respiratory burst in phagocytic cells has been shown to be closely associated with stimulus-induced changes in membrane potential and can be monitored using a luminol-enhanced chemiluminesence (CL) assay. The relationship between current activation and respiratory burst activity in monocyte-derived macrophages was studied using whole-cell voltage-clamp techniques. Current records were obtained from cells maintained in adherent culture. Solutions were exchanged intracellularly using an internal pipette perfusion technique. The activation of a noisy, time-independent outward current was observed upon depolarization from a holding potential of either -30 or -60 mV. A 75% (n=7) decrease in current amplitude upon depolarization to 100 mV was observed when 140 mM CsCl was perfused into the pipette replacing KCl. An 80% block in current amplitude was also observed when Na was substituted for K as the internal cation. This Cs blockable outward current was decreased by 57% (n=9) when Ba (4mM) was present in the external bathing solution. Ba additionally blocked the inward rectifier current in these experiments at -110 mV by 57% (n=9). Monocytes differentiated in suspension culture for 1 to 3 days demonstrated a 42% increase in CL/respiratory burst activity following phorbol myristate acetate stimulation (20 ng/ml) in the presence of 4mM external Ba. A 50% increase in CL was also observed following stimulation of the cells with heat aggregated IgG (100 ug/ml) in the presence of 4mM Ba. These results demonstrate that an enhancement of respiratory burst activity can be brought about by the inactivation of a Ba sensitive, Cs blockable outward current as well as the inward rectifier current and are consistent with the findings that a depolarization response may serve as an intermediary signal that couples ligand-receptor engagement with functional cell activation, leading to particle uptake, degranulation, and the generation of a respiratory burst response. Supported by NIH Grants GM36823 and AI23030.

M-Pos231 SINGLE CHANNEL STUDIES IN CULTURED OLIGODENDROCYTES B. Soliven, S. Szuchet and D.J. Nelson. University of Chicago, Department of Neurology, Chicago, Illinois 60637.

Oligodendrocytes (OLGs) develop processes and form myelin membranes following attachment to a substratum. Cultured OLGs sequentially express an outward current that represents a composite response of an inactivating/transient component and a non-inactivating component; and an inward current which has been identified as an inwardly rectifying K^+ current (Soliven et al., J. Neuroscience, In Press). We attempted to identify single channel events with the corresponding whole-cell currents using patch clamp techniques. In cell-attached patches, inward currents were observed at potentials hyperpolarized to the resting potential in the presence of a 140 mM K^+ pipette solution. The channel conductance ranged from 23 to 36 pS (6 patches) and demonstrated strong rectification. Channel openings were grouped in complex bursts. The mean channel open time distributions could be described in most cases by a double exponential (t_1 = 2.1 msec, t_2 = 84 msec at a pipette potential which hyperpolarized the membrane potential by 40 mV). The channel exhibited at least two closed states (t_1 = 0.83, msec, t_2 = 16 msec). The inclusion of Ba (1mM) in the pipette solution decreased both the frequency of channel openings and the mean channel open time. In outside-out patches, outward currents were observed at depolarized potentials, +50 and +90 mV (with 140 KCl in the pipette and 140 NaCl, 5.4 KCl in the bath) when made from a holding potential of -80 mV. Single channel conductance was 11 pS. Channel currents which were observed showed two open states (t_1 = 1.1 msec, t_2 = 13.2 msec, n=4). External 4-AP decreased the probability of channel opening from 0.26 to 0.12. In summary, cultured oligodentrocytes express at least two distinct populations of K^+ channels whose modulation and expression may be related to process formation and eventually myelin metabolism. (Supported by NIH Grant GM-36823; BS is supported by a Fellowship Grant from National Multiple Sclerosis Society).

M-Pos232 **BRL 34915 INCREASES P_{OPEN} OF THE LARGE CONDUCTANCE Ca^{2+} ACTIVATED K^+ CHANNEL ISOLATED FROM RABBIT AORTA IN PLANAR LIPID BILAYERS.** **Craig H. Gelband, Nicholas J. Lodge, Jane A. Talvenheimo, and Cornelis van Breemen, Dept. of Pharmacology, Univ. of Miami, Miami, FL 33101.**

BRL 34915, a novel anti-hypertensive, lowers blood pressure (Buckingham et al., J. Card. Pharm. 8:798 1986), hyperpolarizes smooth muscle cells (Hamilton et al., Br. J. Pharm. 88:103 1986), and relaxes pre-contracted vascular smooth muscle (Clapham and Wilson, Br. J. Pharm. 87:77P 1986) by a mechanism which is hypothesized to involve the opening of a class of K^+ channels. We have investigated the effects of BRL 34915 on the large conductance Ca^{2+} activated K^+ channel from rabbit aorta in planar lipid bilayers. This Ca^{2+} activated K^+ channel has a conductance of 334 pS (n=10) in symmetrical 250 mM KCl solutions. This channel was selective for K^+ over Na^+ (P_K/P_{Na} = 6.1 with 250 mM KCl cis and 250 mM NaCl trans). In asymmetrical solutions containing 300 mM KCl trans and 100 mM KCl cis, the reversal potential for the channel was -30 mV, which is predicted by the Nernst potential for K^+. This channel also showed characteristic cis (internal) Ca^{2+} and voltage dependence. In symmetrical 250 mM KCl, 1 μM Ca^{2+} cis, 0.05 μM BRL 34915 added to the trans side increased the P_{open} from 0.10 to 0.16 at -40 mV. The single channel conductance did not change in the presence of BRL 34915. Open and closed time histograms were best fit by the sum of two exponential functions. The primary effect of BRL 34915 was to decrease the closed time constant of the long closed state from 233 msec. to 124 msec. and to increase the percentage of closed events exhibiting a short mean closed duration from 42% to 57%. The integral of the distribution of the open events did not change markedly. This decrease in the mean closed time of the long closed state is sufficient to account for the increase in P_{open} of the channel in the presence of BRL 34915. Supported by NIH HL 07188.

M-Pos233 GTP-ACTIVATED POTASSIUM CHANNELS FROM MUSCLE MEMBRANES INCORPORATED INTO PLANAR BILAYERS.

Lucie Parent and Roberto Coronado. Department of Physiology and Molecular Biophysics, Baylor College of Medicine, Houston, TX 77030.

A membrane fraction from rabbit skeletal muscle enriched in T-tubules is shown to contain potassium channels which can be activated by GTP or by the non-hydrolysable analog GTP-y-S. We call this channel K(GTP). Recordings were made in planar bilayers composed of PE:PS=1:1 formed in 0.25M (cis), 0.05M (trans) KCl buffered with 10mM Hepes-KOH pH 7.0. K(GTP) is activated by nucleotide added to the cis solution. ATP or Mg was not required. K(GTP) has a conductance of 60 pS, independent of voltage from -20 to +75mV. K(GTP) usually co-inserts into the bilayer along with K(Ca), the large conductance (305 pS) Ca-activated K channel described in T-tubules. The Ca site for K(Ca) and the GTP site for K(GTP) were always found in the same side of the bilayer (cis). Open probability (P_o) of K(GTP) in the absence of nucleotide is unstable at all holding potentials and decreases continuously after channel incorporation. Millimolar GTP transiently increased P_o more than 5 fold. GTP-y-S (0.1mM) produced a sustained activation (P_o greater than 10 fold) and a significant increase in mean open time. Addition of ATP-KOH (2mM) i) blocked spontaneous activity; ii) blocked activity induced by GTP; and iii) reduced activity induced by GTP-y-S. The block of the spontaneous activity (i above) suggests that K(GTP) may be related to ATP-regulated K channels described previously in muscle. Whether a nucleotide-binding protein regulates K(GTP) is presently investigated. Supported by MRC-Canada, and NIH.

M-Pos234 CHOLINERGIC MODULATION OF GLUCOSE-INDUCED ELECTRICAL ACTIVITY IN MOUSE PANCREATIC B-CELLS

Rosa M. Santos and Eduardo Rojas. Laboratory of Cell Biology and Genetics. NIH. Bethesda

Acetylcholine (ACh) potentiates glucose-induced electrical activity and insulin release in pancreatic B-cells. To identify the acetylcholine receptors, we measured the effects of ACh on pancreatic B-cell membrane potential and input resistance in the presence of muscarinic receptor agonists and antagonists. In the presence of glucose (11 mM), ACh (10 uM) depolarized the membrane during the silent phase between the bursts of electrical activity and caused a 2-fold increase in the burst frequency. Overall spike frequency and fraction of active phase remained unaffected. Muscarine (10 uM) induced similar changes, suggesting that the effect of ACh is mediated by muscarinic receptor. The stimulation of electrical activity by ACh (1 uM) was antagonized by pirenzipine, a muscarinic M1 receptor antagonist (IC_{50}= 0.25 uM). Gallamine, a muscarinic M2 receptor antagonist was without effect at concentrations up to 100 uM. Bethanecol, a muscarinic M2 receptor agonist, was about 100 times less effective than ACh in stimulating electrical activity. Futhermore, ACh (1 uM) increased islet cell input resistance by 25 %. These results indicate that ACh stimulation of glucose-induced electrical activity is mediated by activation of a muscarinic receptor- M1 type. Since ACh induced both a depolarization of the membrane and an increase in input resistance, the data suggest the involvement of K^+- channels.

M-Pos235 PHARMACOLOGICAL CHARACTERIZATION OF SINGLE-CHANNEL K^+ CURRENTS IN DROSOPHILA MUSCLE.

M. Gorczyca and C.-F. Wu, Dept. of Biology, Univ. of Iowa, Iowa City, IA 52242.

A variety of potassium currents have been identified based on their physiological and pharmacological properties. In *Drosophila* muscle, at least four macroscopic potassium currents can be distinguished by differences in their properties as well as sensitivity to mutational alteration. Studies of single channel events underlying these currents have only recently been initiated in muscle membrane vesicles and cultured myotubes.

Mutations affecting channel properties can provide an invaluable tool to the understanding of K^+ channel function and diversity. The resolution of single channel recordings allows detailed examination of pharmacological mechanisms and mutational perturbations. To extend the previous macroscopic studies in larval muscles, and to form the basis for a mutational analysis, we now report single channel currents observed from these muscles *in situ* in wild-type larvae.

Using the inside-out configuration, we have observed several distinct K^+ channel types. The most prominent one is calcium dependent, becoming activated above the concentration range of 10^{-7} to 10^{-8} M. The channel has a very high open probability, displays a conductance of about 20-30pS (130mM K^+ in pipette/2mM K^+ in bath), and is sensitive to TEA. The kinetics and the degree of blocking by 50mM TEA varied in different patches, suggesting the possibility of channel subtypes. This possibility is currently being pursued along with the pharmacological profiles of non-calcium dependent but TEA sensitive channels.

M-Pos236 PURIFICATION AND STRUCTURE DETERMINATION OF CHARYBDOTOXIN, A SPECIFIC PROBE OF Ca^{2+}-ACTIVATED K^+ CHANNELS. M.L. Garcia, G. Gimenez-Gallego, M. Navia, G. Katz, J.P. Reuben, and G.J. Kaczorowski, Dept. of Biochemistry, Merck Institute, Rahway, NJ 07065.

Charybdotoxin (ChTX) has been purified to homogeneity from the venom of the scorpion Leiurus quinquestriatus hebraeus by two successive high performance liquid chromatographies using a mono S ion exchange column and a C_{18} reverse phase column. Analysis of purified ChTX indicates that it is a 37 amino acid highly basic protein of 4.3 KDa which does not possess a free N-terminal residue. The primary structure of ChTX was determined by sequencing peptides obtained from digestion of ChTX with endoproteinase Lys-C, Stapilococcus aureus V-8 protease, and pyroglutamate aminopeptidase (to remove the N-terminal pyroglutamate residue). The C-terminal was confirmed by timed digestion of ChTX with carboxypeptidase A. The sequence of ChTX is:

PYQ-F-T-N-V-S-C-T-T-S-K-E-C-W-S-V-C-Q-R-L-H-N-T-S-R-G-K-C-M-N-K-K-C-R-C-Y-S

Purified ChTX is a potent selective reversible blocker of Ca^{2+}-activated K^+ channels in both GH_3 cells and primary bovine aortic smooth muscle cells (K_i=2.1 nM as determined from single channel analysis). Comparison of the sequence of ChTX with other known toxins reveals sequence homology with neurotoxins obtained from a variety of animal and plant sources. Circular dichroism spectra indicate that ChTX is primarily a β-sheet structure, as has been found with the other homologous proteins. Modeling of the tertiary structure of ChTX was accomplished by comparison with the crystalline structure of α-Bungarotoxin which, although is structurally similar, does not block Ca^{2+}-activated K^+ channels. Together, these studies suggest a model for the structure of ChTX and indicate that this protein is a useful probe for Ca^{2+}-activated K^+ channel function.

M-Pos237 pH SENSITIVITY OF THE VOLTAGE-GATED K^+ CONDUCTANCE IN HUMAN T LYMPHOCYTES. S.C. Lee and C. Deutsch, Department of Physiology, University of Pennsylvania, Phila., PA 19104

A number of growth factors and mitogens have been shown to cause an immediate, transient intracellular alkalinization in mammalian cells, which is mediated by specific activation of the plasma membrane Na^+/H^+ antiporter (Moolenaar, 1986). A growth-factor induced alkalinization of this sort occurs with addition of interleukin-2 to activated T lymphocytes (Mills et al, 1985). In addition, long-term alterations in intracellular pH occur in mitogen-stimulated lymphocytes in culture (Deutsch et al, 1984; Gerson et al, 1982). The intracellular pH of quiescent T-cells is homeostatic, maintaining a value of ~7.15 when extracellular pH is 6.9-7.4. However, mitogen-stimulated cells are non-homeostatic in response to altered extracellular pH, consistent with the observed intracellular acidification as activated cells progress through the cell cycle (Deutsch et al, 1984). It is therefore important to evaluate the effects of pH on the voltage-gated K^+ conductance that is present in lymphocytes and has been implicated in mitogen and interleukin-2 stimulated proliferation (Chandy et al, 1984; Lee et al, 1986). Specifically, pH changes could modulate the voltage-gated K^+ conductance in lymphocytes in a manner similar to that observed for invertebrate neurons (Moody, 1984). We have used patch-clamp techniques applied in the whole-cell mode to determine the pH sensitivity of the macroscopic and single-channel conductances in the T lymphocytes. Our results indicate that the average macroscopic current increases ~3-fold over the pH range from 5.6 to 8.2 with an apparent pK_a of ~6.8. Single-channel conductance is relatively insensitive to pH over this range. (Supp. by NIH AM 27595).

M-Pos238 *OPEN–CHANNEL NOISE IN THE K^+ CHANNEL OF THE SARCOPLASMIC RETICULUM.* A.H. Hainsworth, J.M. Tang, J. Wang, R.A. Levis & R.S. Eisenberg. Department of Physiology, Rush Medical College, 1750 W. Harrison, Chicago IL 60612.

Excised patches from the sarcoplasmic reticulum of skinned lobster muscle fibers contain a K^+ channel with 200 pS conductance over the voltage range ± 100 mV, when bath and pipette contain 460 m**M** K glutamate, 1.2 $CaCl_2$, 5 K_2EGTA, 1 MgATP, 0.9 $MgCl_2$, 25 HEPES, pH 7.0. Two channels in the same patch act as uncorrelated sources of open channel noise. The long lived 170 pS substate shows markedly increased noise. Hexamethonium (7 m**M**) increases noise and blocks outside our recording bandwidth, probably beyond 60 kHz, at a pipette potential of –50 mV.

The main conductance state shows two types of open–channel noise with quite different properties. Type (1) is a zero–mean fluctuation, with an apparently Gaussian distribution of amplitudes (standard deviation ≃ 10 pS, 0 to 1 kHz, –50 mV). Type (2) appears as rapid flickers towards baseline, with a range of amplitudes, rather than any distinct amplitude. The third (central) moment μ_3 of the histogram of open channel amplitudes is a measure of asymmetry about the mean: μ_3 is asymptotically zero for a Gaussian process. For an open channel in the main conductance state, μ_3 is 1.5 pA^3 at –50 mV (130,000 points, 20 μsec/point, filtered at 10 kHz), compared to μ_3 = 0.03 pA^3 for background noise. Asymmetry arises from the flickers of process (2).

Interpretation of the open channel noise (as fluctuations in gating or fluctuations in open channel conductance) requires separation of processes (1) and (2). Level crossing tests are not entirely satisfactory separators; more refined and robust statistical analysis will probably be needed to isolate the processes.

M-Pos239 **DIFFUSION THEORY AND DISCRETE RATE CONSTANTS IN ION PERMEATION.** K.E. Cooper, P.Y. Gates, and R.S. Eisenberg, Dept. of Physiol., Rush Medical College, Chicago, IL 60612.

Using a diffusion theory for discrete rate constants we will show the equivalence of the discrete description and a Nernst-Planck diffusion theory for transport through a channel. We will derive the following diffusion theory expression for the rate constant:

$$k = \frac{1}{D}\int_{\alpha}^{\beta} e^{-\varphi(x)} \left[\int_{x}^{\beta} e^{\varphi(y)} dy \right] dx \qquad (1)$$

where D is the diffusion coefficient, φ is the normalized potential energy of the ion as it moves through a channel (φ contains only the ion-channel interaction potential and the externally applied voltage), and α and β are the positions of the minima on either side of the barrier being crossed.

In the limit of large barriers one can obtain an asymptotic form of equation (1) that has an exponential dependence on the extema of φ (Kramers' equation). The prefactor in this form depends on the second derivative of φ in the wells and at the peak of the barrier and on D. The voltage dependence of the Kramers' form (and of the traditional Eyring formulation) is different from that of equation (1). The size of the discrepancy and its origins will be discussed.

M-Pos240 ***AUTOMATIC DETECTION OF CHANNEL CURRENTS.*** A. Moghaddamjoo, R.A. Levis, and R.S. Eisenberg. Department of Electrical Engineering, University of Wisconsin, Milwaukee WI & Department of Physiology, Rush Medical College, Chicago IL.

Experiments on ionic channels are limited by the labor and difficulty of detecting channel openings. An ideal detector would ***automatically and objectively*** resolve openings, even in the presence of subconductance states, flickers, multiple openings, and substantial noise. We reach for the ideal with a running window edge detector.

If the input to our present version of the detector has signal/noise ≃ 1 *rms*, and looks like

then the output looks like

Most (>99%) data points are correctly classified as closed or open; and estimates of the duration and amplitude of channel states are accurate, within 1%. *(Arrows indicate misclassified data points.)*

M-Pos241 CRITERIA FOR THE COMPENSATION OF PARASITIC IMMITTANCES (SERIES, SHUNT, AND SUMMING NODE) FOR A SET OF THREE FUNDAMENTAL VOLTAGE CLAMP CIRCUITS. Gunter N. Franz, Department of Physiology, West Virginia University Medical Center, Morgantown, WV 26506.

Active compensation sources can be placed at various locations to compensate for several parasitic immittances in voltage clamps of the inverting, non-inverting, and bootstrap type. The compensation methods are suitable to reduce the effects of series and shunt parasitics and of parasitic immittances at the input or summing node of the clamp amplifier.

This poster analyzes several compensation schemes and provides equations representing the criteria for compensation. In general, the compensation criteria are simpler if (1) two or more active compensation sources are added to the circuit, and (2) inverting or bootstrap clamp topologies are used instead of the more common non-inverting type.

M-Pos242 IONIC SELECTIVITIES OF THE VOLTAGE-DEPENDENT CHANNELS PRODUCED BY PARDAXIN, A MARINE TOXIN. Y. L. Shih+, P. Lazarovici*, P. McPhie#, and C. Edwards+, +LCBG, #LBM, NIDDK; *NICHD, NIH, Bethesda, MD. 20892

Pardaxin, a thirty three amino acid polypeptide toxin purified from the secretions of a Red Sea flatfish, forms voltage-dependent channels in bilayer membranes (Lazarovici, et al. J. Biol. Chem. 261:16704, 1986). Bilayers of ethanolamine were formed at the tips of patch clamp pipettes by the double dip method (Suarez-Isla et al. Biochem. 22:2319, 1983). Short duration, stepwise voltage-dependent conductance changes were produced when the side to which the toxin was added was made positive. The selectivities for various cations were estimated from the reversal potentials for the responses obtained with isosmotic solutions on the two sides. The sequence of the relative permeabilities was Rb+ > Na+, K+; tris was not permeant. So far, it has not been possible to measure the permeabilities to Li+, Cs+, and Ca++. Measurements of the secondary structure by circular dichroism have shown little or no differences in solutions of the various test cations.

M-Pos243 Stretch-activated (SA) channels in the neurons of Cepaea (Helicideae) and Lymnaea. E. Bedard, W.J. Sigurdson & C.E. Morris, Biology, U. of Ottawa, Ottawa, Canada K1N6N5.

SA channels of two types have been found in neurons of the terrestrial snail, Cepaea. The most frequently observed one is a flickery channel with a conductance of 58 pS (physiological saline, cell-attached), and a reversal potential (VR) near rest. VR is insensitive to anion substitutions, but shifts progressively in the depolarizing direction with increasing $[K^+]$-pipette. Channel currents are not seen in K^+-free solutions with Na^+ or Ca^{++} as the major cations. Quinidine (but not TEA or 4AP) blocks the channel. The probability of being open for this K^+-permeant channel saturates near -70 mm Hg. In some inside-out patches with symmetrical high NaCl solutions, a non-flickery multiple-conductance Cl^- channel appears during application of suction (about -35 mm Hg). Closure follows within a minute of release of suction rather than within seconds as in the case of the SA K^+ channel. In the freshwater snail, Lymnaea, inside-out patches from neurons contain a similar channel, with a maximum conductance near 100 pS (symmetrical 50 mM Cl^-). This channel, like that of Cepaea, is impermeable to gluconate, but its SA is more equivocal, because it is less reproducible. A preliminary test of several (unidentified) Aplysia neurons revealed SA currents. In one case (cell-attached, physiological saline) channels with VR near rest and a slope conductance of 63 pS (except for infrequent subconductances) showed SA similar to that seen with Cepaea SA K^+ channels. Supported by NSERC, Canada and the Muscular Dystrophy Association of Canada.

M-Pos244 INVESTIGATING THE STEADY-STATE VOLTAGE-DEPENDENT KINETICS OF SINGLE ION CHANNELS: A CASE STUDY FOR THE FAST CHLORIDE CHANNEL. David S. Weiss and Karl L. Magleby. Department of Physiology and Biophysics, Univ. of Miami School of Medicine, Miami, FL 33101.

The membrane potential (V) regulates the activity of many different types of ion channels. The fast Cl channel in cultured skeletal muscle was used to study steady-state voltage-dependent channel kinetics. This channel has a marked voltage sensitivity (open probability increases from 0.04 to 0.56 for V of -90 to -20 mV) and exhibits stable behavior in excised patches enabling the collection and analysis of 1-2 million intervals per experiment. The working hypothesis is that the rates of the conformational changes of the channel directly involved in the gating kinetics are exponentially dependent on V. The goal is to determine the number of kinetics states, transition pathways between these states, which pathways are voltage dependent, and the magnitude and direction of the voltage sensitivities. Steady-state channel activity is collected at each of several Vs. The number of open and shut states are determined from distributions of open and shut intervals. The most likely rate constants for a particular model are then determined for each V and plotted against V on semilogarithmic coordinates. A linear regression is performed for each rate to estimate the rate at zero voltage (y-intercept) and the voltage sensitivity (slope). Starting with these initial values, the data at all the voltages are then fit simultaneously in order to optimize the rate constants and their voltage sensitivities and constrain the models. Our results suggest that most of the rates for the fast Cl channel are voltage dependent. Thus, most of the conformational changes involved in the gating of this channel are associated with charge movement in the electric field of the membrane. Supported by grants AR32805 and NS08138 from the National Institutes of Health.

M-Pos245 **HIGH PERFORMANCE MODULA-2 PROGRAMS FOR DATA ACQUISITION AND ANALYSIS OF SINGLE-CHANNEL EVENTS.**

H. Affolter and F. J. Sigworth, Dept. of Cellular and Molecular Physiology, Yale School of Medicine, New Haven CT 06510.

Modula-2 is a modular, Pascal-like programming language developed by N. Wirth in 1979. We have written a set of library modules for data acquisition and analysis in Modula-2, and use these in programs that run on the $750 Atari 1040ST computer. We have developed new display algorithms that allow this 68000-based computer to draw a vectored graph of up to 8000 data points on its 640 x 400 pixel screen in <100 ms, including the time for scaling, clipping, and erasing a previous trace. We have written routines for stimulating and sampling data both synchronously and in interrupt-driven modes, and have also defined data structures and high-level procedures for data acquisition, storage, menu manipulation, and text windows.

Our programs exploit the fast display capability to allow real-time display during data acquisition and for rapid scrolling through data traces during single-channel analysis.

M-Pos246 CHANNELS FORMED BY COLICIN E1 IN PLANAR LIPID BILAYERS ARE MONOMERS

Stephen L. Slatin. Albert Einstein College of Medicine. Bronx N.Y. 10461.

Colicin E1 is one member of a family of bacterial proteins that kill target bacteria by forming an ion channel in the inner membrane of the victim. These proteins also form voltage-dependent channels in planar lipid bilayers, and can greatly increase the permeabilty of liposomes. The sequence of the whole protein is known, and it has been shown, by the use of site-directed mutagenesis, that the channel-forming region is contained in a domain of less than 88 amino acids very near the C-terminus. Available evidence, from dose/response experiments, suggests that the protein acts as a monomer biologically and in vesicles. The equivalent experiment in planar bilayers suffers from the reluctance of the system to equilibrate. We find that at pH 3.5, where colicin E1 conductance comes to a steady state, the dose/response curve is linear on any particular membrane, which is consistant with a monomer forming the V-dep. channel in this system also. However, the large size of the lumen deduced from reversal potential experiments in bilayers makes it difficult to build a monomeric model of the open channel from the appropriate domain of the protein. To test for the presence of possible E1 dimers, we exposed membranes to whole colicin E1 and a C-terminal fragment of the protein (made in C. Levinthal's lab by cleavage with cyanogen bromide) at the same time. Under the conditions of the experiment, the fragment formed channels with a different voltage dependence than the whole protein. If hybrid dimers had formed they might be expected to have intermediate properties. Instead, two separate populations of channels were maintained. Thus, there is no evidence for a multimeric form of colicin E1 in planar bilayers. [supported by NIH grant GM 29210]

M-Pos247 GADOLINIUM ION IS AN INHIBITOR SUITABLE FOR TESTING THE PUTATIVE ROLE OF STRETCH-ACTIVATED ION CHANNELS IN GEOTROPISM AND THIGMOTROPISM.

B. Millet and B.G. Pickard. Biology Dept.. Washington Univ., St. Louis. MO 63130.

It has been postulated that the transductive step of both geotropism and thigmotropism is the opening of stretch-activated ion channels which permit flow of Ca^{2+} across the plasmalemma (K.L. Edwards and B.G. Pickard, In: The Cell Surface in Signal Transduction, ed. H. Greppin et al., Springer, 1987). The putative role of such channels is not readily tested without an inhibitor (or stimulator) of high specificity; but inhibitors of thigmotropism have not been reported, and the numerous known inhibitors of geotropism also inhibit growth, without which tropic response cannot be expressed. We now report 1) thigmotropism of Zea mays L. roots is inhibited about 65% by pretreatment of tips for 30 min with 10-250 μM $GdCl_3$, 2) orthogeotropism is inhibited about 80% by pretreatment with 250 μM $GdCl_3$ but somewhat less with lower concentrations, and 3) growth is not inhibited over this concentration range (values of $p > 0.8$). In contrast, identical application of $LaCl_3$ does not inhibit the tropisms noticeably at these concentrations, and at 1 mM inhibits orthogeotropism and growth similarly: thus, the geotropic system and the system which mediates tropic response (which requires hormone transport dependent on Ca^{2+} flux) can evidently discriminate the two, closely similar lanthanides. Gd^{3+} might possibly have a general affinity for stretch-activated ion channels, or might have general utility for discriminating different types of Ca^{2+}-permeable channels. In any case, Gd^{3+} could be useful in testing whether ion channels in patched plasmalemma are transducers for thigmo- and geotropism. Funding: NATO, NSF and NASA.

M-Pos248 PURKINJE CELL MEMBRANE MODIFICATIONS BY PARTIAL DEAFFERENTATION IN THE RAT CEREBELLUM.

P. Morain, R.T. Kado and C. Batini. Laboratoire de Neurophysiologie Pharmacologique, INSERM U161, 2 rue Alesia, 75014 Paris, France. Laboratoire de Neurobiologie Cellulaire et Moleculaire, CNRS, Gif-sur-Yvette, France.

The climbing fibers (CF) supplying a major synaptic input to the dendrites of the cerebellar Purkinje cells (PC) in rats can be selectively destroyed by treating the animal with 3-Acetylpyridine (cf.Bardin et.al. J. Comp.Neuro. 213:464-477, 1983). The effects of this deafferentation are severe and permanent impairment of righting reflex and motor coordination. Electrophysiologically, the affected PC have been shown to undergo changes in firing pattern and loss of their inhibitory property with time after treatment.

We have studied the membrane properties of the PC from treated and normal rat cerebella in the brain slice preparation using the single-electrode current clamp technique. PC in normal slices characteristically fired in bursts consisting of simple spikes (SS) followed by dendritic spikes (DS) and ended with a prolonged hyperpolarization. PC from the deafferented animals most often had no bursting activity on impalement but could be made to fire in the same way as the normal PC upon reduction of external sodium or the addition of TTX to the medium. The lack of dendritic activity in the PC from treated animals appears to be due to a voltage sensitive inward rectifying conductance which produces a low conductance state at resting potential and which is not present in the normal PC. These results indicate that removal of the CF input to the PC induces a radical change in the membrane conductances of the PC dendrites.

M-Pos249 REVERSIBLE INSERTION INTO MEMBRANE VESICLES OF A COLICIN E1 CHANNEL-FORMING PEPTIDE.
S. Xu, A.A. Peterson, C. Montecucco[1], and W.A. Cramer, Dept. of Biological Sciences, Purdue University, W. Lafayette, IN, 47907; Institute of General Pathology[1], University of Padua, Padua, Italy. [Intr. by T. S. Baker.]

Colicin E1 and its COOH-terminal channel-forming peptides display maximum binding and insertion into artificial membrane vesicles at acidic pH values near 4.0. At this pH, the thermolytic peptide is relatively inaccessible to exogenous trypsin after insertion into membrane vesicles. Depending on conditions, the M_r 18,000 peptide is either converted to M_r 14,000 or unaffected. The proteolysis involves a tryptic cut at the NH_2-end of the peptide, after K-381 or K-382. However, when the pH of a vesicle suspension, to which peptide has been bound at pH 4.0, is shifted to 6.0, the accessibility to trypsin increases greatly. This has been shown by (i) the large decrease in M_r 18,000, M_r 14,000, or peptide of any size present in the vesicle membrane. (ii) The amount of[^{14}C]-leucine-labeled peptide in the membrane decreases after the pH 4 → 6 shift and treatment with trypsin (PNAS, 82, 1386-1390, 1985). In addition, (iii) when a photoactivable nitrene-generating phospholipid probe was used to label the colicin peptide inserted into the bilayer, the extent of labeling decreases by a factor of 2-3 when the pH is shifted from 4.0 to 6.0; (iv) colicin peptide added to vesicles at pH 4.0 can "hop" to other vesicles if the pH of the donor vesicles is first raised to 6.0 under conditions of high ionic strength. It is proposed that deprotonation of acidic residues in contact with the hydrophobic bilayer destabilizes the partly or fully inserted channel and causes it to be extruded from the membrane. [Supported by NIH GM-18457.]

M-Pos250 TWO FUNCTIONALLY DISTINCT FORMS OF cGMP-STIMULATED CATION CHANNELS IN A BOVINE ROD PHOTORECEPTOR DISK PREPARATION. L.B. Pearce, R.D. Calhoon, P.R. Burns, A. Vincent, and S.M. Goldin (Intr. by Manfred Karnovsky). Dept. of Biol. Chem. and Molec. Pharmacol., Harvard Med. Sch., Boston MA.

Purified bovine disks exhibit cGMP-stimulated release of ^{45}Ca actively accumulated by an ATP dependent uptake system (Puckett and Goldin [1986] Biochem. 25, 1739). Efflux of intravesicular ^{22}Na and actively accumulated ^{45}Ca from this disk preparation, stimulated by continuous superfusion with 8-Br-cGMP, was measured on the 25-100 ms time scale by a novel rapid superfusion method. Activation of cation release was maximal within 25 ms of 8-Br-cGMP introduction. Termination of ^{22}Na efflux over a wide range of test concentrations of 8-Br-cGMP precisely conformed to the sum of two exponential decay processes: a rapid phase (decay constant 200 ms) and a slower phase (decay constant 1.6 s). The kinetics of the biphasic decay of efflux cannot be explained by depletion of a pool of releasable ^{22}Na, but reflect an intrinsic process for channel inactivation. 8-Br-cGMP-stimulated release of ^{45}Ca exhibited identical biphasic decay kinetics. The Ca:Na selectivity ratio is ~0.5:1 for both decay phases. 8-Br-cGMP was less potent (EC50 of 8.4 uM vs. 2.8 uM) but more cooperative (nH of 2.1 vs. 1.1) in its activation of the rapid- vs. the slower-decay phase of ^{22}Na efflux. The slower decay phase was selectively inhibited by 25 uM L-cis-diltiazem. In contrast, Na (5-10 mM) selectively inhibited the rapid-decay phase of 8-Br-cGMP-stimulated ^{45}Ca release. These two pharmacologically distinct phases of decay are hypothesized to represent two functionally distinct forms of cGMP-stimulated channels. The maximum rate of Ca release (5 nmole/mg disk protein/min) may be sufficient to produce a 1 uM change in local cytoplasmic [Ca] within 20 ms.

M-Pos251 A SIMPLE BROMIDE EFFLUX ASSAY FOR CALCIUM AND CYCLIC AMP REGULATED CHLORIDE CHANNELS IN CULTURED MAMMALIAN CELLS. Jeffrey Bingham Smith, Edward J. Cragoe, Jr., and Lucinda Smith. Dept. Pharmacology, University of Alabama at Birmingham, Birmingham, AL 35294 and Merck Sharp & Dohme Research Labs., West Point, PA 19486.

Cultures (35 mm dia) of human forearm skin fibroblasts, transformed human colonic (T84) and bronchial (TBE-1) epithelial cells were incubated in a physiological salts solution containing glucose and 50 uCi 77Br or 82Br for 2 hr. Efflux was initiated by rinsing the cultures 8 times with the efflux medium which was removed and replaced with fresh medium at 10 sec intervals. Isoproterenol, vasoactive intestinal peptide, and forskolin, which increase cellular cAMP, markedly increased Br efflux from T84 and TBE-1 cells as did the Ca transporting antibiotic, A23187. Bradykinin (BK), which increases cytosolic free Ca in the fibroblasts, increased the rate of Br efflux 5 fold from these cells. BK at 20 nM maximally increased Br efflux and Ca mobilization, however, the onset of increased Br efflux lagged the onset of Ca mobilization by 50 sec. Neither furosemide nor SITS had any effect on Br efflux at concentrations that abolished Na/K/Cl symport and sulphate/Cl antiport in the fibroblasts. Certain derivatives of (indanyloxy)alkanoic acid and anthranilic acid, which block Cl channels, potently inhibited BK-evoked Br efflux, whereas other closely related compounds had no effect on efflux. At 50 uM compound nos. 8-10 (DCPIB), 8-4A, and 5-nitro-N-(3,4-dichlorobenzyl)anthranilic acid almost completely blocked BK-evoked efflux, whereas compounds 8-2 (DCPI) and 8-7 had no effect on efflux (see J.Med. Chem. 25:567-579, 1982 for structures). (Supported by Grants HL01671 and AM35818 from the National Institutes of Health and a pilot project from the Cystic Fibrosis Foundation.)

M-Pos252 INTERACTION OF IONS WITH A METABOLICALLY REGULATED K+ CHANNEL, K+(MR), IN PANCREATIC ISLET B CELLS. J. Tabcharani, L. Falke, and S. Misler, Jewish Hospital, St. Louis, MO.

In insulin secreting pancreatic B cells, the K+ channel most apparent at, and most contributory to, Vrest is largely voltage independent but strongly metabolically regulated. Several features of the interaction of rat and human K+(MR) channels with ions are important for its identification and/or function. (1) K+(MR) channels show moderate inward rectification (IR) dependent on intracellular cations. IR seen in cell attached patches can be mimicked in inside-out excised patches on addition of 2-3 mM Mg or 1 mM Mg and 10-20 mM Na to 144 mM KCl_i. This is comparable to IR in delayed rectifier and maxi Ca^{2+} activated K+ channels. (2) Maximum single channel slope conductance γ is dependent on $[K+]_o$, but is less steep than $[K+]_o^{0.5}$ relationship displayed by anomalous rectifier K+ channels which dominate resting P_K in most cells. 3. K+(MR) is permeable to, but blocked by, Rb; it is nearly impermeable to Na, Li, Cs, or NH_4. In inside-out excised patches (pipette containing 144 mM KCl) adding 70 mM $RbCl_i$ to 70 mM KCl_i shifts E_{rev} by -15 mV while substituting 144 mM $RbCl_i$ for KCl shifts Erev by +15 mV (both suggesting $P_{Rb}/P_K = 0.5$); both maneuvers reduce maximum outward current. No outward current was detectable with 144 mM NH_4Cl_i, $LiCl_i$, $NaCl_i$, $CsCl_i$ (extrapolated $E_{rev} > +80$ mV. (4) K+ (MR) activity can be modulated by impermeant cations. In some patches, Mg_i at > 1 mM suppresses mean channel activity (I/i) in the absence of ATP_i but enhances I/i in the presence of ATP_i; $LiCl_i$ > 10 mM causes a voltage dependent increase in I/i in some patches. (5) Asymmetry of TEA action on K+ (MR). TEA_i reduces outward but not inward current in a voltage dependent manner in inside-out excised patch, while TEA_o reduces current in both directions in outside-out patches.

M-Pos253 KINETIC ANALYSIS OF CATION CHANNELS IN FIBROBLASTS: MARKOV AND FRACTAL BEHAVIOR. Andrew S. French and Lisa L. Stockbridge, Department of Physiology, University of Alberta, Edmonton, Alberta, Canada T6G 2H7.

Kinetic behavior in single ion channels is usually analysed by assuming the existence of a small number of discrete open and closed states. The lifetime in each state is assumed to be independent of previous channel history so that transitions occur as a Markov process. A more general theory allows for a large number of states with widely distributed lifetimes, causing the rate of leaving a state, k, to depend on the time scale of observation, t: $k=At^{-B}$ where A, B are constants. In fractal terms $B=D-1$, where D is the fractal dimension (Liebovitch *et al.*, 1987. Math. Biosci. 84:37-68). We used this approach to analyse the kinetic properties of single channels recordings from a calcium-activated potassium channel and a large voltage-activated cation channel, in human and avian fibroblasts. A maximum likelyhood technique was used to produce estimates of k from events within a series of fivefold time ranges, with a doubling of time scale between each range. Confidence limits were measured with m-unit likelyhood intervals. The closed times of both channels were well-fitted by a fractal model over the range from 0.1 ms to 10 s. In contrast, the open times of both channels showed clearly Markov behavior over a wide range of time scales, although they may have fractal behavior at short time scales. Analysis of Markov simulations using the same technique suggests that at least five, and probably many more, closed states exist for these channels. Supported by the Canadian Medical Research Council and the Alberta Heritage Foundation for Medical Research.

M-Pos254 ANALYSIS OF CHAOTIC DYNAMICS OF EXCITATION AND PROPAGATION IN NON-PACEMAKER CARDIAC TISSUES. Dante R. Chialvo, Donald C. Michaels and Jose Jalife. Dept. of Pharmacology, SUNY Health Science Center at Syracuse, NY 13210

Chaotic patterns of excitation and impulse propagation can be demonstrated in cardiac tissues that do not oscillate spontaneously. We investigated the dynamics of such phenomena in isolated sheep Purkinje fibers superfused with Tyrode solution and driven by brief depolarizing current pulses applied through a suction pipette. Microelectrode recordings were obtained 3 to 5 mm from the stimulus site. By using various regimes of stimulus strength, duration and frequency, we defined the behavioral structure in the parameter space. In all experiments, stable locking patterns occurred at relatively low frequencies and levels of current strength. The hierarchy always followed Farey's series and, for a given period-adding sequence, the relation between period of locking and pulse strength was similar to that described for the rotation number in the circle map. Chaotic-like patterns were observed at higher frequencies and current strengths. In a second group of fibers, the dynamics were studied during action potential propagation along a non-homogeneous cell strand. The bifurcation parameters in this case were driving rate and changes in the effective conduction time (latency) induced by segmental uncoupling between cells. At the normal levels of coupling, stimulation at increasing rates during 1:1 led to progressive increase in latency, until 2:1 locking occurred. When the degree of conduction impairment was high, changing the driving rate yielded various locking patterns that resembled those in the first group. Yet, at intermediate levels of coupling, period doubling and irregular dynamics were found as the driving rate was changed between the 1:1 and 2:1 domains. All these observations were reproduced semi-quantitatively in a simple difference equation model. The dynamics in this model are determined by two empirically derived functions: rate-latency of activation and rate-action potential duration. As the driving rate is increased, ordered locking or period doubling bifurcations may occur, depending on the precise shape of the functions. In conclusion, locking phenomena and chaos can be demonstrated in cardiac Purkinje fibers that do not undergo self-sustaining oscillations. Moreover, the model results suggest that the mechanism of such dynamics may be related to the non-monotonicity of the rate-latency function.

M-Pos255 ASYMMETRIC CHARGE MOVEMENT IN MAMMALIAN CARDIAC MUSCLE CELLS: NA AND CA CHANNEL COMPONENTS. Bruce P. Bean and Eduardo Rios. Department of Neurobiology, Harvard Medical School, Boston, MA 02115 and Department of Physiology, Rush Medical College, Chicago, IL 60612.

We used whole cell recording to study asymmetric charge movement in isolated rabbit and rat ventricular cells. Ionic currents were eliminated with an internal solution of (in mM) 120 TEA Cl, 5 $MgCl_2$, 10 EGTA, 10 HEPES, pH 7.4 and an external solution of 154 TEA Cl, 10 $BaCl_2$, 6 $CdCl_2$, 0.1 $LaCl_3$, 10 uM TTX, 10 HEPES, pH 7.4. With a holding potential of -100 mV, using 10-20 mV hyperpolarizations to correct for linear capacitance, extra charge movement was evident for depolarizations positive to -70 mV. The extra ON charge saturated at about +20 mV. Saturating depolarizations moved extra charge of 10-20 fC/pF. The OFF charge on repolarization was usually slightly smaller than the ON charge. Holding the cell at -50 mV resulted in a prominent decrease in the ON charge (by 30-40%) with less reduction of the OFF charge. The voltage-dependence of the reduction of ON charge matched that of Na channel inactivation. The charge movement remaining at a holding potential of -50 mV seems to be largely Ca channel gating current, since 1) it is reduced at more positive holding potentials with a voltage-dependence like that of Ca channel inactivation, and 2) it is reduced - sometimes almost abolished - by application of 10 uM D600 followed by long depolarizations.

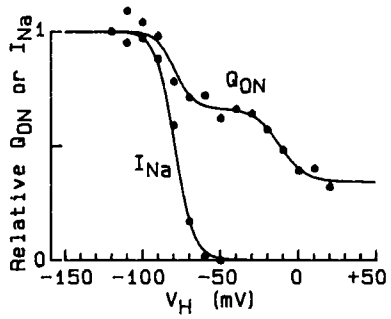

M-Pos256 INTERACTION OF INTRACELLULAR ION BUFFERING WITH TRANSMEMBRANE COUPLED ION TRANSPORT Richard Kline, Leonard Zablow & Ira Cohen., Columbia U., NYC 10032 & SUNY Stony Brook, NY 11794

The role of the Na/Ca exchanger in the control of cellular excitability and tension development is of current interest in cardiac physiology. It has been suggested that this coupled transporter is responsible for rapid changes in intracellular Ca^{++} activity (aCai) during single beats, generation of plateau currents which control action potential duration, and control of intracellular Na^+ activity (aNai) during Na/K pump suppression as may occur during terminal stages of ischemia. Its actual behavior is complex for at least two reasons. First, the exchanger transports two ionic species and thus its instantaneous flux rate depends on both aNai and aCai. Second, the alteration in aCai which is caused by a given transmembrane Ca^{++} flux, and which controls the subsequent exchanger rate, is a complex function of available intracellular Ca^{++} buffering. The buffers convert only a small and variable fraction of the change in total calcium concentration arising from transmembrane Ca^{++} fluxes into changes in activity. Using a number of simplifying assumptions, we model changes in aNai and aCai under the influence of Na/Ca exchange, Na/K ATPase and Ca-ATPase pumps, and passive Na^+ and Ca^{++} currents during mock experimental protocols. We conclude that: 1) Na/Ca exchange alone cannot maintain aNai at low levels during prolonged Na/K pump blockade; 2) since the relationship between the rise of aNai and aCai during Na/K pump blockade and their fall upon pump reactivation may differ due to exchanger-buffer interaction, the tension vs. aNai, and TI current vs. aNai relations should show hysteresis; and, 3) the exchanger and its resultant currents can contaminate measurements of Na/K pump currents.

M-Pos257 TIME INDEPENDENT ACETYLCHOLINE ACTIVATED POTASSIUM CURRENT IN THE EMBRYONIC CHICK ATRIUM, Tony L. Creazzo (Intr. by Richard D. Veenstra). Medical College of Georgia, Department of Anatomy, Augusta, Georgia 30912.

Several recent reports indicate that the acetylcholine activated K+ current ($I_{K(ACh)}$) in cells from adult hearts is time dependent. Whether $I_{K(ACh)}$ in the embryonic chick heart was time dependent was examined using the whole-cell variation of the patch clamp technique. Atrial myocytes were isolated from day 15 embryos. These cells were spherical with a diameter of 17.8 ± 2.2 μm^2 (S.D., n=9). The membrane capacitance was 9.5 ± 3.1 pF (n=9) or 0.93 $\mu F/cm^2$. The input resistance was quite high at approx. 2 GΩ. The I-V relationship for $I_{K(ACh)}$ was determined from the computed difference in the current during 200 msec voltage steps in the presence or absence of 1.0 μM ACh. The quasi instantaneous I-V relationship was not significantly different from the I-V taken at 200 msec whether in 4 or 25 mM $[K+]_o$ (ANOVA). Relaxations of $I_{K(ACh)}$ were not observed and, thus, $I_{K(ACh)}$ was not time dependent. The slope conductance was linear at potentials negative to E_{rev} and inwardly rectified at potentials positive to E_{rev}. The average slope conductance in 4 mM K+ was 660 pS (n=7) and 700 pS (n=5) in 25 mM K+. E_{rev} was -73 ± 7 mV (n=7) in 4 mM K+ and -34 ± 11 mV (n=5) in 25 mM K+. E_{rev} increased 62 mV per 10 fold increase in $[K+]_o$. The maximum outward current was approx. 30 pA in either 4 or 25 mM K+. The current was completely blocked by 1 μM atropine, 0.5 mM Ba++ or 1 mM 4-AP. It was calculated that there were approx. 2000 $I_{K(ACh)}$ channels per cell ($2/\mu m^2$). It is possible that time dependence of $I_{K(ACh)}$ develops after day 15 of incubation.

M-Pos258 VOLTAGE- AND TIME-DEPENDENT EFFECTS OF VERAPAMIL UPON THE Ca^{++} CURRENT AND $[Ca^{++}]_i$ TRANSIENT IN CARDIAC MYOCYTES. James Johns and Luc Hondeghem, Vanderbilt Univ., Nashville, TN.

Verapamil is well-known to block the calcium current of ventricular myocardium in a time- and voltage-dependent fashion. In the present study we quantified its effects upon the $[Ca^{++}]_i$ transients in collagenase-dispersed guinea pig ventricular myocytes loaded with FURA-2. The cells were voltage or current clamped using the whole cell recording mode of the patch clamp technique. $[Ca^{++}]_i$ was estimated using the ratio of FURA-2 fluorescence with illumination at 340 and 380 nm. At 25°C, under control conditions, following a 1 minute rest period, the $[Ca^{++}]_i$ transient declined from the 1st to the 2nd pulse, and then increased to reach a steady state (see figure).

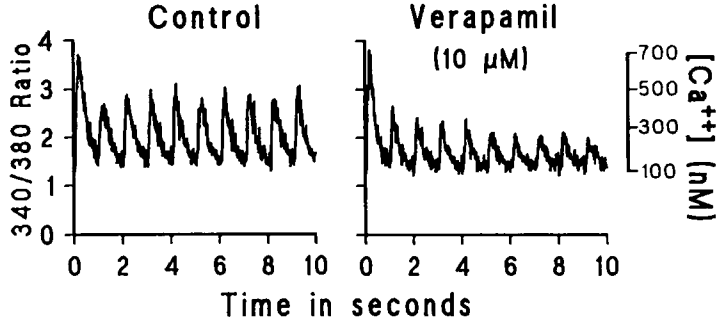

Verapamil (10 μM) had little effect upon the amplitude of the first two $[Ca^{++}]_i$ transients following a 1 minute rest period, but decreased the subsequent transients in a use-dependent fashion, so that a reduced steady state $[Ca^{++}]_i$ resulted. Thus, after a rest period when block of calcium channels is minimal and intracellular stores are well-filled, verapamil does not interfere with the release of calcium. We conclude that verapamil not only reduces calcium currents, but also reduces calcium transients in a use-dependent fashion, probably because of decreased transsarcolemmal flux and depletion of the releasable intracellular pool.

M-Pos259 SLOW DEACTIVATION OF I_K CURRENT AS A BASIS FOR WENCKEBACH PERIODICITY IN SINGLE VENTRICULAR MYOCTYES. Mario Delmar, Donald C. Michaels and Jose Jalife. SUNY Health Science Center at Syracuse, NY 13210.

Slow recovery of excitability and rate-dependent activation failure in heart cells are associated with changes in the amplitude and shape of subthreshold responses induced by depolarizing inputs scanning the diastolic interval. The ionic mechanism of this interval-dependence of the subthreshold response was studied in single guinea pig ventricular myocytes, obtained by enzymatic dissociation. Transmembrane voltage and/or currents were recorded using patch clamp electrodes in the whole cell configuration at 32 °C. Sodium and calcium currents were abolished respectively by adding tetrodotoxin (30 uM) and $CoCl_2$ (2 mM) to the HEPES Tyrode perfusate. Hence, only the potassium outward currents, i_{K1} and i_K remained operative. In current clamp studies, regenerative, i_{K1}-mediated active responses were elicited by 500 msec depolarizing pulses. After repolarization, single test depolarizing pulses applied at brief delays caused only passive responses, whereas those applied at long intervals induced progressively larger regenerative responses. The role of i_K relaxation was characterized in voltage clamp experiments. Partial I_K activation was induced by 500 msec pulses to +20 mV from holding potentials (HP) between -80 and -90 mV. Upon repolarization, single 100 msec pulses to +10 mV were applied at various test intervals. The instantaneous current jump elicited by the test pulse at a given interval reflected the degree of deactivation of i_K, whose time course followed a single exponential with a time constant (T) of 216.9 ± 20.5 (n=15). Our results show that the inward going rectification of i_{K1} and the slow time course of i_K deactivation are the major determinants of the amplitude and shape of subthreshold responses elicited after an action potential. These data fully explain the ionic bases of Wenckebach periodicity and other rate-dependent conduction block processes in the heart.

M-Pos260 CHAOTIC DYNAMICS OF REPETITIVE VAGAL CONTROL OF THE SINUS NODE: A MATHEMATICAL MODEL.
Donald C. Michaels, Dante R. Chialvo and Jose Jalife. Dept. of Pharmacology, SUNY Health Science Center at Syracuse, NY 13210

A model of the cardiac pacemaker was used to study the dynamics of the response to repetitive vagal stimulation. The central region of the sinoatrial node was simulated as a 15 x15 array of resistively coupled pacemaker cells. Cells were randomly assigned one of ten intrinsic cycle lengths. Under control conditions, the pacemakers mutually entrained to a common frequency and a dominant region became apparent. Single acetylcholine (ACh; "vagal") pulses applied to a randomly selected 60% of the cells resulted in a shift of the dominant pacemaker to a new region of the array, a delay in the next spontaneous firing, and an increase in apparent conduction time. When ACh pulses were applied repetitively over a range of stimulus intensities and frequencies, a variety of stimulus:response patterns were obtained including phase-locking (e.g., 1:1, 2:1, 3:2, etc) and irregular (i.e., chaotic) dynamics. A map of the parameter space indicated that at lower stimulus intensities, phase locking followed the typical Farey sequence. At higher intensities, regions of irregular dynamics were found. In another group of simulations, qualitatively similar results were obtained when a single pacemaker cell was perturbed with repetitive ACh pulses. Chaotic behavior in both types of simulation was investigated using phase-plane (orbital) plots, Poincaré mapping, and return mapping. On the route to truly irregular dynamics, period doubling bifurcations (2:2, 4:4 and 8:8) were obtained both spatially and in the parameter plane. The attractor in the return map during chaotic activity resembled the Lorenz tent map. However, the interactions of neighboring cells exhibiting chaotic dynamics resulted in characteristic alterations of the attractor geometry that could not be simulated by the addition of random noise. Our results suggest that irregular dynamics obeying the rules derived from other chaotic systems are present during vagal stimulation of the sinus node. These chaotic dynamics may provide insight into the mechanisms of dynamic vagal control of heart rate and may help to explain clinically relevant disturbances of cardiac rate and rhythm.

M-Pos261 EVIDENCE FOR THE PRESENCE OF I_F CURRENT IN THE RABBIT TRICUSPID VALVE PACEMAKER CELLS.
Justus Anumonwo, Mario Delmar, George Rozanski and Jose Jalife. Dept. of Pharmacology, SUNY Health Science Center at Syracuse, NY 13210.

It has been previously demonstrated that atrioventricular valve cells have spontaneous activity. We studied the bases of this activity in whole tissue and in single cell preparations. In whole tissue experiments we used the loose-patch voltage clamp technique and 30 tissue strips of 200 by 200 microns. We report here the presence of an I_F current in the rabbit tricuspid valve. With a holding potential of -50 mV, hyperpolarizing pulses applied into the range of diastolic depolarization (-60 to -90 mV) produced slow time-dependent inward currents. Steady-state current-voltage (I-V) plots showed that whereas the current was depressed by low Na (35 mM), noradrenaline (1.5 mM) increased its magnitude and rate of activation. Decreasing the temperature from 37 to 25 °C reduced the magnitude and slowed the time course of current activation. Cs (2 mM) markedly depressed the current and changed the slope of the I-V relation. All effects were reversed upon washout. In spontaneously active preparations, Cs (1 - 10 mM) changed the biphasic diastolic depolarization to monophasic, but the spontaneous activity persisted. Single myocytes were obtained by collagenase treatment which yielded cells of rod-like and spindle shapes of various sizes. All cells were striated and some were spontaneously active in Tyrode solution. Preliminary single cell voltage clamp experiments using the suction pipette demonstrate that in the presence of Ba (1 mM), a Cs-sensitive, hyperpolarization-activated inward current can be elicited upon hyperpolarizing from holding potentials of -50 mV. The time course of this current is similar to that described for the whole tissue. In addition, we recorded an inward current with behavior and voltage dependency similar to that described for I_{Ca} in other cardiac cells. Further, a Ba-sensitive inward rectifier (I_{K1}) with an N-shaped instantaneous I-V relation was also demonstrated. A pronounced time-dependent inactivation process was apparent for this inward rectifier. It is concluded that the I_F current is present in the valve cells and that although it contributes to the diastolic depolarization, it is not the only factor involved in pacemaking. Moreover, I_{K1} inactivation might also be involved in diastolic depolarization.

M-Pos262 ACTIVE GENERATOR PROPERTIES AND MARGIN OF SAFETY FOR PROPAGATION IN ANISOTROPIC SHEEP VENTRICULAR MUSCLE.
Carmen Delgado, Mario Delmar, Dante Chialvo, and Jose Jalife. Dept. of Pharmacology, SUNY Health Science Center, Syracuse, NY 13210.

Action potential propagation in cardiac muscle is slower in the transversal (T) than in the longitudinal (L) axis of the cells. Moreover, L propagation shows a lower action potential upstroke velocity (Vmax) and amplitude, together with a slower foot potential. Recently, we reported that when intercellular coupling is impaired, T propagation is more vulnerable to block. We have now studied the relationship between active membrane properties and margin of safety, defined as the range of active generator properties at which successful propagation in the T or L direction is maintained. After determination of fiber orientation, thin pieces of sheep epicardial ventricular muscle (2 x 2 x 0.5 mm) were cut into an "L" shape according to such an orientation. Following equilibration,threshold current and strength interval curves for L and T were studied in twelve preparations. The threshold for T propagation was 15.5 ± 4.01 uA, whereas for L propagation it was 28.6 ± 8.3 uA ($p<0.05$). In nine of twelve experiments, the refractory period was shorter for L than for T propagation. In a second group of experiments preparations were exposed to Tyrode solution containing increasing concentration of KCl, while recordings were obtained simultaneously from T and L through appropriately placed pairs of extracellular and intracellular microelectrodes. The changes in Vmax, T and L effective conduction velocities (CV's) and degree of anisotropy (measured as the ratio of T/L CV), as well as time to complete blockade were monitored during and after the transition from 4 to 20 mM KCl. In one experiment, simultaneous T and L conduction block was observed. However, in seven of eight experiments, effective CV decreased more for T (45%) than for L (20%) and the time to conduction block was briefer for T (4.9 min) than for L (6.7 min). Further, in contrast to what is predicted by linear cable theory, the relationship between CV^2 and Vmax was not linear. At the time of T block, Vmax had decreased to 74% and 63% for T and L, respectively. We conclude that, although under physiological conditions excitability is higher for T, when active generator properties are impaired as a result of high potassium or premature stimulation, the margin of safety for propagation is higher in the L than in the T direction.

M-Pos263 DEFECTIVE MYOPLASMIC Ca^{2+} HOMEOSTASIS IN VENTRICULAR MUSCLE IN DIABETIC CARDIOMYOPATHIC RATS. J.R. López[1], T. Bányász[2], T. Kovács[2], F.A. Sréter[3], and G. Szűcs[2], [1]Centro de Biofísica y Bioquímica, Instituto Venezolano de Investigaciones Científicas, Apartado 1827, Caracas, Venezuela; [2]Department of Physiology, Debrecen Medical School, Debrecen, Hungary; [3]Department of Anesthesia, Massachusetts General Hospital and Harvard Medical School and Department of Muscle Research, Boston Biomedical Research Institute, Boston, MA 02114.

Diabetes mellitus is frequently associated with cardiac dysfunction. Altered myocardial Ca^{2+} transport has been reported in diabetes (Wood, J., et al., *Am. J. Physiol.*, **247**:R120, 1984). We have measured the intracellular free calcium ion concentration $[Ca^{2+}]_i$ by means of Ca^{2+}-selective microelectrodes in ventricles of diabetic and non-diabetic rats. Wistar rats weighing 300 g were made diabetic with a single intravenous injection of streptozotocin (Sigma, 55 mg/kg) in citrate buffer (pH 4.5) injected into the femoral vein under ether anesthesia. The animals were killed by decapitation after 8 wk. Hearts were excised, atria and connective tissue removed, and small segments of ventricle transferred to a temperature controlled chamber for electrophysiological measurements. The $[Ca^{2+}]_i$ in the non-diabetic ventricular cells was 0.10 ± 0.01 μM (mean ± SEM) while it was 0.31 ± 0.02 μM in the diabetic myocytes. No differences in the resting membrane potentials were observed (-85.0 ± 1.0 mV in non-diabetic and -86.0 ± 1.0 mV in diabetic cells). These results show that in diabetic ventricular muscle there is an imbalance in the regulation of the intracellular calcium concentration. [Supported by grants from MDA and CONICIT of Venezuela S1-1277 to JRL and NIH Center Grant GM15904 to the Department of Anesthesia].

M-Pos264 GEOMETRICAL EFFECTS ON CARDIAC ACTION POTENTIAL INITIATION. R.C. Tan, B.M. Ramza and R.W. Joyner. Depts. of Pediatrics and Physiology, Emory University, Atlanta, GA, 30322 and The University of Iowa, Iowa City, IA, 52242

We propose that the process of action potential initiation is fundamentally different for isolated cells as compared to a region in a multi-dimensional syncytium, such that the current threshold (I_{th}) for the syncytium is much more sensitive to decreased G_{Na} because an active response in a liminal area is required prior to initiating syncytial propagation. We tested this hypothesis by measuring the alterations in I_{th} produced by Lidocaine (L) and/or elevated K^+ (8K) in isolated rabbit ventricular cells versus rabbit papillary muscles. With 50 uM L and/or 8K the I_{th} for the papillary muscle was more than doubled, with larger effects for the combined interventions and for rapid pacing (2.5 Hz). In contrast, even 100 uM L and 8K at 2.5 Hz pacing produced no significant elevation in I_{th} for the isolated cells. We also used numerical simulations of action potential initiation in an isolated isopotential cell represented by the Beeler-Reuter cardiac membrane model as compared to a radially symmetric disk of excitable cells with stimulation at the central element of the disk model. Decreasing G_{Na} of the membrane model produced only a small difference in I_{th} for the isopotential model, but large differences in I_{th} for the disk model.

Our results can be explained by the absence of an electrical load on the isolated cells, whereas the electrical load of the surrounding cells of the syncytium creates the necessity of a liminal area of activation. This liminal area of activation is increased when the availability of Na current from each cell is decreased, leading to an increase in the I_{th} for local stimulation of the syncytium. These results help to explain the selective action of antiarrhythmic agents on blocking abnormal impulse initiation.

M-Pos265 MECHANISM OF THE VERATRIDINE-INDUCED INCREASE IN CYTOSOLIC Ca^{2+} AND RATE OF RESPIRATION OF CARDIAC MYOCYTES. Rafael Moreno-Sánchez and Richard G. Hansford (Intro. by William Guggino). Gerontology Research Center, National Institute on Aging, Baltimore, MD 21224.

We studied the effect of the Ca^{2+} blockers verapamil(V), nitrendipine(N) and dichlorobenzamil (DCB) on the increase in cytosol free Ca^{2+} ($[Ca^{2+}]c$) and the rate of O_2-uptake induced by depolarization of isolated rat cardiac myocytes with veratridine. Respiration was measured with an O_2-electrode and $[Ca^{2+}]c$ by Quin 2 fluorescence. 25μM veratridine increased $[Ca^{2+}]c$ from a resting value of 94+22 (n=13) to 778+103nM (n=10): O_2-uptake increased from 30+5 (n=31) to 182+30 (n=31) ng-atom O_2/mg/min. The veratridine-induced increase in $[Ca^{2+}]c$ was inhibited by 39+8% (n=11), 88+6% (n=3) and 37+10% (n=5) by 2.5μM V, 25μM V and 2μM N, respectively. Veratridine-induced O_2-uptake was inhibited by 18+6% (n=7), 86+2% (n=4), 6+1% (n=4), 55+4% (n=4) and 94+2% (n=6) by 2.5μM V, 25μM V, 2μM N, 2.5μM DCB and 25μM DCB, respectively. The increment in $[Ca^{2+}]c$ caused by a low concentration of veratridine (5μM) was potentiated by isoproterenol (139+7 (n=7) for control vs 161+7nM (n=7; P<0.001) for isoprel): preincubation with 2.5μM V prevented the effect of isoprel ($[Ca^{2+}]c$=109+7nM, n=5). Equally, 2.5μM V or 2μM N completely reversed the increase in $[Ca^{2+}]c$ seen on adding 25 mM K^+ to cells in a low-Na^+ (<5.5mM) medium. As isoprel is known to stimulate Ca^{2+} channel activity and as Na^+/Ca^{2+} exchange would be expected to be at low activity in low-Na^+ medium, these findings suggest that 2.5μM V and 2μM N are fully effective in Ca^{2+}-channel blockade. Therefore the higher concentrations of Ca^{2+} blockers needed to inhibit the veratridine-induced increase in $[Ca^{2+}]c$ and O_2-uptake imply that these processes depend largely (approx. 60%) on Na^+/Ca^{2+} exchange.

M-Pos266 ELECTROPHARMACOLOGICAL EVIDENCE FOR A NONEXTRACELLULAR ADENOSINE RECEPTOR IN RAT HEART
John Bianchi, John D. Gallagher, and Rafael Rubio*. Deborah Research Institute, Browns Mills, NJ and *University of Virginia, Charlottesville, VA

Studies of the effect of adenosine (ADO) in heart have also included dipyridamole (DIP) or nitrobenzylthioinosine (NBMPR) to block ADO transport. As ADO is transported by a facilitated mechanism down a biochemical gradient, ADO blockade and exogenous ADO (10^{-6}M) will enhance intracellular as well as extracellular ADO. To investigate possible intracellular ADO effects, rat atrium was superfused in Krebs-Henseleit buffer and action potentials were recorded. Superfusate included adenosine deaminase (ADA), ADA + NBMPR (10^{-6}M) [I], or ADA + NBMPR + homocysteine thiolactone (hCys,10^{-6}M [II] which crosses cell membranes and lowers intracellular free ADO by chemical conjugation. ADO alone shortened action potential duration (APD). Addition of ADA restored APD to control. Over time, ADA + NBMPR shortened APD during normoxia or hypoxia, whereas hCys reversed this response but alone had no effect. Results are summarized (control APD_{50} = 30.6 ± 0.8, APD_{90} = 78.3 ± 1.0:

	ADO	ADA	I	II
APD_{50}	15.3±0.6	27.6±0.8	13.5±0.6*	29.4±0.6
APD_{90}	47.1±0.9	103.5±1.5	58.2±1.0*	89.4±0.8

[mean ± SEM; 5 studies; *p<0.001 v. control]

These studies suggest the existence of a nonextracellular ADO receptor which can mediate some ADO effects.

M-Pos267 **SODIUM AND INTRACELLULAR pH DEPENDENCE OF I_{K1} CONDUCTANCE**
Robert E. Ten Eick, Edward J. Cragoe Jr. and Robert D. Harvey (Intr. by R. Novak)
Department of Pharmacology, Northwestern University, Chicago, IL 60611

The conductance of the inward-rectifying K^+ current (I_{K1}) in isolated cat ventricular myocytes is decreased by reducing the extracellular Na^+ concentration. Using a whole cell patch clamp technique, possible mechanisms underlying this effect of Na^+ were investigated. Possible explanations included: 1) block of inward K^+ current by the Na^+ substitute; 2) changes in membrane surface charge associated with removal of extracellular Na^+; 3) increases of intracellular Ca^{+2} due to suppression of Na-Ca exchange; 4) reduction of a Na^+-dependent K^+ conductance due to a subsequent decrease of intracellular Na^+; 5) reduction of I_{K1} conductance (g_{K1}) associated with reduction of intracellular pH due to suppression of Na-proton exchange. The findings support the hypothesis that the effect of removing Na^+ is mediated through a decrease in intracellular pH. These include observations that: 1) reducing internal pH by reducing external pH causes a decrease in g_{K1}, and recovery from this acidification requires extracellular Na^+; 2) the effect of reducing pH_o is attenuated by dialyzing with a low pH internal solution; 3) g_{K1} is reduced by exposure to the Na-proton exchange inhibitor dimethylamiloride, and this effect is absent in the absence of Na^+. The results did not support the other hypotheses. These findings imply that physiological or pathological processes such as ischemia and metabolic or respiratory acidosis which can produce intracellular acidosis should be expected to effect permeation through the I_{K1} channel.

M-Pos268 SPONTANEOUS LOSS OF INACTIVATION IN RAT NEONATAL HEART CELLS STUDIED USING THE WHOLE CELL VOLTAGE CLAMP TECHNIQUE.
L. Ebihara, C. Jeck, Department of Pharmacology, Columbia University, College of Physicians and Surgeons, New York, NY 10032.

Sodium currents in rat neonatal heart cells were studied at 22°C using the patch electrode whole cell recording technique. We observed a progressive, spontaneous loss of inactivation of the sodium current 15-20 minutes after disrupting the cell membrane. This process involved a slowing of inactivation rather than the complete removal of inactivation. It was associated with a shift in inactivation and activation parameters of the sodium current to more negative potentials. When the temperature was raised to 36°C, the slowing of inactivation as well as the time dependent shifts in inactivation and activation were greatly accelerated. Slowing of inactivation frequently became discernable within less than 1 minute after entering the cytoplasmic compartment. Substitution of KF, CsCl or K aspartate for CsF in the pipette failed to prevent loss of inactivation. The inclusion of agents that promote enzymatic phosphorylation such as ATP and creatinine phosphate were also without effect. However, we observed that the amount of leakage current and the rate of exchange of the pipette solution with the cell interior seemed to influence this process. When the sodium current at 36°C was studied under conditions which minimized the slowing of inactivation, the decay of the sodium current followed a monoexponential time course at all potentials. Supported by NIH grants HL28223 and HL 28958.

M-Pos269 Calculation of Time Constants for Intracellular Diffusion in Whole Cell Patch Clamp Configuration. C. Oliva, I. Cohen, & R. Mathias. Physiology & Biophysics, SUNY Stony Brook, NY 11794.

The patch clamp technique with internal perfusion has been widely employed to study the effects of alterations in intracellular milieu. We have modelled this internal perfusion process by making a number of simplifying assumptions, and solving, numerically, the one-dimensional diffusion equation. In our model, substances diffuse into the cell from a perfusion point which is located in the pipette, and close to the tip. No conduction or convection occurs. Results of our model for pipettes with tips of two different shapes, cylindrical and conical, will be presented. In both cases, key variables determining the time constant to achieve a steady state are the geometry of the pipette and the cell volume. The effect of the tip geometry can be related to the pipette electrical resistance. Thus, for a 2 MΩ pipette, and a rectangular parallelepiped canine cardiac Purkinje cell of 30 um in height and width and 180 um in length, the perfusion process, for a substance with a diffusion coefficient of 10^{-5} cm^2/sec, would have a time constant of about 5 min. We derived an approximate expression for the final time constant to achieve steady state by examining the small s series expansion of the Laplace Transform of the average intracellular concentration. We found this time constant, for both a cylindrical and a conical pipette, to be: $\tau = V R / D \rho$. Where V is the cell volume, R is the pipette resistance between the point of perfusion and the pipette tip, D is the diffusion constant of the substance, and ρ is the resistivity of the pipette filling solution. This final time constant is in good agreement with numerical calculations. Supported by NIH grants EY06391, HL36075, HL20558, PPG HL28958.

M-Pos270 Na/K PUMP CURRENT ELICITED BY REPETITIVE ACTIVATION OF I_{Ca}. F.Chang and I.Cohen. Dept. of Physiology & Biophysics, HSC, SUNY at Stony Brook, Stony Brook, NY 11794.

A two microelectrode voltage clamp technique was applied to canine Purkinje strands of short length (<1.5mm) and narrow radius (<0.15mm).Repetitive activation of the calcium current was achieved by applying trains of depolarizing voltage clamp pulses, (pulse duration 50 to 250 msec and frequency 2.5 to 10 Hz) from -40 to 0 mv. A 2 minute long train of depolarizing pulses in Tyrode containing 2 mM Ca^{2+} was followed by a slowly decaying outward current that was blocked by Dihydrooubain (10^{-4}M) or eliminated by D600. Reducing external Ca^{2+} to 0.1 mM dramatically reduced this post-drive Na/K pump current. Substitution of 2 mM Sr^{2+} for Ca^{2+} reduced the post-drive current, while substitution of 2 mM Ba^{2+} for Ca^{2+} eliminated it. Addition of Ba^{2+} to 2 mM calcium Tyrode had no effect. We further examined the dependence of the post-drive current on clamp membrane potential during the train with a two pulse protocol. Increasing the amplitude of the second pulse following a 50 msec depolarizing pulse reduced the post-drive current, while applying a hyperpolarizing pulse following the depolarizing pulse increased post-drive current. Control experiments demostrate that recovery from inactivation of I_{Ca} was unlikely to be responsible for this voltage dependence. Instead these results suggest that repetitive activation of I_{Ca} can result in a Na^+ load through Na:Ca exchange which generates a post-drive Na/K pump current. Supported by HL 20558 and PPG HL 28958.

M-Pos271 $[Ca^{2+}]_i$ in ventricular muscle fibers. Effects of hypoxia. López, J. R., Sánchez, V., Linares, N., Cordóvez, G. Centro de Biofísica y Bioquímica, Instituto Venezolano de Investigaciones Científicas Apdo. 21827 Caracas, Venezuela.

Cellular damage due to hypoxia has been attributed to different factors, but the precise sequence of events has not been resolved. One possible mechanism of hypoxic injury is calcium overload, due to an increase in Ca^{2+} influx and/or release of Ca^{2+} from intracellular stores. We have measured the intracellular free calcium concentration ($[Ca^{2+}]$) by means of calcium selective microelectrodes in cardiac muscle cells isolated from the left ventricle under different experimental conditions. The calcium selective microelectrodes were prepared and calibrated as has been described previously (López et al, Biophys. J. 43:1, 1983). Hypoxia was induced by equilibrating the Tyrode solution with 98% N_2/5% CO_2 (PO_2 about 4-7 mm Hg). The intracellular resting free $[Ca^{2+}]$ was 0.12 ± 0.01 μM (M ± SEM) in non hypoxic muscle cells. In hypoxic cells, the $[Ca^{2+}]_i$ remained in the control range during the initial 8-10 minutes. However, it reached a new concentration of 0.26 ± 0.02 μM (M ± SEM) after 10-12 minutes. The results of this study show that hypoxia in ventricular muscle cells induces a small but, significant increase in intracellular free $[Ca^{2+}]$. The fact that we could revert the change in $[Ca^{2+}]_i$ by re-oxygenation shows that the increase in myoplasmic $[Ca^{2+}]$ precedes the loss of plasma membrane structural integrity. (Supported by CONICIT S1-1277, Muscular Dystrophy Association, and Elmor of Venezuela).

M-Pos272 ELECTROPHYSIOLOGICAL INFLUENCE OF THYROID STATE ON ISOLATED CARDIAC VENTRICULAR MYOCYTES. James P. Morgan, G. Maurice Briggs, and Judith K. Gwathmey. Dept. of Medicine and Cardiovascular Division, Harvard Medical School and Beth Israel Hospital, Boston, MA 02215.

The isolated cardiac myocyte is a valuable model for studying cardiac function. It is of interest to know if the myocyte directly reflects changes in the physiological state of the animal. To investigate this we produced a hyperthyroid condition in ferrets with injections of thyroxine. Myocytes were then enzymatically isolated from both hyperthyroid and euthyroid animals. Myocytes were stimulated at 1 Hz and 37°C and action potentials were recorded using standard intracellular techniques. There was no significant difference in the resting membrane potential (-82 ± 1 vs -83 ± 1 mV) or action potential amplitude (97 ± 5 vs 102 ± 4 mV). However the action potential duration was significantly less in the hyperthyroid myocytes (172 ± 5 vs 211 ± 7 ms). The hyperthyroid myocytes also developed delayed afterdepolarizations and triggered automaticity while the control mycoytes did not even at stimulation rates up to 4 Hz. We conclude that electrophysiological changes observed in the isolated cardiac myocyte of hyperthyroid animals directly reflect the hyperthyroid condition. Further, this predisposes hyperthyroid animals to triggreed arrhythmias. Supported by HL39091, HL31117, HL01611, grant in aid and fellowship from the American Heart Association, Massachusetts affiliate.

M-Pos273 MECHANISM OF ATP-INDUCED INCREASE IN INTRACELLULAR Ca^{2+} CONCENTRATION IN RAT CARDIAC MYOCYTES. A. Christie and S-S. Sheu, Dept. of Pharmacol., U. of Roch., Rochester, NY 14642.

Exogenous ATP causes perturbation of membrane permeability in many cell types by an unknown mechanism. We have shown that extracellularly applied ATP increases cytosolic Ca^{2+} concentration ($[Ca^{2+}]_i$) in isolated rat ventricular myocytes (Biophys J 49:351a). Using the Ca^{2+} indicator quin-2, we investigated the mechanism by which ATP increases $[Ca^{2+}]_i$. As shown, treatment with the slowly hydrolyzable ATP analog, α,β-methyleneadenosine 5'-triphosphate (AMP-CPP, 100 μM) causes a slow rise in $[Ca^{2+}]_i$ and prevents a subsequent ATP-induced increase in $[Ca^{2+}]_i$. Conversely, treatment with a nonhydrolyzable ATP analog, β,γ-methyleneadenosine 5'-triphosphate (AMP-PCP, 100 μM) did not affect resting $[Ca^{2+}]_i$ or inhibit a subsequent ATP-induced increase in $[Ca^{2+}]_i$. The requirement of a hydrolyzable terminal phosphate group gives some evidence that a kinase is involved. Subsequent experiments have shown that the Ca^{2+} response is Mg^{2+} dependent and that selective phosphorylation of several extracellular membrane-bound proteins occurs. We hypothesize that ATP increases $[Ca^{2+}]_i$ by serving as a substrate for a kinase which phosphorylates an extracellular membrane-bound protein(s) thereby increasing sarcolemmal permeability to Ca^{2+}.

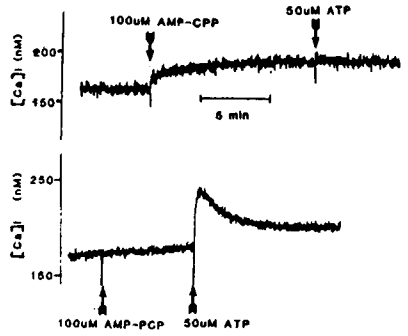

M-Pos274 IDENTIFICATION OF TWO TIME-DEPENDENT COMPONENTS OF "SLOWLY-INACTIVATING" SODIUM CURRENT IN CANINE CARDIAC PURKINJE FIBERS. Gary A. Gintant, Masonic Medical Research Lab., Utica, NY 13501

Previous studies have demonstrated a slowly decaying inward current in cardiac Purkinje fibers (potential range -70 to 0 mV) which lasts seconds after the initial fast sodium current, is blocked by tetrodotoxin (TTX), and has been interpreted as a "slowly-inactivating" sodium current. This slow sodium current was further characterized using shortened (<1.25 mm) canine cardiac Purkinje fibers and a two microelectrode voltage clamp technique (35-37°C). Slow sodium current was assessed as the difference in membrane current (after the initial sodium spike) during 10 sec test pulses in the absence and presence of a maximal TTX conc. ($3x10^{-5}$ M). Slow sodium current could be separated into an earlier rapid component (≅ 1 sec duration), a later slower component well described as an exponential (tau ≅ 3 sec), and a constant. The amplitude of the second time-dependent component increased with stronger depolarizations (test pulse range -60 to -20 mV) while its time constant remained largely unaffected. Hyperpolarizing prepulses (10-20 mV, 1 sec duration, holding pot. -70 mV) applied immediately prior to test pulses increased the amplitude of the first component, but had no effect on either the amplitude or time constant of the second component. Depolarizing prepulses (5-10 mV) diminished the first component, but had no effect on the second component. Lithium substitution for sodium diminished the amplitude of the second component (10-15%) without altering its kinetics. These observations suggest that the slow sodium current consists of at least two time-dependent components. The second (slower component) is activated even when the fast sodium spike and the first component of slow sodium current is greatly reduced, and may affect excitability of depressed cardiac fibers.

M-Pos275 EFFECTS OF METABOLIC SUBSTRATES ON INTRACELLULAR pH IN FERRET VENTRICLE. L.A. Blatter, Dept. of Pharmacol., Mayo Foundation, Rochester, MN 55905, and J.A.S. McGuigan, Physiol. Inst., Universität Bern, Switzerland (Intr. by J.S. Shiner, Physiol. Inst., Universität Bern, Switzerland)

Since metabolic substrates as well as intracellular pH (pH_i) can influence the performance of the heart, we investigated the connection between different metabolic substrates and pH_i in right ventricular trabeculae and papillary muscles of adult ferrets. pH_i measurements were made by single barrelled liquid membrane ion-selective microelectrodes based on a neutral ion carrier (Ammann et al., Anal. Chem. 53, 2267-2269, 1981) at 25° C. In Tyrode solution (composition in mmol/l: Na 155, K 5, Ca 5.4, Mg 0.5, Cl 164.5, Hepes 5; pH 7.4) containing pyruvate (5 mmol/l), solution P, the mean pH_i was 7.32 ± S.D. 0.12 (n=51) and the average membrane potential was -77.8 mV ± 4.4 mV. Upon changes to Tyrode with glucose (5 mmol/l), solution G, or substrate-free Tyrode (SF) pH_i changed to 7.46 ± 0.13 (n=32) and 7.45 ± 0.16 (n=24) respectively. Changes from P to G caused a reversible intracellular alkalinization as did changes from P to SF. The ΔpH_i changes were: P → G +0.15 (n=19) G → P -0.12 (n=18), P → SF +0.17 (n=13), SF → P -0.13 (n=12), G → SF +0.07 (n=10), SF → G -0.11 (n=9). Preliminary results show that the acidification on changing from glucose to pyruvate can be reduced by α-cyano-4-hydroxycinnamate. These findings would be consistent with carrier-mediated membrane transport for pyruvate coupled to cotransport of H^+-ions and/or countertransport of OH^--ions (de Hemptinne et al., Am. J. Physiol. 245, C178-C183, 1983).

M-Pos276 SIALIC ACID RESIDUES AND SURFACE CHARGE MODULATION OF I_f IN CULTURED PACEMAKER CELLS FROM RABBIT SINOATRIAL NODE. Bernard Fermini and Richard D. Nathan. Department of Physiology, Texas Tech University Health Sciences Center, Lubbock, TX 79430.

We tested the hypothesis that sialic acid (NANA) constitutes much of the negative surface charge that is functionally associated with hyperpolarization-activated channels in single (Type II) pacemaker cells. A highly purified preparation of neuraminidase (Sigma Type X) was used to remove (an estimated) 85% of the surface NANA from cells after periods of 3-7 days in culture. Activation-voltage relationships for I_f were determined from normalized current tails that were elicited at -60 mV and that followed 10-sec voltage steps between -70 and -140 mV. External $[K^+]$ was 5.4 mM and $[Ca^{2+}]$ was 1.8 mM. Within 35 min of rupturing the patch, the half-activation potential ($V_{1/2}$) had shifted to more negative potentials in 2 cells and to less negative potentials in 2 other cells. Because of such "run down," I_f was measured, in different populations of cells for different conditions, just after initiating the whole-cell clamp. Incubation of cells with neuraminidase (1.0 U/ml for 1 hr at 37°C) failed to affect $V_{1/2}$ or the Boltzmann equation slope factor (k) significantly. The mean (±SEM) $V_{1/2}$ and k for 5 controls were -84.9 ± 4.6 mV and 10.4 ± 2.3 mV, whereas the corresponding values for 9 cells treated with neuraminidase were -79.0 ± 2.0 mV and 8.5 ± 0.8 mV. Our results suggest that sialic acid residues are not responsible for the surface charge that is associated with the modulation of I_f in these pacemaker cells. Supported by NIH grant HL 20708. Dr. Fermini holds a fellowship from the Canadian Heart Foundation.

M-Pos277 INVESTIGATIONS OF THE INOTROPIC MECHANISMS OF NON-TOXIC AND TOXIC DOSES OF OUABAIN IN ISOLATED ADULT VENTRICULAR MYOCYTES. M. Horackova, Dept. of Physiology and Biophysics, Medical School, Dalhousie University, Halifax, N.S. Canada B3H 4H7.

We used enzymatically dissociated rat ventricular myocytes to study $^{45}Ca^{2+}$ transport in the presence of ouabain (10 nM, 1μM, and 100 μM) in Tyrode solution containing 1 mM $CaCl_2$. The $^{45}Ca^{2+}$ content in suspensions of quiescent dissociated myocytes was determined by Millipore filtration technique described previously (Desilets and Horackova, BBA 721:144-157, 1982). During $^{45}Ca^{2+}$ uptake and $^{45}Ca^{2+}$ efflux experiments, 10 nM ouabain decreased Ca^{2+} content, 1 μM didn't change it appreciably, and 100 μM increased it significantly. Qualitatively the same results were obtained at 22°C and 35°C. Furthermore, we studied ouabain's effects on electrical and contractile activities in the superfused myocytes. Ouabain did not significantly affect the electrical activity of isolated, electrically stimulated myocytes, but it increased the contractility, i.e. the amplitude of the shortenings of these myocytes in a dose-dependent manner. Thus, the positive inotropic (contractropic) effect of ouabain at therapeutic doses (≤10 nM) occured in spite of decreased Ca^{2+} content, while at high toxic doses the positive inotropic effect was accompanied by an increment in Ca^{2+} content. These data support the hypothesis that the mechanisms of positive inotropy of ouabain are different at therapeutic and toxic concentrations of this drug and that inhibition of Na^+-K^+ pump may not be responsible for the increased contractility at therapeutic concentrations. Supported by MRC Canada and Nova Scotia Heart Foundation.

M-Pos278 STUDIES OF DIABETIC CARDIOMYOPATHY IN ISOLATED ADULT RAT VENTRICULAR MYOCYTES. M. Horackova and S. Mullen (Intr. by A.Y.K Wong) Dept. of Physiology and Biophysics, Medical School, Dalhousie University, Halifax, N.S. Canada B3H 4H7.

The effects of chronic experimental diabetes on electrophysiological properties, contractile behavior, $^{45}Ca^{2+}$ transport and ultrastructural characteristics were studied in enzymatically dissociated ventricular myocytes. Diabetes was induced in adult rats by an intravenous administration of streptozotocin (55 mg/kg) and animals were killed 8-10 weeks later. Myocytes from diabetic rats exhibited electrical behavior similar to that of myocytes from control rats, but their contractile properties were altered. Their sensitivity of the twitch contractions to various positive and negative inotropic agents (isoproterenol, norepinephrine, phenylephrine, acetylcholine, ouabain and veratridine) was greatly diminished. However, a part of the contractile responses (the tonic "sustained" contractions) were increased in the diabetic myocytes, indicating that the myopathic changes are not caused by a decreased sensitivity of myofilaments. The contractions (shortenings) were recorded by a video system. Furthermore, the diabetic myocytes also exhibited a significant decrease in total Ca^{2+} content, as determined by $^{45}Ca^{2+}$ flux experiments. The ultrastructure of the diabetic myocytes was affected only slightly, without any serious degenerative changes. These investigations offer for the first time a comprehensive picture of changes related to diabetic cardiomyopathy as they occur at the level of cardiomyocytes. Supported by grants from MRC Canada (MT-4128) and Nova Scotia Heart Foundation to Dr. M. Horackova.

M-Pos279 PERSISTENT ACTIVATION OF I_{ACh} by ATP-γ-S IN SINGLE ATRIAL CELLS. A.S. Otero, G.E. Breitwieser†, and G. Szabo. University of Texas Medical Branch, Galveston, TX, 77550, and †Johns Hopkins University, Baltimore, MD, 21205.

The effects of intracellular ATP analogs on the K^+ current (I_{ACh}) activated by acetylcholine (ACh) were examined in isolated frog atrial cells using the whole cell patch clamp technique. Intracellular perfusion with high (0.5-2.5 mM) concentrations of adenosine-5'-[γ-thio]triphosphate (ATPγS) caused a slow, receptor-independent activation of I_{ACh}. Application of 1 μM ACh to the bath for a period of 1 minute after 10-15' of perfusion caused a further increase on I_{ACh}. This effect of ACh could not be decreased upon wash-out of agonist. Intracellular perfusion with 0.1 mM ATPγS did not elicit spontaneous activation of I_{ACh}. However, application of ACh after 5' of perfusion produced a small, persistent I_{ACh} (8.6%). After 10' of perfusion, 57% of the ACh-induced current was resistant to wash-out. When the pipette contained 0.1 mM ATPγS and 1 mM GTP the effects of ATPγS were abolished; on the other hand, perfusion of cells with 0.1 mM ATPγS + 0.5 mM GDP enhanced the effect of ATPγS, producing 73% persistent activation after 5'. Adenylimidodiphosphate (AppNHp; 2 mM) had not detectable effect on I_{ACh}. Thin layer chromatography analysis of two different lots of ATPγS used in these experiments did not reveal contamination by GTPγS. The results suggest that the effect of ATPγS on I_{ACh} may reflect transfer of the thiophosphate group to GDP, catalyzed by intracellular enzymes. Formation of GTPγS under these conditions would then lead to activation of I_{ACh} via the GTP-binding protein which links muscarinic ACh receptors to a K^+ channel in frog atrial cells. This work was supported by NIH grant HL37127 to G.S. and AHA-TX to A.O..

M-Pos280 EFFECTS OF NOREPINEPHRINE ON INTRACELLULAR SODIUM ACTIVITY AND MEMBRANE POTENTIAL IN BEATING AND QUIESCENT PURKINJE FIBERS OF SHEEP HEART. D.Y. Wang, Q.Y. Gong and C.O. Lee, Dept. of Physiology, Cornell University Medical College, New York, N.Y. 10021.

The effects of norepinephrine on Na-K pump and i_f in sheep cardiac Purkinje fibers were studied by measuring intracellular sodium activity (a^i_{Na}) and transmembrane potential. The a^i_{Na}, twitch tension, and action potential (or resting membrane potential) were simultaneously measured during exposure of the fibers to norepinephrine ($5x10^{-7}$ - $5x10^{-6}$M) in the presence and absence of strophanthidin (10^{-6} - $5x10^{-6}$M), cesium (2 - 3 mM), and high $[K^+]_o$ (15 - 30 mM). In the beating fibers (1Hz), norepinephrine decreased a^i_{Na} from 8.8±1.1 mM to 8.2±1.0 mM (mean±SD, $P < 0.005$), prolonged the duration of action potential (APD), and hyperpolarized the diastolic membrane potential. Inhibition of Na-K pump by strophanthidin reduced or abolished the decrease in a^i_{Na}, the prolongation of APD, the hyperpolarization of diastolic membrane potential by norepinephrine. In quiescent fibers, however, norepinephrine increased a^i_{Na} from 7.7±1.6 mM to 8.5±1.6 mM (mean±SD, $P < 0.005$), and depolarized the resting membrane potential from 72.8±3.1 mV to 64.0±3.5 mV (mean±SD). The increase of a^i_{Na} and the depolarization of resting membrane potential by norepinephrine were almost abolished by cesium that could block i_f. The changes of a^i_{Na} and resting membrane potential by norepinephrine were also abolished by the high $[K^+]_o$ that depolarized the cell membrane by 20 - 35 mV. The results indicate that norepinephrine stimulates the Na-K pump and increases i_f in sheep cardiac Purkinje fibers. In the beating fibers, the decrease in a^i_{Na} might be due to a dominant effect of norepinephrine on the Na-K pump. In the quiescent fibers, the increase in a^i_{Na} might be due to a dominant effect of norepinephrine on i_f that is voltage-dependent. (Supported by USHPS HL 21136).

M-Pos281 RESTORING FORCES IN RAT CARDIAC MYOCYTES AND ULTRASMALL TRABECULAE

HENK E.D.J. ter Keurs and Tatsuo Iwazumi, University of Calgary, Canada

Restoring forces in cardiac muscle have been proposed to play an important role in the phase of early filling of the beating heart. In order to identify the structures responsible for the the development of restoring forces in cardiac muscle we have used a technique that allows study of the mechanical properties of single cells (Iwazumi T. Bioph. J. 1986;51,479a). Myocytes were isolated from Rat heart, excised under ether anesthesia, by collagenase digestion. Trabeculae consisting of a chain of single cells were dissected manually. Preparations were skinned with Triton-X100 in relaxing solution and attached to a force tranducer and a motor such that a segment of 5 to 10 sarcomeres could be studied. The relation between force and sarcomere length in myocytes, which had a slack length of 1.87 um (SLs) showed small opposing forces (less than 4% of force (Fa) developed upon activation at a pCa = 5.5 and at a SL = 2.0 um) between SLs and SL = 1.60 um. An increase of restoring force at a SL< 1.6 um caused to segments to buckle. Sls in trabeculae was 1.87 um as well. Restoring force increased with decreasing SL < SLs in trabeculae without buckling unless SL was shorter that 1.3 um. At SL = 1.5 um restoring force was 20% of Fa. We conclude that intracellular restoring forces at SL > 1.6 um are small while the large restoring force in trabeculae largely results from the collagen meshwork in the extracellular elastic matrix of myocardium.

M-Pos282 THE FORCE RESPONSE TO SUDDEN LENGTH CHANGES IN RAT MYOCARDIUM

Peter H. Backx and Henk E.D.J. ter Keurs, University of Calgary Canada

To characterize the instantaneous elasticity of cardiac muscle we have developed a method to measure force in response to sudden sarcomere length (SL) changes. Rat cardiac trabeculae were dissected from the right ventricle and studied in a modified Krebs-Henseleit medium. Rapid cooling contractures (RCC) were induced by rapidly changing from K-H medium at 25 C to a Na-free medium (Li=140mM) with a Ca concentration of 10 mM at 5 C. Muscle and SL changes were completed in .25 ms. Force was measured with a silicon strain gauge (freq.resp:10kHz), SL with laser diffraction techniques with a lateral effect photodiode (freq.resp:50kHz). The response to rapid changes of SL consisted of an initial immediate change of force (T1) followed by a slower exponential change (T2). The half time of T2 was 3 ms during the RCC. Rapid transients were studied during the first ten seconds of the RCC. The initial response of force (T1) could clearly be distinguished from the rapid redevelopment of force (T2) during RCC but not during twitches at 25 C. Residual force during T1 was zero at steps of -12nm/sarc.The relation was linear for steps between -8nm/sarc and +6nm/sarc. We conclude that tension transients of rat myocardium during quick changes of SL closely resemble those of skeletal muscle.

M-Pos283 DYNAMIC STIFFNESS MEASUREMENTS OF SINGLE FROG VENTRICULAR HEART CELLS. Leslie Tung, Department of Biomedical Engineering, Johns Hopkins University, Baltimore, MD 21205

A fiber-optic based, ultrasensitive force transducer described previously (Tung, Pflugers Arch 407:109, 1986) has been modified to enable stiffness measurements to be made from single frog ventricular heart cells during the active development of contraction. The transducer was mounted on a piezoelectric bimorph crystal, so that the position of the transducer and consequently the length of the heart cell could be varied. The new optical signal recorded by the transducer now contains force and length components. The two components can be separated by analyzing the equivalent mechanical circuit for the piezoelectric crystal, the force probe and the heart cell, which in the simplest case form a "compliance-divider". Shown below is a recording of a single cell twitch with an 0.9 μm, 200 Hz sinusoidal perturbation applied to the cell length. The length component appears as an oscillation which is superimposed on the slower force component. The reduction in amplitude at the peak of contraction compared to that at rest indicates a rise in cell stiffness. As in intact muscle, stiffness plotted against level of force shows a linear relationship. These measurements of dynamic cell stiffness are potentially applicable to microstructural models of myocardial tissue properties, and for sufficiently small length perturbations, to studies of crossbridge mechanics.

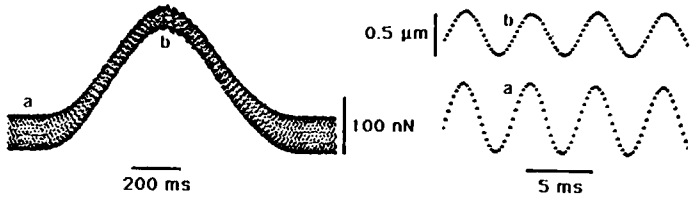

M-Pos284 MOBILITY AND FLUORESCENCE POLARISATION OF TnCDANZ FOLLOWING INJECTION INTO BARNACLE MUSCLE CELLS. P.J. Griffiths, C.C. Ashley & J.D. Potter*. University laboratory of Physiology, Parks Road, Oxford, U.K. *Department of Pharmacology, University of Miami, Miami, Fl.

Dansylaziridine-labelled Ca^{2+}-binding subunit (TnCDANZ) of the regulatory protein, troponin, has been injected into single fibres. Its Ca^{2+}-dependent fluorescence provides an indication of the time course and degree of occupancy of native TnC low affinity Ca^{2+}-binding sites during contraction (Griffiths et al, FEBS letters, 176, 144). However, injected TnCDANZ may bind non-specifically inside the cell or exchange with native TnC over time. The state of added TnCDANZ was studied by injecting TnCDANZ (barnacle type II, mol. wt. 15K) into barnacle muscle fibres ($[TnCDANZ]_i$=70μM). After 24 hours, a myofibrillar bundle was taken from the fibre and illuminated at 325nm. The washout of TnCDANZ was measured as decline in fluorescence at 520nm. The mean diffusion coefficient (D) of TnCDANZ efflux was $0.95X10^{-7}cm^2.s^{-1}$ at 11°C (μ=150mM, n=11). Globular proteins of mol. wt. 15K should have a D value of about $7X10^{-7}cm^2.s^{-1}$ in free solution, but usually have a much smaller value inside a muscle (eg: aequorin). After 40min efflux, less than 5% of initial TnCDANZ load remained in the bundle. Fluorescence polarisation studies of TnCDANZ indicated a limiting polarisation (P_0) of 0.27 and an excited state lifetime of 10.1ns (λ=520nm). After 48 hrs incubation of TnCDANZ-injected fibres at 12°C, TnCDANZ polarisation at 20°C was 0.123± 0.032; in free solution it was 0.133. At 520nm, TnCDANZ accounted for 76-93% of total fluorescence of injected fibres (polarisation of uninjected fibres, 0.223). These findings indicate at least 95% of TnCDANZ injected into a muscle fibre remains unbound up to 48 hrs post-injection. (Supported by the MDA, MRA & NIH AR37701-021).

M-Pos285 CORRESPONDENCE BETWEEN THE FALL IN STIFFNESS, SHORTENING AND A-BAND WIDTH FOLLOWING EXPOSURE OF ISOLATED CARDIAC MYOCYTES TO HIGH SALT. Allan J. Brady, & Kenneth P. Roos. Department of Physiology, UCLA School of Medicine, Los Angeles, CA. 90024-1760.

Exposure of isolated Triton X-100 skinned cardiac myocytes to KCl concentrations greater than 0.17M in relaxing solutions, pH 7.1, results in a decline in stiffness in attached cells, a shortening of unattached cells and a narrowing of the A-bands. The rates of stiffness decline and shortening increase with increased salt concentration. Neither stiffness decline nor shortening is described by a single exponential. Half-times for stiffness decline in KCl solutions (0.19-0.56M) ranged from 2890 to 16 seconds. Half-times for shortening ranged from 1625 to 7 seconds in similar solutions. Stiffness declines to about 10% control and shortening occurs to about 60% initial length (SL = 1.19μm) in all these solutions. A plot of ln half-time vs. ionic strength shows the correspondence of these two processes. A plot of the A-band length data of Higuchi & Ishiwata (Biophys. J. 47:267-275, 1985) superposes well on these data. These data indicate that as the myosin of the A-band is extracted in high salt 1) passive stiffness declines and 2) the unattached cell shortens to about the thin filament length consequent to the loss of A-band material. It is concluded that in the intact cell the cytoskeleton maintains a compressive stress on the myofilament system and that strain in the cytoskeleton is relieved by myofilament extraction. Supported by USPHS HL-30828 (AJB) and HL-29671 (KPR).

M-Pos286 **SARCOMERE DYNAMICS AND UNIFORMITY IN TWITCH CONTRACTIONS OF RAT CARDIAC MYOCYTES.**

Kenneth P. Roos*, A. Christyne Bliton, Mark J. Patton, & Stuart Taylor.
*Cardiovascular Research Laboratory, UCLA School of Medicine, Los Angeles, CA. 90024-1760, and Department of Pharmacology, Mayo Foundation, Rochester, MN. 55905.

Ca^{2+}-tolerant cardiac myocytes, prepared by standard 1% collagenase retrograde coronary perfusion of adult rat hearts, were imaged during electrically induced twitch contractions in 2.0 mM Ca^{2+} with a digital processing and analysis system. 20 to 50 μm square portions (∿¼-½) of a myocyte were projected through a standard visible light microscope objective onto a 128 pixel photodiode matrix array for digital recording. 40 sequential frames were captured at 50 to 175 Hz during an entire twitch contraction for later analysis. Images were digitally processed to enhance and analyze striations as follows: with background subtraction, homomorphic filtering, fast Fourier transforms, gray scale manipulation, convolutions, masking, and false color rendering. Striation spacing from 4-15 contiguous sarcomeres were tracked and objectively measured frame-to-frame throughout the contraction/relaxation cycle. Striation intensity profiles and numerical values were calculated and displayed with each image. We have found that the sarcomeres contract and relax smoothly and homogeneously at close to the same maximum rates (∿3-4 segment lengths/sec). After an initial fast relaxation, there is a longer, slower phase. The relative time course of contraction and relaxation was identical among segments in the cell. However, the absolute sarcomere length and change of length sometimes varied among laterally adjacent groups of sarcomeres. These findings were reproducible among twitches from the same cell. Video recordings will be shown of original and processed images in motion annotated by their histograms and numerical values. Supported by USPHS HL-29671 (KPR); USPHS NS/AM-22369, & NSF DMB-8503964 (ST).

M-Pos287 THE STARLING'S LAW OF THE HEART, MYOCARDIAL LENGTH DEPENDENT ACTIVATION, AND THE TROPONIN-C MOIETY

Arvind Babu and Jagdish Gulati
Division of Cardiology, Albert Einstein College of Medicine, Bronx, NY 10461

Increase in end-diastolic volume orders the performance of the heart as a pump. This property, known widely as the Starling's law of the heart, has a primary physiological basis in the length dependence of the developed tension by the myocardial cells. Here we examine whether troponin-C moiety is the critical length transducer in the muscle cells. From the effects of length on the pCa-force relationships it is known that cardiac muscle has 3 to 5 fold greater sensitivity to length changes (in the 1.4um to 2.4um sarcomere length range) than the skeletal fibers. To see if these differences arose due to the differences in the TnC moiety we studied the activation properties of the cardiac muscle with native-CTnC and STnC. Thin trabeculae from hamster ventricles were used. The pCa-force relationships (20°C; ionic strength 190mM) on the skinned trabeculae were determined at 1.9um and 2.4um lengths, and were found to be separated by 0.13pCa units (pCa50). Next 70-75% of the native CTnC was extracted and replaced with STnC from fast-twitch muscle. The STnC-loaded trabeculae indicated a length dependent separation of only 0.02pCa units. In contrast, the CTnC-loaded trabeculae gave the same response as native myocardium. The results show that the TnC moiety is a critical length sensor in cardiac muscle. We suggest that the length dependence of the order seen in the present study on trabeculae governs the Starling's law of the performance of the heart in the organism, assuming that there is only partial activation (below 50% of the maximum possible level) of the heart during each beat.

M-Pos288 MYOCARDIAL ADAPTATION TO CREATINE DEFICIENCY IN GPA FED RATS. Ventura-Clapier, R.; Mekhfi, H.; Hoerter, J.; Lauer, C.; Legssyer, A. Introduced by A. Shrier.

Functional importance of creatine kinase has been questioned on the basis of the depletion of creatine by feeding poorly metabolized structural analogs of creatine to animals. However, the possibility that adaptative changes take place during the long term feeding has not been eliminated. Effects of creatine depletion on the functional properties of myofilaments have been studied after 5-10 weeks feeding with 1.5% ß-guanidinopropionate (GPA). ^{31}P-NMR of whole rat heart showed phosphocreatine depletion between 50-90% and GPAP accumulation from ≈ 30 to 70 nanomoles/mg Prot. Ventricular hypertrophy was observed in GPA-fed animals due to both decreased body weight and increased ventricular weight ; the ventricular weight to body weight ratio (VW/BW) increased from 2.56 to 3.32. On thin left ventricular fibres, skinned by Triton X100 (1%), the Ca sensitivity was unchanged in GPA-treated rats compared to control paired animals. However, the time constant of isometric tension recovery following a step change in length was significantly increased in GPA-fed rats compared to control. This increase was correlated to the increase in VW/BW. Both hypertrophy and decreased contraction rate were similar to those seen under pressure overload and suggest the possibility of isoenzymic changes in myosin. Thus, creatine depleted rat heart seems to undergo adaptative processes, leading to an improvment in the economy of contraction.

M-Pos289 Direct Evidence of Changes in Myofilament Sensitivity to Ca^{++} During Hypoxia and Reoxygenation in Ferret Papillary Muscles. Roger J. Hajjar, Judith K. Gwathmey. The Beth Israel Hospital and Harvard Medical School, Boston, MA.
Metabolic factors which affect the sensitivity of the myofilaments to calcium and the maximum Ca^{++}-activated tension seem to be the most important contributors to early hypoxic failure. We were interested in examining the changes in myofilament sensitivity during hypoxia and reoxygenation in intact myocardium. In order to produce steady activation in ferret papillary muscles loaded with aequorin, a bioluminescent calcium indicator, we stimulated the muscles at a frequency of 15-20 Hz after exposure to ryanodine, a sarcoplasmic reticulum inhibitor. Steady levels of tension and free intracellular calcium ions ($[Ca^{++}]_i$) were reached and a sigmoidal %Force vs -log($[Ca^{++}]_i$) was constructed. At various stages during hypoxia (5mn, 10mn, and 15mn) and 3mn after reoxygenation steady force and $[Ca^{++}]_i$ were recorded. Force vs $[Ca^{++}]_i$ relation was shifted to the right by 0.11, 0.18, and 0.24 pCa (-log($[Ca^{++}]$) units and down to 66%, 48%, and 67% of maximal force at 5mn, 10mn, and 15mn after start of hypoxia respectively. During reoxygenation, the Force vs $[Ca^{++}]_i$ relation was shifted up by 36%. These changes indicate that during hypoxia, a decrease in the sensitivity of the myofilaments to Ca^{++} and a depression of the maximal Ca^{++}-activated force occur, whereas during reoxygenation there is an increase in the maximal Ca^{++}-activated force. Our results correlate well with the depressant effects on tension development of increases in inorganic phosphate (P_i) and decreases in pH in skinned fiber experiments, which indicate that P_i and pH are probably the most important contributors of contraction failure during hypoxia in mammalian myocardium.
Support: HL39091 and Biomedical Research Grant Beth Israel Hospital.

M-Pos290 ADDITIONAL EVIDENCE THAT BETA ADRENERGIC STIMULATION ENHANCES V_1 ISOMYOSIN IN MYOCARDIUM WITH A MIXED ISOMYOSIN PROFILE. Michael R. Berman, Jon N. Peterson and William C. Hunter. Biomedical Engineering, Johns Hopkins University, Baltimore, MD 21205

Winegrad and colleagues (Circ. Res. 55:565-574, 1984) recently presented biochemical evidence that beta adrenergic stimulation enhances the force generating capabilities of V_1 isomyosin. We present evidence from mechanical studies which is consistent with their observations. Small amplitude sinusoidal length oscillations at several discrete frequencies were applied to rabbit right ventricular papillary muscles in barium contracture. The ratio of and the phase difference between the oscillatory force and length signals at each frequency were used to construct complex stiffness spectra. Amplitude spectra exhibited a minimum at a frequency earlier identified with V_3 isomyosin (Berman et al., Biophys. J. 51:465a, 1987). After addition of 10 uM isoproterenol, a beta adrenergic agonist, some (but not all) spectra showed a striking change: a second minimum appeared in the amplitude spectra, at a frequency (2.7±0.2 Hz, n=4) consistent with that reported (Shibata et al., Circ. Res. 60:770-779, 1987) for V_1 isomyosin. Since rabbit papillary muscle contains mostly V_3 isomyosin, but may contain as much as 20% V_1, we interpret these observations as indicating that beta adrenergic stimulation enhanced the force generating capability of the existing V_1 isomyosin sufficiently so that a V_1 signature appeared in the complex stiffness spectra. It is possible that such pharmacologically induced changes in the "effective" V_1/V_3 ratio might play a role in the moment to moment modulation of contractility in the working myocardium. Supported by RO1-HL38488 (MRB).

M-Pos291 ALTERATIONS IN INTRACELLULAR FREE CALCIUM AND PH DURING GLOBAL ISCHEMIA IN THE ISOLATED PERFUSED RAT HEART. Frank Lattanzio, Jr., Dept. of Pharmacology, Univ. of Nevada School of Medicine, Reno, NV 89557

Isolated rat hearts were perfused with 37° Hepes-Tyrode's and exposed to 2 micromolar indo-1 AM and/or BCECF AM for 30 min to permit monitoring of intracellular free calcium and pH by epicardial fluorescence. Systolic calcium transients were greater than 600 nM with a time averaged intracellular free calcium of approx. 150 nM and an intracellular pH of 7.1 in controls. After initiation of global ischemia, systolic calcium transients ceased and the time-averaged intracellular calcium fell to approx. 30 nM for 10-15 min before increasing, concomitant with contracture. In contrast, intracellular pH decreased rapidly and then reached a plateau at pH 6.0-6.3 after 10-15 min. When reperfusion was started at the onset of contracture, intracellular free calcium rose briefly and then declined with the resumption of cardiac function. However, global ischemia for 30 min evoked an elevated intracellular free calcium and contracture that was maintained upon reperfusion, even after pretreatment with 500 nM nitrendipine. Nitrendipine did reduce the rates of increase in intracellular free calcium and pH during global ischemia. Intracellular pH rapidly returned to control levels upon reperfusion in all cases. These data suggest that blockade of calcium channels may moderate some of the adverse effects of global ischemia, but other systems, such as sodium-proton and sodium-calcium exchange, also increase intracellular free calcium during global ischemia and reperfusion. This research was supported by grants from AHA (Nevada Affiliate), NIH SCOR HL 17651-13 and the Bently Scholar Award.

M-Pos292 THE EFFECT OF GROWTH HORMONE SECRETING TUMORS ON THE Ca^{2+} SENSITIVITY OF RED AND WHITE SKELETAL MUSCLE FROM ADULT RATS. Xiaoping Xu*, J. M. Forrer#, P. M. Best*, & P. J. Bechtel#. Depts. of *Physiology and #Animal Science, University of Illinois, Urbana, Il 61801.

When female Wistar-Furth rats are injected with GH3 cells small tumors are formed which secrete growth hormone (GH) (and other hormones) resulting in large increases in body weight and muscle mass. To determine the effect of the GH3 tumors on muscle function we have measured the pCa-tension relationship of red (soleus) and white (peroneus long. & brev.) muscles. Muscles from adult rats (24mos) were studied after GH3 injected animals weighed 54% more than age matched controls (40% increase in muscle mass). Ca activated tension was recorded from skinned (sarcolemma removed) muscle fibers. Fibers from adult rats were skinned mechanically while those from newborn rat fibers (10d old) were treated with 0.5% Brij to solubilize the sarcolemma. Solutions contained 2mM EGTA, 2mM MgATP, 1mM Mg, 15mM CP, 100mM monovalent cations and MOPS buffer (pH=7 at 20°C), I=0.15. The pCa of the solutions varied from 8 to 4. Fibers from GH3 injected rats with GH3 tumors were more sensitive to Ca than those from control rats. For soleus muscle, the pCa producing 50% of maximal tension (T_{max}) was 5.7 in rats with GH3 tumors and 5.5 in controls. The slope of the pCa-tension curve was the same for both groups (Hill n=2.4). Soleus fibers of newborn rats without tumors were less sensitive to Ca than both adult controls and GH3 tumor rats (pCa=5.1 for 50% T_{max}, n=2.4). For peroneus fibers the pCa at 50% T_{max} shifted from 5.2 to 5.5 after tumor growth while the slope changed from 1.4 to 2.4. The results show that significant changes in Ca sensitivity, and thus in physiological function, occur in muscles undergoing rapid growth induced by GH secreting tumors. Support: NIH AR32062 (PMB), IAES.

M-Pos293 REGULATION OF CROSS BRIDGE CYCLING IN CARDIAC MUSCLE, S. Winegrad, A. Weisberg and S. Weindling. Dept. of Physiology, School of Medicine, University of Pennsylvania, Phila., PA 19104-6085.

The contractile properties of mammalian cardiac muscle are regulated by an adrenergically controlled mechanism. This has been demonstrated by measurements of maximum Ca-activated force in bundles of cells permeabilized with either EGTA or non-ionic detergent and by measurement of Ca and actin activated ATPase in cryostatic sections of quickly frozen hearts. Maximum velocity of unloaded shortening, maximum Ca-activated force, and ATPase activity have been measured under different conditions to determine when in the cross bridge cycle the regulation occurs. Maximum velocity of shortening of hyperpermeable fibers containing only one isozyme of myosin (either V_1 or V_3) is unchanged by beta adrenergic agonists or cAMP even when maximum Ca-activated force has been increased by 150%. Maximum velocity of shortening is increased when both myosin isozymes are present; this is consistent with data already reported indicating a selective positive effect of beta agonists on V_1 force generators. Beta agonists increase Ca-activated myosin ATPase by enhancing substrate binding without altering V_{max} for the enzymatic reaction. In response to beta agonists, V_{max} of actin activated myosin ATPase, however, is increased by 50-100%. These data suggest that the reaction(s) regulated by beta adrenergic stimulation are most likely involved in the binding of the cross bridge to actin or hydrolysis following binding. Measurements of phosphate burst are being carried out to make the distinction (Supported by N.I.H. grants HL 16010 and HL 33294).

M-Pos294 VARIATION IN CONTRACTILE FORCE WITH CROSS-SECTIONAL AREA IN PAPILLARY MUSCLE. L.-E. Lin, G. McClellan and S. Winegrad. Dept. of Physiol., Univ. of Penna., Philadelphia, PA 19104.

Papillary muscles from the right ventricle of rat hearts were dissected in oxygenated Kreb's solution maintained at either 2 to 4°C or at room temperature (18-22°C). The papillary muscles were mounted in oxygenated Kreb's at room temperature and stretched until significant passive tension developed. After mounting, the muscles were skinned with 1% Triton X-100 in 5mM ATP, 3mM EGTA relaxing solution. Maximum calcium activated force was measured in activating solutions with pCa's of 9.0, 5.2, 5.0, and 4.5, and containing 5mM ATP and 15mM creatine phosphate.

Maximum force per unit area depends on cross-sectional area. In papillary muscles maintained at room temperature, this relationship appears to follow a single exponential with forces around 80mN/mm^2 for the small muscles and declining to around 4mN/mm^2 for the large. After exposure to cold, the relationship between force and cross-sectional area is shifted to a lower level with small muscles developing around 40mN/mm^2. This decline in force after "cold shock" can be reversed in about 50% of the papillary muscles by exposing them to 3 X 10^{-7}M isoproterenol in the Kreb's and detergent solutions. When the papillary muscles are superfused for 30 minutes in oxygenated Kreb's before skinning, the maximum force per unit area produced by the small muscles decreases significantly, and the dependence of force on the cross-sectional area is decreased. These results are suggestive of a mechanism that reduces maximum developed force in vitro and is not diffusion limited. This mechanism appears to be related to the one by which beta adrenergic agonists enhance force development by cardiac contractile proteins. (Supported by American Heart Association Grant in Aid.)

M-Pos295 ENHANCEMENT OF LOAD BEARING CAPACITY AFTER LOAD CLAMPS IN SINGLE SKINNED CARDIAC CELLS. Nora M. De Clerck and Dirk L. Brutsaert, University of Antwerp, Antwerp, Belgium.

The effects of changing isometric versus isotonic loading conditions on the load bearing capacity were studied in single skinned (mechanical dissection + Brij-58 treatment) rat cardiac cells (n= 65; room temperature). As these cells were deprived of all membranous systems, any contribution of the excitation-contraction coupling mechanism could be outruled. All experiments were performed under steady state activation by solutions with a set concentration of free calcium.

When during steady isometric contraction, the cell was unloaded to preload and subsequently re-loaded to full isometric conditions, an enhancement of active isometric force was observed. Similarly, in steady afterloaded contractions, an unloading and re-loading step induced an increased shortening level of the cell. The amount of increase in contractile activity did not correlate with the amplitude or duration of the clamp; it was not affected by the skinning procedure, by changing the initial sarcomere length (1.9-2.4 μm) before contraction or by activating with different concentrations of free calcium (pCa 4.5-6). The present enhancement of contractile activity might be attributed to different steady states of the crossbridges, during a constant level of steady state activation.

M-Pos296 DOES AXIAL STRESS ON THICK FILAMENTS INDUCE AN ACTIVE PROCESS WITHOUT CA^{++}? T. Iwazumi Dept. of Medical Physiology, University of Calgary, Calgary, Alberta, Canada T2N 4N1

Single cardiac myocytes were axially compressed by utilizing a new mounting method which allowed a very short segment of the myocyte (about 5 sarcomere long) to be securely mounted between length control and force transducers (Iwazumi, Biophys. J. 51; 479a), and their elastic properties were measured up to 50 KHz. The stiffness spectrum of the passive myocyte showed monotonical increase with frequency for the most part of the sarcomere lengths from 1.6 μm to 2.5 μm. However, abrupt changes of the spectral shape occured at three different sarcomere lengths. Among them the most interesting was the one at the buckling point less than 1.6 μm. The stiffness spectrum of slightly buckled myocytes showed the shape identical to that of isometrically contracting myocytes (a sharp trough at about 20 Hz, a broad peak at above 100 Hz, and another broad trough at about 800 Hz) and when the myocyte was activated at the same length, the spectrum shifted upward (i.e., stiffer) without changing the shape. Therefore, it seems likely that axially compressed thick filaments were in an active state without Ca^{++} thus sarcomeres could not return to the rest length after removal of Ca^{++}. The latched sarcomeres could be returned to the rest length only after they were forcefully stretched. The force required to unlatch the myocyte was about ^.1 mg weight.

M-Pos297 CONTRACTILE DYNAMICS OF RAT SKELETAL MYOCYTES MEASURED BY HIGH-SPEED DIGITAL IMAGING MICROSCOPY. Martha L. Rolli, Laurel A. Wanek, and Stuart Taylor. Department of Pharmacology, Mayo Foundation, Rochester, MN 55905.

We studied microscopic contractile behavior of rat skeletal muscle in primary cell culture with an immersion objective lens, incoherent light, a self-scanning quartz-windowed silicon photodiode area array, and high-speed digital capture, storage and processing of images. Photographic film or TV image detection systems do not provide the equivalent features of wide dynamic range (12 bits), speed (partial frame rates of 300 Hz or greater), and image manipulation. Thigh muscles were removed from 1-3 day old pups, dissociated, and plated in sterile, untreated dishes with polystyrene or Teflon bottoms. We used no chemicals to select for non-myogenic cells (i.e., to inhibit growth, metabolism, proliferation, or induce myoblast fusion). It is well known that contraction can occur in long, branching, striated cells (myotubes) as well as round or spherical aggregates of myoblasts (myosacs; myoballs). Electrophysiological studies are usually carried out on only a fraction of cells from such cultures. We compared myotubes and myoballs with intermediate types of myocytes that co-exist in a given culture dish. Starting at about 3 days we observed two types of spontaneous contraction, slow reversible blebbing and rapid local twitching. The same cells contracted rapidly and more uniformly when impaled by an intracellular microelectrode or when stimulated by current injected via the electrode. Contraction was reversibly increased by increasing stimulus strength or duration. Increased external $[K^+]$ also caused contraction. Homomorphic filtering and edge enhancement allowed objects to be followed in complete cycles of contraction/relaxation. Video recordings of original and processed images of myocytes in motion will be shown. Supported by USPHS NS-22369, NSF DMB-8503964 and a Research Center Grant from the MDA.

M-Pos298 INTER-FIBER AND INTRA-FIBER DIFFERENCES IN MAXIMUM SPEED OF SHORTENING CORRELATED WITH MYOSIN ISOFORM COMPOSITION IN FROG MUSCLE. K.A.P. Edman and C. Reggiani, Department of Pharmacology, University of Lund, S-223 62 Lund, Sweden.

The velocity of shortening at zero load (V_0) was determined in single fibers of the anterior tibialis muscle of R. temporaria using the slack test method (Edman, J. Physiol. 1979. 291:143-159). V_0 was also measured in short (ca. 0.5 mm), consecutive segments along the intact fiber by recording the relative position of markers on the fibre surface during isotonic shortening near zero load (Edman & Reggiani, J. Physiol. 1984. 351:143-159). There was a considerable variation of V_0 among individual twitch fibers. V_0 of the single fibers was linearly related to the myofibrillar ATPase activity determined in the same fibers. Our original observation (J. Physiol. 1985. 365:147-163) that V_0 varies along the length of a muscle fiber was confirmed. The segmental differences of V_0 were found to be proportional to the myofibrillar ATPase activity in the same fiber segments.

The isomyosin composition of the fibers was studied by incubating transverse sections of the fibers with two monoclonal antibodies (A1 and A2) raised against the myosin heavy chains. The intensity of antibody staining (horse radish peroxidase reaction) was determined spectrophotometrically. Staining intensity with A2 varied in direct proportion to V_0 whereas staining with A1 was inversely related to V_0 in the individual fibers. These results show that at least two different isomyosins (with respect to the heavy chain composition) coexist in frog muscle fibers, V_0 being determined by the ratio of these isomyosins in the fiber. Substantial differences in the relative intensity of staining of A1 and A2 were observed along the length of individual muscle fibers. Such variation in isomyosin composition is likely to contribute to the segmental differences in V_0 within a fiber.

M-Pos299 CONCANAVALIN A BINDING TO MUSCLE MYOFIBRILS. L. J. Mundschau and M. L. Greaser, Muscle Biology Laboratory, University of Wisconsin, Madison, WI 53706

Concanavalin A (Con A) is a lectin which binds specifically to glycoproteins having alpha D glucose or alpha D mannose residues. A fluorescein isothiocyanate derivative of Con A (Con A-F) has been used to stain rabbit psoas myofibrils. Strongest staining occurred in two perpendicular zones in the A band, each approximately 0.2 μm from the M line. The Z lines and the entire A bands also stain but with less intensity. The spacing of the Con A-F staining in the A band did not appear to be affected by sarcomere length in the range of 2.0 to 3.0 μm. The staining patterns were not markedly affected by the method of fixation (i.e. 0.1% glutaraldehyde, methanol at -20°C, acetone at -20°C, 1% formaldehyde, or 3.7% formaldehyde). Myofibrils extracted with KI had brightly stained Z lines with some weak staining of the filamentous material between them. Myofibrils whose A bands had been partially removed using Hasselbach-Schneider solution also showed increase Z line fluorescence as well as staining at the ends of the I filaments. Formamide extraction removed the Z lines and also the Con A-F staining in the same region. Although the protein constituent(s) involved in Con A binding have not been determined, the translocation of staining sites with different protein extractants is similar to that found previously using antibodies against titin. Supported by NIH-HL 32938.

M-Pos300 CHARACTERISTICS OF A MODIFIED CARDIAC HMM

S.S. Margossian, J. Lefford and H.S. Slayter, Montefiore Medical Center, Bronx, New York, 10467 and Dana-Farber Cancer Institute, Boston, MA 02115

Dog cardiac myosin was digested with trypsin and alpha-chymotrypsin in efforts to obtain a homogeneous preparation of cardiac HMM. The digestions were performed as a function of protease concentration, pH, nucleotides, divalent cations and temperature. Under all conditions used, the tryptic HMM had the heavy chains cleaved into two fragments migrating with a mobility corresponding to M_r of 65kDa and 50kDa respectively. At pH 8-8.5, the heavy chains were somewhat protected; a 130kDa band was still present in addition to the two smaller, 65kDa and 50kDa pieces. On the other hand, chymotryptic digestion produced an HMM with the heavy chains split into a doublet of M_r's about 130kDa and 120kDa. Higher pH protected the heavy chains from hydrolysis. The presence or absence of divalent cations or of ATP did not alter the pattern of tryptic digestion. The purified subfragment migrated as a single peak during sedimentation velocity and had an M_r of 320kDa calculated from sedimentation equilibrium data. Electron microscopy showed it to consist of two globular heads attached to a tail about 38 nm long. It was enzymatically active and could bind to actin. The neutral protease from myopathic hamsters removed the residual LC2 totally and the modified, LC2-deficient HMM reassociated with stoichiometric amounts of isolated LC2. Thus, a new HMM was produced with a clipped tail, lacking the hinge region and nicked heavy chains that were held together through non-covalent interactions under non-denaturing conditions. (Supported by NIH grant HL 26569 to SSM).

M-Pos301 PROBING THE SUBSTRUCTURE OF CARDIAC S1 BY TRYPSIN AND IDENTIFICATION OF LIGHT CHAIN AND ACTIN BINDING SITES

S.S. Margossian, V. Hatcher, W. Stafford and S. Taylor. Montefiore Medical Center, Bronx, NY 10467 and Boston Biomedical Research Institute, Boston, MA 02114.

The substructure of dog and rat cardiac myosin S1 (V_3 and V_1 myosin isoforms respectively) was probed by limited proteolysis using trypsin (S1 to trypsin weight ratio of 1000 to 1). At pH 8.0 and in 0.1 M NaCl, the rate of cleavage of dog S1 heavy chain was significantly higher than that of rat S1. Neither divalent cations nor nucleotides had any effect on the rate. In each instance the end products were three fragments with M_r's of 50kDa, 25kDa and 20kDa. Using ^{125}I-labeled purified LC1, LC2 and actin, their binding region within the S1 substructure was identified by the gel overlay method. Both light chains and actin bound to the 20kDa fragment. In parallel experiments, LMM, rod and S1 from the two myosin isoforms were run on pyrophosphate gels to determine the region within cardiac myosin heavy chains responsible for their differential mobilities on these gels. LMM and rod had identical mobilities, whereas both S1's moved as doublets: the slower-moving band being more intense in dog S1, while the reverse was true for rat S1. Thus, the results suggest that the variations in heavy chains detected by native gels were within the S1 region, a result supported by the different susceptibilities of the two S1's to proteolysis. (Supported by NIH grant HL 26569 to SSM).

M-Pos302 EFFECT OF NUCLEOTIDE STRUCTURE ON CARDIAC MYOSIN S1 TRANSIENT KINETICS. J.H. Hazzard, D.H. Tollin and M.A. Cusanovich, Dept. of Biochemistry, Univ. of AZ, Tucson, AZ 85721.

The transient kinetics of nucleotide binding and hydrolysis by cardiac myosin subfragment 1 (S1) have been measured by stopped-flow for the naturally-occurring nucleotides TTP, CTP, UTP and GTP. The results are compared to those previously obtained for ATP (Hazzard, J.H. and Cusanovich, M.A. (1986) Biochemistry 25, 8141). All four nucleotides are hydrolyzed by cardiac S1, although the observed rate constant for hydrolysis is substantially lower than that for ATP, decreasing in the order ATP>TTP>CTP>UTP>GTP. The magnitude of the characteristic fluorescence enhancement of the S1 observed upon nucleotide binding and hydrolysis varies with nucleotide concentration. The dependence is similar for all nucleotides, with the observed fluorescence enhancement increasing as nucleotide concentration decreases. Thus, although the observed rate constant for binding of TTP, CTP, UTP and GTP to S1 is lower than that for ATP, binding is still fairly rapid as much of this phase of the reaction is occurring in the dead time of the stopped-flow instrument. The amplitudes of the fluorescence enhancement are similar to that for ATP with the exception of the enhancement due to GTP binding, which is only one-third of that observed with ATP. In terms of the dependence of the observed rate constant and of the magnitude of the fluorescence enhancement on nucleotide concentration, the pyrimidine nucleotides have properties more similar to ATP than does the purine nucleotide GTP. This suggests that the substituents on the 6-membered ring are more important in these reactions than is the additional 5-membered ring in the purines. The individual kinetic constants for nucleotide binding and hydrolysis have been determined by computer modeling in an extension of the method used in the previous ATP analysis. These results are presented and discussed in terms of the sensitivity of the S1 active site to nucleotide structure.

M-Pos303 THE COMPLEX FORMED BETWEEN 1-N^6-ETHENOADENOSINE DIPHOSPHATE AND MYOSIN SUBFRAGMENT-1 EXISTS IN TWO CONFORMATIONS. Shwu-Hwa Lin and Herbert C. Cheung, Graduate Program in Biophysical Sciences and Department of Biochemistry, University of Alabama at Birmingham, Birmingham, AL 35294

The emission of the ATP analogue, 1-N^6-ethenoadenosine diphosphate (εADP) decays monoexponentially. When bound to myosin subfragment-1 (S-1), 60 mM KCl, 30 mM TES, pH 7.5 and 26 °C, the decay became biexponential with decay times τ_1 = 24 ns (A_1 = 81%) and τ_2 = ~8.0 ns (A_2 = 19%). We have measured this emission decay over the temperature range 6-26 °C by pulse fluorimetry. The ratio of the amplitudes A_1/A_2 increased from about 2 to 4 with increasing temperature, while τ_1 and τ_2 increased only slightly. The fractional intensities of the two decay components are $f_1 = (A_1\tau_1)/(A_1\tau_1 + A_2\tau_2)$ and $f_2 = (A_2\tau_2)/(A_1\tau_1 + A_2\tau_2)$. A plot of logarithm (f_1/f_2) vs. $1/T$ was linear, yielding a value of $\Delta H° = 16$ kcal-mol^{-1}. These results demonstrate the presence of two populations of the εADP·S-1 complex. The two species are in equilibrium which can be shifted by thermal perturbation. The population that predominates at low temperature has a short decay time (τ_2) whereas the high temperature conformation has a long decay time (τ_1). Supported in part by NIH grant AR 31239

M-Pos304 THE N-TERMINAL SEGMENT OF S-1 AND THE BINDING OF NUCLEOTIDES. Theresa Chen, Jane Liu, and Emil Reisler, Department of Chemistry and Biochemistry and the Molecular Biology Institute, University of California, Los Angeles, CA 90024.

Binding of Mg nucleotides to the active site of myosin subfragment 1 exposes a new site near the N-terminus of myosin for tryptic or subtilisin attack (Hozumi, T., Biochemistry 22, 799-804 (1983); Applegate and Reisler, Biochemistry 23, 4779-4784 (1984); Mornet et al, J. Mol. Biol, 183, 479-489, (1985). Such cleavage causes partial inactivation of S-1 ATPase activities (Hozumi, T., J. Biochem 100, 11-19 (1986). We have now found that after removal of the nucleotides on Penefsky columns, the cleaved S-1 loses all of its ATPast activities. If the nucleotides are added back to the cleaved S-1 and allowed to incubate overnight, the ATPase activities are restored. Yet, the addition of MgATP or MgADP to the cleaved and nucleotide free S-1 prior to its reactivation does not result in the normal enhancement of tryptophan fluorescence. Moreover, MgATP and pyrophosphate do not dissociate the cleaved S-1 from actin. Taken together, our data indicate that the combined effects of proteolytic cleavage of S-1 at its N-terminus segment and the removal of bound nucleotides are to alter the protein-nucleotide interactions. Thus, structural continuity in this part of myosin heavy chain must play an important role in maintaining the native conformation of myosin heads and in particular around the site required for nucleotide binding.

M-Pos305 TOPOGRAPHY OF MYOSIN S1: IDENTIFICATION OF SITES ON THE 25 kDa DOMAIN THAT ARE CLOSE TO SH-1 BY INTRAMOLECULAR CROSSLINKING. Renné Chen Lu & Anna Wong, Dept. of Muscle Res., Boston Biomed Res. Inst. & Dept. of Neurology, Harvard Medical School, Boston, MA 02114

The thiol specific photoactivatable reagent benzophenone iodoacetamide (BPIA) can be selectively incorporated into the most reactive thiol, SH-1, of myosin S1 and upon photolysis an intramolecular crosslink is formed between SH-1 and the N-terminal 25 kDa region of S1. If a Mg^{2+}-nucleotide is present during photolysis, crosslinks can be formed either with the 25 kDa or the central 50 kDa region (Lu et al., PNAS 83 6392, 1986). Comparison of the peptide maps of crosslinked and uncrosslinked S1 heavy chains indicates that the segment located about 12-16 kDa from the N-terminus of the heavy chain can be crosslinked to SH-1 via BPIA independently of the presence of a nucleotide, whereas the segment located 57-60 kDa from the N-terminus can be crosslinked to SH-1 only in the presence of a Mg^{2+}-nucleotide (Sutoh & Lu, Biochemistry, 26, 4511, 1987). To determine more precisely the residues that are close to SH-1, S1 was crosslinked with radioactive BPIA and degraded with proteolytic enzymes. Peptides containing crosslinks were isolated by liquid chromatography and subjected to amino acid sequence analyses. The results show that Glu-88, Asp-89 and Met-92 are the three major sites in the 25 kDa region that are corsslinkable to SH-1, Cys-707, via BPIA. These sites are very near the reactive lysine residue (Lys-83), but relatively remote in the primary structure from the site (Trp-130) where one of the nucleotide analogues binds. This work was supported by N.I.H. grants AR28401 and RR0571.

M-Pos306 THERMAL UNFOLDING & DEGRADATION OF THE 50 kDa DOMAIN DO NOT AFFECT THE PROXIMITY RELATIONSHIP OF THE 25 & 20 kDa DOMAINS. Renné Chen Lu, Anna Wong and Terence Tao, Dept. of Muscle Res., Boston Biomed. Res. Inst., & Dept. of Neurol., Harvard Med. Sch., Boston, MA 02114

Recently Setton & Muhlrad (ABB 235, 411, 1984) and Burke et al. (Biochemistry 26, 1492, 1987) have shown that the 50 kDa region, but not the 25 and 20 kDa regions, becomes susceptible to tryptic cleavage after S1 has been thermally denatured and then renatured by cooling, suggesting that the 25 and 20 kDa regions, but not the 50 kDa region, can refold to their native states. We have used the photocrosslinking and resonance energy transfer techniques to address the question of whether the 25 and 20 kDa regions maintain the same proximity relationships in native S1 as in S1 of which the 50 kDa region has been degraded. Previously we have shown that SH-1 can be crosslinked either to the 25 or the 50 kDa region via benzophenone iodoacetamide (BPIA) (Lu et al., PNAS 83, 1986). We found that degradation of the 50 kDa region does not prevent the crosslinking of SH-1 to the 25 kDa region, nor does a crosslink between the 20 and 25 kDa regions protect the 50 kDa region from degradation. However, the formation of a crosslink between the 20 and the 50 kDa regions prevented the latter from enzymatic degradation after thermal denaturization. Resonance energy transfer measurements show that the distance between the reactive lysine residue (Lys-83) and SH-1 (Cys-707) (Takashi et al., Biochemistry 21, 5661, 1982) remains the same after the degradation of the 50 kDa region. It appears that thermal unfolding and degradation of the 50 kDa region do not greatly disturb the part of S1 structure involving the 25 and 20 kDa regions. Supported by grants from N.I.H. (AR28401, AR21673, and RR0571).

M-Pos307 INTRINSIC FLUORESCENCE STUDIES OF THE UNFOLDING OF RABBIT SKELETAL MYOSIN ROD AND LIGHT MEROMYOSIN (LMM). Lan King and Sherwin S. Lehrer, Department of Muscle Research, Boston Biomedical Research Institute, Boston,MA 02114

The myosin rod, which is composed of the LMM region and the S2 region exhibits multiple unfolding transitions, indicating regions of different stability. We have determined by spectroscopic method that each chain of rod and LMM contained about two tryptophan, in agreement with the cDNA-derived sequence of rabbit skeletal leg muscle LMM (K. Maeda et.al., Eur. J. Biochem. 167,97,1987). To obtain information about the relative stability of the tryptophan containing regions in these rod-like molecules we compared unfolding profiles obtained with the 222 nm circular dichroism (CD) which measures helix content and three fluorescence parameters: intensity (F), spectral shift (Δ), and polarization (p), measures of local environment and flexibility. Three major thermal helix unfolding transitions with the same midpoints, 43°C ,47°C, 53°C, for both rod and LMM were detected with CD. From the fractional loss of helix associated with each transition it appears that most of the S2 region of rod melts in 47°C transition. No change in F, p or Δ was associated with the 43°C transition but changes in the fluorescence parameters were observed for the higher temperature transitions for both rod and LMM. In contrast to temperature-induced unfolding, only two main transitions were observed for rod and LMM with denaturant-induced unfolding, both CD and fluorescence giving the same midpoints for each system. The transition midpoints of the rod were slightly shifted to greater denaturant concentration and were slightly broadened relative to LMM. These results suggest that: i.) the least stable part of the rod is in LMM bordering the tryptophan containing region, ii.) the presence of the S2 region slightly affects the unfolding of the tryptophan region in LMM. (Supported by NIH, NSF and MDA)

M-Pos308 EFFECT OF FILAMENT LENGTH ON MYOSIN EXCHANGE BETWEEN SYNTHETIC THICK FILAMENTS. I. Tan, E. Zlotchenko and A. D. Saad. Department of Cell Biology and Anatomy, Cornell University Medical College, New York, New York 10021. (Introduced by S. M. Goldfine)

Previous studies using a fluorescence energy transfer (FET) assay (Saad, A. D., et. al (1986) Proc. Natl. Acad. of Sci. USA 83:9483-9487) and electron microscopy have shown that extensive exchange of myosin occurs between synthetic thick filaments. To further examine this process, myosin exchange was compared for filaments of different lengths. Chicken pectoralis myosin was labeled with either donor (5-(2-((iodoacetyl)aminoethyl) aminonaphthalene-1-sulfonic acid) or acceptor (5-iodoacetamidofluorescein) fluorochromes. Donor labeled myosin and acceptor labeled myosin were separately assembled into filaments of different lengths. Short (0.5um) filaments were obtained by quick dilution from high salt (0.5M KCl, 10mM Imidazole, pH 6.8) to low salt (0.125M KCl); intermediate length (1.0 - 1.5um) filaments were prepared by a sequential dilution method (Pepe et. al (1986) Prep. Biochem. 16:99-132) and long (4 - 5um) filaments were formed by dialysis. Filaments morphology was examined by immunolabeling. Monoclonal antibody MF20 bound to all of the filaments at identical 14.5nm intervals indicating a similar axial packing of myosin within these filaments. To examine exchange, donor labeled filaments were mixed with acceptor labeled filaments (0.25 mg/ml total concentration) and the subsequent change in fluorescence monitored. The extent of exchange was very similar for the three types of filaments examined. Since preferential end exchange would have resulted in higher exchange in shorter filaments, these results provide further support for a mechanism of exchange involving the entire length of synthetic thick filaments. (Supported by NIH - AM37653 and New York Heart Assoc.)

M-Pos309 EXPRESSION OF HIGHLY DEUTERATED PROTEINS FOR THE STUDY OF MUSCLE CONTRACTION AND ITS CONTROL Mendelson, R., Stone, D. B., Sparks, L., Reinach, F. *, *Crespi **, H. A. & Bivin, D. B. C.V.R.I.,* Biochem./Biophys., Univ. of Calif., San Francisco, CA; ** Univ. of Sao Paulo, Sao Paulo, Brazil; ** Argonne Nat. Lab., Chicago, IL

In neutron diffraction and NMR experiments the deuteration of a single member of a macromolecular complex allows one to study either that member exclusively or to render it "invisible". We have reported that deuterated actin can be extracted from the slime mold Dictyostelium discoideum grown on deuterated E. coli. This actin (66% deuterated) was made invisible in neutron scattering experiments by solvent contrast-matching in 95% D_2O. We have now embarked on an experimental program to study the mechanism of muscle contraction and its control using highly deuterated (>99%) proteins. Neutron scattering experiments using these proteins involves rendering protonated material invisible by setting the deuteration level of the buffer at 41%, thereby allowing one to see only the deuterated members of a complex. The high deuteration level produces scattering with maximal contrast and signal-to-noise. We have found that highly deuterated contractile proteins can be economically generated by growing bacterial clones which over-express fusion proteins using an approach similar to that used by Seeholzer et al. P.N.A.S. 83, 3634 (1986). The growth medium used was a highly deuterated algal hydrolysate in pure D_2O. We currently grow this algae at a deuteration level of >99%. To date, we have expressed deuterated chicken-light chain 2 and chicken fast muscle alpha-tropomyosin fusion proteins with high yield (2-20 mg/l). We expect to study the positions of muscle crossbridges and TM using these proteins. Supported by N.I.H. grants HL-16683 and HL-07192 and a CALCOR grant from Univ. of Calif.

M-Pos310 PROPERTIES OF CHICKEN MYOSIN REGULATORY LIGHT CHAIN ISOLATED FROM ESCHERICHIA COLI. Lakshmi D. Saraswat and Susan Lowey, Rosenstiel Research Center, Brandeis University, Waltham, MA 02254.

The 19-kD myosin light chain (LC2) has been implicated in the calcium regulation of invertebrate striated and vertebrate smooth muscles. In the latter, myosin is activated by phosphorylation of the light chain by a calcium-calmodulin-dependent kinase. Despite considerable sequence homology between smooth and skeletal muscle light chains, the functional significance of LC2 in vertebrate striated muscle contraction remains unclear. To increase our understanding, variants of chicken pectoralis LC2 have been synthesized in E. coli, using cDNA obtained from a λgt-11 library (Reinach and Fischman, 1985). The insert in clone L10 was digested with nuclease to remove the 30-nucleotide 5′ untranslated region, and ligated to the bacterial expression vector, pKK223-3. Transformation of E. coli produced two variants: a full length LC2 without methylation of the N-terminal alanine, and a truncated LC2 starting at methionine 19. The proteins can be isolated by immuno-affinity chromatography, and will be characterized by gel filtration, reactivity with a monoclonal antibody specific for LC2, and intrinsic fluorescence. The effect of divalent cations on the conformation of the mutant proteins will be compared to native LC2. Site-directed mutagenesis has been initiated to introduce cysteine residues into LC2. Thiol reactive spectroscopic probes can then be used to study conformational changes within the myosin head during activation. Supported by grants from NIH (AR17350) and NSF (PCM-8204125).

M-Pos311 STRUCTURAL CHANGES INDUCED IN SCALLOP HMM BY CA^{2+} AND ATP. Ling-Ling Young Frado and Roger Craig. Anatomy Department, U. Mass. Medical School, Worcester, MA 01655.

Relaxed, native scallop thick filaments change in structure from a helically ordered to a disordered form when they bind Ca^{2+} or lose their bound ATP (Vibert and Craig, J. Cell Biol. 101, 830, 1985). We have used biochemical and ultrastructural methods to investigate the effects of Ca^{2+} and ATP on the structure of purified scallop heavy meromyosin. In low salt in the presence of ATP, the papain digestion rate of the HMM heavy chain was approximately 5x higher in the presence of Ca^{2+} than in its absence. In the absence of ATP this Ca^{2+}-sensitivity was abolished. In low salt in the presence of ATP but the absence of Ca^{2+}, two peaks with slightly different Stokes radii were observed in the HMM elution profile from an HPLC gel filtration column. On addition of Ca^{2+} or removal of ATP, a single peak with the larger Stokes radius was obtained. At low salt in the presence of ATP but absence of Ca^{2+}, low angle rotary shadowing showed that at least 36% of molecules had their heads bent down towards their tails. Addition of Ca^{2+} reduced this number to about 24%, while removal of ATP reduced it to less than 10%. These results suggest that the relaxed state (ATP, low Ca^{2+}) of scallop striated muscle myosin favors a bent-down, proteolytically protected arrangement of heads on myosin molecules in solution, which may be related to the low ATPase and helical ordering of relaxed filaments. In the activated state (or when ATP is removed), the heads may become more flexibly attached to the myosin tail, which may underlie the transition to disorder occurring when intact filaments are activated or lose their ATP. Supported by grants from NIH and MDA.

M-Pos312 ORIGIN OF MYOSIN HEADS ON LIMULUS THICK FILAMENTS. Rhea J.C. Levine & Peter D. Chantler, Department of Anatomy, The Medical College of Pennsylvania, Philadelphia, PA 19129.

Although 3-D reconstruction of Limulus thick filaments suggests that each of the 2 S-1s/surface subunit arises from an axially sequential myosin molecule, the resolution is insufficient to be sure. To distinguish between this arrangement and one in which both S-1s originate from the same molecule, we examined the effect of 0.6M KCl on untreated filaments and those in which nearest S-1s were cross-linked by the 22Å, bifunctional agent, $Bis_{22}ATP.V_i$. If intramolecular bonds form between S-1s from the same molecule, surface myosin should dissolve in 0.6M KCl, leaving a paramyosin core, as with untreated filaments. If intermolecular bonds form between S-1s from different myosins, then exposure to 0.6M KCl might result either in the release of surface myosin as long polymers, or in its retention.

Filaments with well-ordered, helical surface lattices were incubated on rigor buffer for 15' (on EM grids) to remove bound ATP, then for 1-5' on buffer plus 0.5mM $Bis_{22}ATP$, followed by 15' on the same solution plus 1mM V_i. Controls were: untreated filaments; those treated, but without the V_i step; and filaments that were fully treated, then incubated for 15' on buffer plus 1-2mM DTT. Some grids were negatively stained and examined at each step; all remaining were incubated for 15' on 0.6M KCl, prestaining.

Only filaments treated with $Bis_{22}ATP.V_i$ (not followed by DTT) retained surface myosin and appeared intact, with central bare zones, after exposure to 0.6M KCl. On all control grids, only smooth cores, with occasional myosins attached, were seen. Thus, $Bis_{22}ATP.V_i$ formed intermolecular bonds that prevented myosin solubilization by high salt. This strongly supports the origin of the 2 S-1s/surface subunit from different myosin molecules.

Supported by: NIH grants: AM33302 & HL15835 to the Penna. Mus. Inst. (RL) & NSF grant DCB 860226 (PC).

M-Pos313 MYOSIN/PARAMYOSIN PHOSPHORYLATION IN MOLLUSCAN MUSCLES. Loriana Castellani and Carolyn Cohen, Rosenstiel Research Center, Brandeis University, Waltham, MA 02254.

Phosphorylation of paramyosin in molluscan catch muscles is well established. More recently, the myosin from the anterior byssus retractor muscle (ABRM) of Mytilus edulis has been shown to be phosphorylated in the rod by an endogenous kinase. We are carrying out studies of different muscle types in a variety of molluscs to compare the phosphorylation patterns of both proteins. Myofibrils were prepared from catch and non-catch muscles in clams, mussels, oysters and scallops. Phosphorylation was measured at three salt concentrations (40, 120 and 360 mM NaCl) in the absence of Ca^{2+} using radio-labeled ATP. At low ionic strength phosphorylation is readily observed in the myosin heavy chain of all catch, but not of non-catch muscles. As the ionic strength increases, the degree of phosphorylation decreases. In contrast, paramyosin phosphorylation occurs both in catch and non-catch muscles, and it is greatly enhanced by ionic strength. These results provide part of the information required to identify the targets of phosphorylation that may be related to control of catch. Supported by grants from NIH, NSF and MDA.

M-Pos314 **THE SYNTHESIS OF A NOVEL CLASS OF RIBOSE-MODIFIED NUCLEOTIDE ANALOGS. I. AFFINITY PURIFICATION OF SKELETAL MYOSIN SUBFRAGMENT-1**
Scott Braxton and Ralph G. Yount, Biochemistry/Biophysics Program, Washington State University, Pullman, WA 99164-4660.

In order to prepare stable ribose modified nucleotide analogs, a new synthetic approach to prepare carbamate derivatives has been devised. The nucleotide is activated with carbonyldiimidazole; then reacted with an amine in organic solvents to form a 2' or 3' carbamate. These carbamates are stable between pH 2 and 11.4 ($t_{1/2}$ ~ 50 days at 25°C). The ATP analogs are substrates for myosin subfragment-1 (S1) and are also trapped at the nucleotide binding site by the Co(II/III) phenanthroline system or by the addition of vanadate. This method has recently been extended to include fluorescent derivatives of ATP (see Neuron, Cremo & Yount, these abstracts).

One such ATP analog was attached to agarose through a 20 atom leash and used for affinity purification of S1. SDS-PAGE shows that the affinity purified S1 is substantially cleaner than control S1. In addition, the specific activity has increased to 120% of control. The affinity purified S1 also traps to a greater extent than does control S1. After trapping it is possible to remove all protein which does not have ADP trapped at the active site by a second passage over the affinity column.

The synthetic procedure outlined above has been used to prepare carbamates of GTP, 2'dAMP and cAMP in addition to ATP and should prove to be of general utility for the stable derivatization of nucleotides at the ribose ring.
Supported by grants from MDA and NIH (DK05195).

M-Pos315 **SYNTHESIS AND CHARACTERIZATION OF NEW FLUORESCENT PHOTOAFFINITY ATP ANALOGS: INTERACTION WITH THE ACTIVE SITE OF SKELETAL MYOSIN SUBFRAGMENT 1.** Joan Neuron, Christine Cremo, and Ralph G. Yount, Biochemistry/Biophysics Program and the Dept. of Chemistry, Washington State University, Pullman, Washington 99164.

Three new fluorescent and photoreactive ATP analogs; dansyl-2N3ADP (DEDA-2N3ADP), fluorescein-2N3ADP (FA-2N3ADP), and N-methylanthraniloyl-2N3ADP (MANT-2N3ADP) have been synthesized and characterized. For DEDA-2N3ADP and FA-2N3ADP, dansylethylenediamine or fluoresceinamine have been attached to the 2' or 3' position of the ribose ring via a stable carbamate linkage (See S. Braxton and R. G. Yount, these abstracts). The products are purified by DEAE ion exchange, LH-20 hydrophobic chromatography, and HPLC.. MANT-2N3ADP is a photoreactive analog of MANT-ADP (Hiratsuka et al. J. Biochem,(1984), 96, 147). These three new probes are shown to photoincorporate with high efficiency onto skeletal myosin subfragment 1 (S1) by prior trapping at the active site as the Co^{2+}-nucleotide diphosphate-V_i complex (Goodno, et al., Meth. in Enz.,(1982) 85, 116). The fluorescence properties of these probes free in solution and bound at the active site of S1 will be presented. These probes are potentially useful as donors and/or acceptors for long range distance measurements by fluorescence energy transfer techniques within the myosin head, within the actomyosin complex, or with other ATP binding proteins.
Supported by grants from MDA and NIH (DK05195).

M-Pos316 BINDING OF DYNEIN, MYOSIN AND MYOSIN FRAGMENTS TO DNA. Julian Borejdo & Marco Giordano. Cardiovascular Research Institute, University of California, San Francisco, California 94143.

It was found by agarose gel electrophoresis and by ultracentrifugation that dynein, myosin and chymotryptic fragments of myosin bind strongly to DNA. Binding of myosin fragments to DNA quantitatively retarded the migration of nucleic acid through the gel, and increased the light scattering by DNA. These findings provided a convenient way to study the binding. Electron microscopic observations showed that the binding resulted in the formation of loops and kinks in DNA. Ca^{2+}-, Mg^{2+}- and EDTA-activated ATPase of HMM was unchanged by DNA, but its actin-activated ATPase was decreased. The effect of ionic strength, actin and various nucleotides on binding showed that the protein interacted with DNA through its nucleotide binding site, which is on the globular portion of the molecule. We speculate that this binding simulates the interaction of cytoplasmic ATPases with chromatin during cell anaphase and therefore that it is important during cell mitosis.

M-Pos317 **Subdivisions of leg type 2B fibers in rabbit and rat skeletal muscles.** K. Mabuchi, Y. Mabuchi, F.A .Sréter, and J .Gergely. Dept. of Muscle Res., Boston Biomedical Research Institute; Dept. of Neurology and Anesthesia, Mass. General Hosp.; Dept. of Biol. Chem. and Mol. Pharmacol., and Dept. of Anesthesia, Harvard Med. School, Boston, MA, 02114.

Previous work has shown that 2B fibers of adductor magnus, tibialis anterior and masseter muscles of the rabbit contain at least two subpopulation of myosin heavy chains - distinguishable by electrophoretic migration velocity and peptide patterns - distinct from both type 2A and slow forms (Mabuchi et al., Muscle & Nerve 7:431-438, 1984). In this work we have used monoclonal antibodies (McAbs) to characterize 2B fibers of various muscles of the rabbit and the rat. We fond that the majority of the rabbit adductor magnus 2B fibers contains a unique myosin which is distinguishable by McAbs from the specific isoform in extraocular muscles (cf. Wieczorek et al., J. Cell Biology 101:618-629, 1985), and from the 2B myosin found in the majority of the fast leg muscles. The rat muscles studied by us (adductor magnus, semimembranosus, tibialis anterior, extensor digitorum longus and psoas) contain two population of type 2B fibers; one predominant in the white portions and the other abundant in the red, mitochondria-rich, region. Antibody reaction patterns and peptide maps clearly distinguish these isoforms from slow and 2A types. (Supported by grants from NIH (R37-HL 5949 and GM 15904), MDA and Mass. Affiliate, AHA).

M-Pos318 INTERACTION BETWEEN SMOOTH MUSCLE TROPOMYOSIN AND REDUCED CALDESMON. Philip Graceffa, Dept. of Muscle Research, Boston Biomedical Research Institute, Boston, MA 02114.

We have previously provided evidence for the interaction between chicken gizzard tropomyosin and caldesmon by showing that caldesmon (in the absence of DTT) dramatically enhanced the specific viscosity of tropomyosin in the absence of salt (1). Since a recent study has shown that, in the absence of DTT, caldesmon is oxidized to disulfide-crosslinked oligomers which can be reversed by DTT reduction (2), we repeated the viscosity experiments in the absence and presence of DTT. Caldesmon, in the absence of DTT and salt, enhanced the specific viscosity of tropomyosin 12-fold which dropped to a 1.6-fold enhancement upon addition of DTT. This indicates that reduced caldesmon interacts with tropomyosin in the absence of salt, although it enhances tropomyosin's viscosity much less than does oxidized caldesmon. As evidence for the interaction of tropomyosin with reduced caldesmon at a more physiological ionic strength we found that in 0.1M NaCl, 3mM $MgCl_2$, 1mM DTT, pH 7, caldesmon enhanced the fluorescence of MIANS-labeled tropomyosin. In conclusion, our work indicates that tropomyosin interacts with both oxidized and reduced caldesmon. Furthermore, we conjecture that disulfide-crosslinked caldesmon bundles tropomyosin end-to-end polymers, which form at low salt, with a resulting dramatic increase in viscosity in much the same way that disulfide-crosslinked caldesmon bundles actin filaments with an enhancement of actin viscosity (2). Supported by NIH grant AR-30917.

(1) Graceffa, P. (1987) FEBS Lett. 218, 139-142.
(2) Lynch, W.P., Riseman, V.M., and Bretscher, A. (1987) J. Biol. Chem. 262, 7429-7437.

M-Pos319 CALDESMON: MOLECULAR WEIGHT AND SUBUNIT COMPOSITION BY ANALYTICAL ULTRACENTRIFUGATION. Walter F. Stafford and Philip Graceffa, Dept. Muscle Research, Boston Biomedical Research Institute, Boston, MA 02114.

The subunit mass of chicken gizzard caldesmon has been reported to be between 120-150 kDa using methods which are sensitive to the shape of the molecule. It is also controversial whether caldesmon exists as a monomer or dimer. We determined the molecular weight by means of sedimentation equilibrium centrifugation, a method which does not depend on the shape of the molecule. We found that, in 0.1-0.3M NaCl, $\pm$3mM $MgCl_2$, 1mM dithiothreitol, pH7, caldesmon behaved as a single monodisperse component with a molecular mass of 97 $\pm$ 3 kDa. SDS polyacrylamide gel electrophoresis of this caldesmon showed a single band with an apparent subunit mass of 137 kDa, in agreement with previous work. A comparison of this apparent subunit mass with the molecular weight indicates that caldesmon is a monomer in solution. Sedimentation velocity experiments showed a single component with a value of $s^{o}_{20,w}$ of 2.65S from which a value for Stokes' radius (R_s) was calculated to be 8.7 nm, both numbers in agreement with previously measured values. This value of R_s corresponds to a frictional ratio (f/f_{min}) of 2.8, consistent with the known asymmetry of caldesmon. Supported by NIH grant AR-30917.

M-Pos320 PHOSPHORYLATION OF GIZZARD CALDESMON. Jean-Claude Abougou and D. J. Hartshorne, Muscle Biology Group, University of Arizona, Tucson, AZ 85721.

Caldesmon is a thin-filament protein abundant in smooth muscle that binds calmodulin. It inhibits the Mg^{2+}-ATPase activity of skeletal and smooth muscle actomyosin and due to this has been proposed as a putative regulatory protein. Caldesmon also is phosphorylated, and it was suggested that this alters its inhibitory properties (Ngai, P.K. and Walsh, M.P. Biochem. J. [1987] 244, 417-425). The latter finding, however, is controversial and our intent was to characterize the phosphorylation reaction in more detail. It was shown that: 1) The presence of caldesmon kinase is variable in different preparations. Part of the variability is due to the use of ammonium sulfate fractionation. Caldesmon kinase precipitates at lower $(NH_4)_2SO_4$ concentrations (~30% saturation) than caldesmon. A caldesmon preparation collected at 30-65% saturation is low or devoid of kinase activity and this can be restored by the addition of the 0-30% fraction. 2) Titration of endogenous kinase activity in caldesmon preparations with calmodulin results in maximum activity at considerably less than the caldesmon stoichiometry. This implies that the kinase activity is not a property of caldesmon but reflects a contaminant protein and that the competition for calmodulin by caldesmon is not appreciable, i.e. the affinity of caldesmon for calmodulin is relatively weak. 3) The sites of phosphorylation on caldesmon by the endogenous kinase are the same as the sites for the Ca^{2+}-calmodulin kinase from rat brain (kindly donated by Dr. H. Schulman) and are distinct from the protein kinase C sites. Supported by NIH grants HL23615 and HL20984.

M-Pos321 BINDING AFFINITY OF CALDESMON TO CALMODULIN IN THE PRESENCE AND ABSENCE OF SMOOTH MUSCLE ACTIN. Kurumi Y. Horiuchi and Samuel Chacko, Department of Pathobiology, University of Pennsylvania, Philadelphia, PA.19104.

Caldesmon is an actin binding protein which also binds to calmodulin in the presence of Ca^{2+}. Binding of caldesmon to actin inhibits the actin-activated ATPase of phosphorylated smooth muscle myosin. Calmodulin releases this inhibition in the presence of Ca^{2+}. In this study we determine the affinity of caldesmon to calmodulin and how this affinity is modified by ionic conditions and smooth muscle actin. The binding affinity of caldesmon to calmodulin is studied using immobilized calmodulin. The binding constant is 0.8×10^6 M^{-1} at 0.05 M ionic strength. Raising the ionic strength causes a decrease in the affinity of caldesmon to calmodulin. Caldesmon binds to calmodulin both in the presence and absence of Mg^{2+} although the binding constant is maximal at around 1 mM free Mg^{2+}. The apparent binding affinity of caldesmon to calmodulin decreases in the presence of smooth muscle actin. The intrinsic binding constant of caldesmon to actin is obtained from Dixon Plots and it is found to be 0.33×10^6 M^{-1} in the presence of Ca^{2+}-calmodulin. Smooth muscle actin containing stoichiometric amount of tropomyosin binds caldesmon at a higher affinity than actin devoid of tropomyosin. As in the case in the binding of caldesmon to calmodulin, an increase in ionic strength lowers the binding affinity of caldesmon to actin; however, in the latter case, this effect is more pronounced. The affinity of caldesmon to actin is decreased more than three fold on raising the ionic strength from 0.05 to 0.11 M compared to 1.5 fold for the affinity of caldesmon to calmodulin. Supported by grants from NIH and NSF.

M-Pos322 BINDING OF CALDESMON TO SMOOTH MUSCLE MYOSIN Mitsuo Ikebe, Jane Koretz*, and Sheila Reardon, Dept. of Physiology and Biophysics, Case Western Reserve University, Cleveland, OH 44106, *Department of Biology, Renoselaer Polytech. Institute Science Center, Troy, NY 12180

Caldesmon is a major actin-and calmodulin-binding protein. Addition of caldesmon to smooth muscle myosin induced the formation of small aggregates of myosin in the absence of Ca^{2+} calmodulin, but not in the presence of Ca^{2+} calmodulin. The binding site of myosin was studied by using caldesmon-Sepharose 4B affinity chromatography. Subfragment 1 was not retained by the column, while heavy meromyosin (HMM) and subfragment 2 were bound to the caldesmon affinity column in the absence of Ca^{2+} calmodulin. The binding of HMM to the column was inhibited by Ca^{2+}-calmodulin. Therefore, the binding site of caldesmon on the myosin molecule was concluded as the subfragment 2 region and binding of caldesmon to myosin was abolished in the presence of Ca^{2+} and calmodulin. Cross-linking of actin and myosin mediated by caldesmon was studied. While actomyosin was completely dissociated in the presence of Mg^{2+}-ATP, the addition of caldesmon caused aggregation of the actomyosin$_{Mg^{2+}}$. By low speed centrifugation at which actomyosin was not precipitated in the presence of Mg^{2+}-ATP, the aggregate induced by caldesmon was precipitated and the composition of the precipitate was found to be actin, caldesmon and myosin. In the presence of Mg^{2+}-ATP, pure actin did not bind to myosin-Sepharose 4B affinity column and caldesmon bound to myosin-Sepharose 4B affinity column. When actin was mixed with caldesmon and applied to the column, not only caldesmon but also all of actin was retained to the column. These results indicate that caldesmon can cross-link actin and myosin. This may play a role for the tension maintenance of smooth muscle with low energy usage. (Supported by N.I.H. grant AR 38888, by Syntex Scholarship and by American Heart Association Northeast Ohio affiliate. M.I. is Established Investigator of A.H.A.)

M-Pos323 **Ca^{2+}-CALMODULIN INTERACTION WITH CALDESMON.** **Saleh El-Saleh* and Michael Walsh++ from the *Department of Physiology and Biophysics, University of Cincinnati, College of Medicine, Cincinnati, OH 45267 and the ++Department of Medical Biochemistry, Faculty of Medicine, University of Calgary, Calgary Alberta Canada T2N 4N1.**

The interaction between chicken gizzard caldesmon and Ca^{2+} calmodulin was investigated using the Ca^{2+} calmodulin-induced fluorescence enhancement of intrinsic tryptophan fuorescence in caldesmon as a probe for this interaction. In the absence of Mg^{2+} the saturation of the induced tryptophan fluorescence (25% enhancement) was achieved at 1.0-1.2 moles of Ca^{2+} calmodulin/mole of caldesmon when measured at pH 7.0 μ = 120 and pCa = 4.0. The association constant under these conditions was $2.01 \times 10^8 M^{-1}$, a value that is 224 fold higher than that reported by Christopher et al. (JBC, 1987, 262, 116). In the presence of Mg (1 mM free), stoichiometric levels of Ca^{2+} calmodulin binding to caldesmon were obtained with the tryptophan fluorescence reaching 28% at full saturation. The K_a, under these conditions, was enhanced by about 2 fold ($3.46 \times 10^8 M^{-1}$). On the other hand, the Ca^{2+}-dependent changes in the induced tryptophan fluorescence exhibited greater Ca^{2+}-sensitivity ($pCa_{50\%} \simeq 7.25$) in the presence of Mg as compared to its absence ($pCa_{50\%} \simeq 6.6$). The enhancement of Ca^{2+}-sensitivity (+ Mg) was greater than the Ca^{2+}-dependent binding of Ca^{2+} to calmodulin as determined from the Ca^{2+}-dependent change in tyrosine fluorescence in calmodulin ($pCa_{50\%} \simeq 5.6$, +Mg). It was also higher than the Ca^{2+}-dependent interaction and acivation of myosin light chain kinase by calmodulin (Johnson et al., 1981, JBC, 256, 12194; Mg 3mM, μ = 150, pH 7.0). It is possible, therefore, that a cooperative Ca^{2+} effect may occur in the narrow range of the high pCa levels (8.0-7) leading to the disinhibition of the acto-myosin ATPase (or interaction) by caldesmon·calmodulin, followed by activation of MLCK (pCa range 7-4).

M-Pos324 CALDESMON AND THE STRUCTURE OF VERTEBRATE SMOOTH MUSCLE THIN FILAMENTS. W. Lehman*, C. Moody+, and R. Craig+. *Dept. of Physiology, Boston Univ. School of Medicine, Boston, MA 02118 and +Anatomy Dept., Univ. of Massachusetts Medical School, Worcester, MA 01605.

Several approaches are being used to determine the structural interactions of caldesmon on vertebrate smooth muscle thin filaments. (1) Immunological studies: Polyclonal antibodies developed against and specific for the 40 KDa actin-calmodulin-binding domain of chicken gizzard caldesmon cause native gizzard thin filaments to associate laterally and label the thin filaments at approx. 40 nm intervals (i.e. with a spacing identical to the known repeat of tropomyosin). The results suggest that caldesmon interacts discretely with tropomyosin on smooth muscle thin filaments. Thin filaments crosslinked by these antibodies are sufficiently well-ordered for optical diffraction studies. In contrast, thin filaments immunoprecipitated by polyclonal antibodies developed against the entire caldesmon molecule (or against tropomyosin) cause the filaments to bundle without revealing periodicity (Lehman and Marston (1986)). We presently are also developing monoclonal antibodies in order to map the domain structure of caldesmon molecules and determine domains of caldesmon associated with the thin filament. (2) Paracrystal studies: Although smooth muscle caldesmon dissociates from thin filaments under conditions conventionally used for actin paracrystal formation (25-50 mM divalent cations), we find that ordered gizzard thin filament paracrystals, retaining caldesmon, can be formed in solutions containing lower concentrations of $MnCl_2$. Such paracrystals may prove useful in optical diffraction studies. (3) Rotary shadowing: Our method for rotary shadowing of intact thin filaments results in an excellent degree of preservation. Such preparations will be used to test whether caldesmon projects from the thin filaments.

M-Pos325 **THE CALMODULIN BINDING DOMAIN OF CHICKEN GIZZARD MYOSIN LIGHT-CHAIN KINASE CONTAINS TWO NON-OVERLAPPING ACTIVE SITE-DIRECTED INHIBITORY SEQUENCES.** Carolyn J. Foster and Federico C.A. Gaeta (Intr. by B.J.R. Pitts), Depts. of Cardiovascular Pharmacology and Medicinal Chemistry, Schering Research, Bloomfield, New Jersey 07003.

The calmodulin (CaM) binding domain of chicken gizzard myosin light chain kinase (MLCK) contains clusters of basic aminoacids similar to the basic cluster essential for recognition of the substrate, myosin light chain, by the enzyme. Kemp, et al., (JBC, **262**, 2542 (1987)) have proposed that the region contains an inhibitory pseudosubstrate sequence. We have synthesized a number of peptides based on the region 480-516 (^{480}AKKLSKDRMKKYMARRKWQKTGHAVRAIGRLSSMAMI^{516}) of MLCK. Direct inhibition of MLCK was studied using CaM-independent enzyme (CIM) prepared by proteolysis, while binding to CaM was inferred when the ability of a peptide to inhibit was different in the presence and absence of CaM and Ca^{2+}. Our results show that the ability to bind CaM resides in both ends of the sequence, since peptide 494-504 was a poor CaM binder, while peptides extended in either direction (480-504 or 494-512) were good CaM binders. Peptide 480-504 bound to CaM in the presence of Ca^{2+}, and CaM reversed MLCK inhibition in a concentration-dependent fashion. The ability to inhibit the enzyme also resides in several distinct regions. The non-overlapping peptides 480-493 and 494-504 were both potent inhibitors of CIM (IC_{50}=10μM and 2.2μM, respectively), and were competitive with peptide substrate. The combined peptide 480-504 was an extremely potent inhibitor (IC_{50}=11nM), and it displayed unusual kinetics. It was apparently competitive with ATP and non-competitive with the peptide substrate. These results support the premise that this region of MLCK is capable of acting as an internal inhibitory domain, and that CaM activates MLCK by binding to the same region thus exposing the catalytic site.

M-Pos326 STUDY OF THE INHIBITORY REGION OF SMOOTH MUSCLE MYOSIN LIGHT CHAIN KINASE Mitsuo Ikebe*, Bruce E. Kemp++ and David J. Hartshorne+, *Dept. of Physiology and Biophysics, Case Western Reserve University, Cleveland, OH 44106, +Dept. of Nutrition and Food Sci., University of Arizona, Tucson, AZ 85721, and ++Department of Medicine, University of Melbourne, Heidelberg, Australia

Previously we showed that smooth muscle myosin light chain kinase (MLCK) is hydrolyzed by trypsin to the 64K inactive fragment which can be further cleaved to the 61K active kinase fragment and proposed the existence of the inhibitory region in the amino acid sequence of MLCK. We studied the location of the inhibitory region in the amino acid sequence by using synthetic peptides. 5 peptides were used named SM I, SM II, SM III, SM IV, and SM V. These correspondended to residues 480-501, 480-493, 493-504, 483-498, 493-512. Ki of these peptides against 61K active Ca^{2+} calmodulin independent kinase were 40nM, 1.5μM, 3μM, 40nM, and 3μM. Therefore residues 483-498 are thought to be an inhibitory region of MLCK. It was also found that the inhibition of the activity of 61K active fragment by SM I and SM IV is competitive to ATP. This suggests the ATP binding site is in close proximity to this inhibitory region. Although SM V was a rather poor inhibitor of 61K fragment, SM V was a potent inhibitor for native MLCK. The inhibition was competitive to calmodulin. Since SM V does not inhibit 61K active fragment well, SM V is likely to bind to calmodulin and compete with the binding of MLCK for calmodulin. The activity of native MLCK was also inhibited by SM I and IV. The inhibition was competitive to calmodulin. Since SM I and IV inhibit the 61K active fragment which lost calmodulin binding site, SM I and IV bind to MLCK and this binding is probably competitive with the binding of calmodulin to native MLCK. (Supported by N.I.H. grants AR 38888,and by Syntex Scholarship Award. M.I. is Established Investigator of A.H.A.)

M-Pos327 LOW RESOLUTION MAPPING OF CALMODULIN-MYOSIN LIGHT CHAIN KINASE (MLCK) INTERACTIONS USING SYNTHETIC MLCK PEPTIDES. Donald K. Blumenthal*, Rachel E. Klevit°, & Harry Charbonneau° (*Univ. of Texas Health center, Tyler, TX 75710; °University of Washington, Seattle, WA 98185).

Peptides corresponding to the calmodulin-binding domain of skeletal muscle MLCK (residues 577-595; KRRWKKNFIAVSAANRFKK) exhibit many of the calmodulin-binding properties of intact MLCK, and have been used as models for studying calmodulin-MLCK interactions at the molecular level. A series of cysteinyl-containing synthetic MLCK peptids has recently been prepared for the purpose of incorporting sulfhydryl-reactive probes in a site-specific manner. Acrylodan, a polarity-sensitive fluorescent label, was incorporated into the peptides, KRRWKKAFIAVSAAARFKKC-amide and KRRCKKAFIAVAAARFG-amide. In the absence of CaM, the two acrylodan-labeled peptides have nearly identical emission spectra (Em max = 520 nm). In the presence of Ca^{++}/CaM, the former peptide exhibits a modest blue-shift in its emission spectrum (20 nm), whereas the latter peptide exhibits a substantial blue-shift (50 nm). In the presence of the thrombin-generated fragment of CaM (residues 1-106) the acrylodan group at the 4-position of the peptide undergoes nearly identical spectral changes upon interaction with CaM (1-106) as with intact CaM, whereas the label at the C-terminus of the peptide does not experience any change in its emission spectrum in the presence of CaM(1-106), even though complex formation can be dectected by changes in peptide fluorescence anisotropy. These data suggest that the N-termini of the MLCK peptides align with the N-terminus of calmodulin. Additional data in support of this conclusion were obtained using the peptide CKRRWKKAFIAVSAAARFG-amide, labeled with iodoacetamido-PROXYL. Proton NMR spectra obtained using this spin-labeled peptide indicate that only residues in the N-terminus of CaM are perturbed.

M-Pos328 **A DUAL STRUCTURAL/CATALYTIC ROLE FOR MYOSIN LIGHT CHAIN-KINASE IN SMOOTH MUSCLE? J.D. Strauss, P. deLanerolle, J. Lin, D.G. Ferguson and R.J. Paul. Depts. of Physiology & Biophysics, Universities of Cincinnati (45267-0576), Illinois, and Iowa.**

In previous studies (Fed. Proc. 45:762) we have shown that polyclonal anti-MLCK Fab inhibit force in skinned guinea pig taenia coli (TC) smooth muscle; however, force was inhibited to a greater degree than myosin phosphorylation. Anti-MLCK Fab also relaxed contractions elicited after incubation with ATPγS, suggesting a role for MLCK in addition to catalysis. In order to distinguish between these possible functions, we developed and screened a series of monoclonal antibodies against MLCK purified from turkey gizzard. Antibodies from several clones (K-47, K-36, K54, K-12, and K-39) were tested for their ability to bind to TC proteins by Western blot analysis, their ability to inhibit myosin kinase in vitro, and for their effects on isometric force (F_o) (pCa = 5) in skinned smooth muscle. IgG found not to react with t.coli proteins had no effect on F_o. K-47 bound to guinea pig MLCK on blots but had no effect on either MLCK activity or force. K-36 induced a relaxation to 0.7 F_o at 90 min compared to a level of 0.22 F_o in the presence of goat polyclonal IgG against MLCK; K-36, however, had little effect on in vitro MLCK activity. Conversely, K-54 inhibited in vitro MLCK activity but had no effect on force. These results are consistent with a dual structural and catalytic role for MLCK. This is being further studied by immunogold labeling of these antibodies in skinned TC. In preliminary experiments, fibers treated with these primary antibodies retain substantial amounts of indirect immunogold label while control samples did not retain any label. The localization of these antibodies and the structural integrity of these fibers after antibody treatment is being evaluated using transmission electron microscopy. Supported in part by NIH HL 23240, HL 22619, HL 34979 (DGF) and T.G. HL 07571 (JDS).

M-Pos329 PURIFICATION AND CHARACTERIZATION OF MYOSIN LIGHT CHAIN KINASE FROM SHEEP UTERINE MUSCLE. Mary D. Pato, Ewa Kerc, and Steve Lye*, Dept. of Biochemistry, University of Saskatchewan, Saskatoon, Saskatchewan, Canada S7N 0W0; *Dept. of Obstetrics and Gynecology, St. Joseph Hospital Research Institute, St. Joseph Hospital, University of Western Ontario, London, Ontario, Canada N6A 4V2.

Phosphorylation-dephosphorylation of the 20,000-Da light chains of smooth muscle myosin is the major mechanism regulating contractile activity of smooth muscle. Phosphorylation of myosin by myosin light chain kinase (MLCK) has been shown to be required for the actin-activation of the myosin Mg ATPase activity and for muscle contraction. Recently, we have purified MLCK from pregnant sheep uterine muscle. The purification procedure included gel filtration on Sephacryl S-300, ion-exchange on DEAE-Sephacel and affinity chromatography on a calmodulin-Sepharose column. The purified enzyme migrated as a single band on a SDS-polyacrylamide gel with a M_r = 160,000. It is inactive in the absence of Ca^{2+} and calmodulin and is a substrate for cAMP-dependent protein kinase. The polyclonal antibodies we have raised against the uterine MLCK also cross-reacted with MLCK from turkey and chicken gizzards.

Supported by a grant from the Medical Research Council of Canada.

M-Pos330 EFFECTS OF PEPTIDE INHIBITORS OF MYOSIN LIGHT CHAIN KINASE (MLCK) ON CONTRACTILITY IN SKINNED SMOOTH MUSCLE. **J.C. Rüegg, J.D. Strauss, R.J. Paul, B. Kemp, M. Chen, A.-Y. Li, M. Ikebe and D.J. Hartshorne. Depts. of Physiology & Biophysics, Medicine, and Muscle Biology Group, Universities of Heidelberg (FRG), Cincinnati, Melbourne (Australia), Case Western and Arizona.**

We studied the effects of synthetic peptides, based on the cDNA sequences of chicken gizzard MLCK, which inhibit myosin kinase activity in vitro. A 20 amino acid peptide, WP, (-494—513-) containing a MLCK phosphorylation site, has been shown to bind to calmodulin with a Kd of ↶1 nM (Lukas et al., Biochem 5:1458, 1986). SM-I, a 22 amino acid peptide (-480—501-), inhibits both MLCK and a proteolytic fragment of MLCK whose activity is independent of Ca^{2+}-calmodulin. Skinned fibers from chicken gizzard and guinea pig taenia coli were prepared as previously reported (Experientia 41:1002, 1985). Both WP and SM-I reduced isometric force as well as velocity. Maximal contractions induced by 20 μ M Ca^{2+} at 0.1 μ M calmodulin could be completely relaxed by WP at 1 μ M. This relaxation could be antagonized by addition of calmodulin. WP (1 μ M) shifted calmodulin dose-response curves to the right. Using WP as a calmodulin-buffer, force was graded in a free calmodulin range of 0.1 to 10 nM. However, additional force could be developed by [calmodulin] > [WP]. Contractions elicited after exposure to ATPγS were not inhibited by either WP or SM-I. Inhibition by SM-I (1 μ M) was dependent on [ATP] with little effect at 7.5 mM and ↶ 40% relaxation at 1 mM. SM-I relaxation was not readily reversible, but could be antagonized by calmodulin. Our results suggest that WP is a calmodulin antagonist, unique in terms of its potency and that SM-I may inhibit by a different mechanism, possible acting directly on MLCK. These peptides should allow a more detailed evaluation of the roles of calmodulin and MLCK in the regulation of smooth muscle contractility. Supported in part by NIH HL 22619, HL 23240 (RJP), HL 07571 (JDS), and HL 23615, HL 20984 (DJH).

M-Pos331 EFFECTS OF PEPTIDE FRAGMENTS OF MYOSIN LIGHT CHAIN KINASE ON THE SHORTENING OF SINGLE SMOOTH MUSCLE CELLS. G.J. Kargacin, M. Ikebe, T. Ito and F.S. Fay. Dept. of Physiology, U.Mass. Med. Ctr., Worcester, MA 01655

Myosin light chain kinase (MLCK) is thought to play a central role in smooth muscle activation. The enzyme catalyzes the phosphorylation of the 20 kD myosin light chains and is regulated by Ca^{++} and calmodulin. In vitro, tryptic hydrolysis of MLCK produces a 64 kD fragment with minimal enzymatic activity. Further hydrolysis produces a 61 kD fragment with high activity that is independent of Ca^{++}-calmodulin (Ikebe et al., J.B.C. 260, 1987). We report here a study carried out in vivo with skinned single smooth muscle cells. Cells were isolated enzymatically from the stomach of the toad Bufo marinus and were skinned with saponin. Myosin light chain kinase (MW 130 kD) was isolated from turkey gizzard smooth muscle and the purified enzyme subjected to tryptic digestion to yield a 61 kD fragment. This fragment lacked the Ca^{++}-calmodulin binding site of the native kinase and was able to induce shortening of skinned cells in Ca^{++}-free solution at rates comparable to those seen during Ca^{++}-dependent activation of the cells. Two synthetic peptide copies (SM 1, amino acids 480 to 501; and SM 4, amino acids 483 to 498) of the inhibitory region of the native kinase inhibited the shortening induced by the 61 kD fragment in a dose dependent manner. Preliminary results from the microinjection of the 61 kD fragment into intact cells indicate that it induces them to irreversibly contract. Our results support the hypothesis that MLCK plays an important role in smooth muscle regulation and suggest that the Ca^{++}-calmodulin binding site on the enzyme is near or part of an inhibitory region. Supported by NIH grants HL14523, AM07341, AR38888 and a SYNTEX Scholarship Award to M.I. M.I. is an Established Investigator of the American Heart Association.

M-Pos332 CALMODULIN-BINDING PEPTIDE FROM MYOSIN LIGHT CHAIN KINASE INHIBITS CONTRACTION IN SKINNED TRACHEAL SMOOTH MUSCLE. K.E. Kamm, T.F. Feltes and J.T. Stull, Depts. of Physiology and Pediatrics, Univ. Tx Hlth. Sci. Ctr. Dallas, Dallas, TX 75235.

Fibers of bovine tracheal smooth muscle were chemically skinned to test the hypothesis that synthetic peptides with high specificity might be used to evaluate particular contributions of intracellular reactions to the regulation of contractility. A synthetic peptide (CBDP) of the calmodulin (CaM)-binding domain of rabbit skeletal muscle myosin light chain kinase (MLCK), which binds CaM with high affinity (Kd=1 nM) and inhibits purified MLCK competitively in respect to CaM (Blumenthal et al., PNAS USA 82:3187, 1985), was used. At 6 μM CBDP, Ca^{2+}/CaM-dependent MLCK activity in diluted (1:90) homogenates of bovine tracheal smooth muscle was inhibited >95%. Inhibition was reversed by addition of 12 μM CaM. For tracheal muscle fibers chemically skinned in Triton X-100 followed by freeze-glycerination, force of contraction with 2 μM Ca^{2+} increased from 30 ± 20 to 300 ± 14 (5) mg on addition of 2 μM CaM (Ca^{2+}/CaM), moreover, repeated applications of Ca^{2+}/CaM resulted in reproducible cycles of contraction-relaxation. Mean values of phosphorylation were 0.03 ± 0.03 (6) for relaxed fibers and 0.61 ± 0.05 (4) mol phosphate per mol light chain for Ca^{2+}/CaM contracted fibers. Pretreatment of fibers with 20 μM CBDP resulted in 80% inhibition of force in response to Ca^{2+}/CaM. Inhibition was reversed following a 90 min wash. These results are consistent with Ca^{2+}/calmodulin-dependent regulation of smooth muscle contraction and demonstrate the potential for further investigations of sites of regulation with the use of peptide inhibitors. (Supported by HL 26043 and 32607).

M-Pos333 SITES OF MYOSIN LIGHT CHAIN PHOSPHORYLATION IN CONTRACTING SMOOTH MUSCLE. K.E. Kamm, J.C. Colburn, L.-C. Hsu, C.H. Michnoff and J.T. Stull, Dept. Physiol., Univ. Tx. Hlth. Sci. Ctr. Dallas, Dallas, TX 75235.

Since purified smooth muscle myosin light chain can be phosphorylated at 5 distinct sites by both myosin light chain kinase (MLCK) and protein kinase C (PKC) in vitro, we determined specific sites phosphorylated in smooth muscle cells. Bovine trachealis was incubated in ^{32}P-PO_4 and subsequently stimulated with 10 μM carbachol for 1 or 30 min. After 1 min in carbachol myosin light chain was 59 ± 4% monophosphorylated (LCP) and 9 ± 2% diphosphorylated (LCP2). At 30 min the distribution was 45 ± 4% LCP and 4 ± 1% LCP2. At both 1 and 30 min ^{32}P-LCP contained phosphoserine and demonstrated a single ^{32}P-labelled spot after trypsin digestion and two dimensional thin layer electrophoresis and chromatography. The migration of this spot was identical to that obtained with trypsin-digested tracheal light chain monophosphorylated by MLCK. At both 1 and 30 min ^{32}P-LCP2 contained both phosphoserine and phosphothreonine with a ^{32}P-labelled spot migrating similarly to trypsin-digested tracheal light chain diphosphorylated by MLCK. The peptide maps for LCP and LCP2 were distinct from the peptide maps obtained from tryptic digests of tracheal light chain phosphorylated by protein kinase C. Thus, stimulation of bovine tracheal smooth muscle with a high concentration of carbachol results in the formation of both LCP and LCP2 although the amount of LCP is substantially greater than LCP2. MLCK, but not PKC, appears to catalyze myosin light chain phosphorylation both with short and prolonged periods of stimulation (Supported by HL26043 and HL32607).

M-Pos334 MYOSIN LIGHT CHAIN PHOSPHORYLATION AND THIOPHOSPHORYLATION IN SKINNED CHICKEN GIZZARD AT LOW MG^{2+}. R. Emmet Kenney[+], P.E.Hoar[+], W.G.L. Kerrick[+#]. Depts. of [+]Physiology & Biophysics and [#]Pharmacology, Univ. of Miami School of Medicine, Miami, FL 33101.

The relationship between tension and phosphorylation of the 20,000 dalton light chain of myosin was examined in a skinned preparation of chicken gizzard vertebrate smooth muscle at low levels of free Mg^{2+} (0.1 mM). When skinned fiber bundles were contracted in the presence of Ca^{2+}, 2mM $MgATP^{2-}$, and 0.1 mM Mg^{2+}, light chain phosphorylation occurred rapidly, proceeding to a plateau level by ten minutes. Tension developed slightly later and reached steady-state values slightly after the phosphorylation. The relationship between the percent of light chains phosphorylated and percent maximum tension in 0.1 mM free Mg^{2+} was steep. Maximum steady-state tension occurred at low levels of light chain phosphorylation (0.2-0.25 moles of phosphate/mole of light chain). This rapid phosphorylation and steep relationship between steady-state tension and light chain phosphorylation was similar to results seen in this laboratory at high levels of free Mg^{2+} (1.0 mM). In contrast, when $MgATP\gamma S^{2-}$ was used to thiophosphorylate light chains, the rate of thiophosphorylation at low Mg^{2+} was less than that seen at high Mg^{2+}. The amount of tension associated with a given level of thiophosphorylation at 0.1 mM Mg^{2+} also was lower than that seen at the higher Mg^{2+} (1.0 mM). The reasons for these differences are at present unclear.

Supported by: NIH AR 37447-01A1, Muscular Dystrophy Association, American Heart Association (National and Florida Affiliate).

M-Pos335 ATPase ACTIVITY IN SKINNED GIZZARD CELLS CORRELATES WITH FORCE DEVELOPMENT. P.E. Hoar, and W.G.L. Kerrick. Depts. of [+]Physiology & Biophysics and [#]Pharmacology, Univ. of Miami Sch. of Medicine, Miami, FL 33101.

Bundles of skinned gizzard cells were used to measure the relationship between force, myosin light chain phosphorylation, and ATPase activity. ATPase activity was determined in an optical system (Guth K. & Wojciechowski R., Pflugers Arch. 407:552-557, 1986) which measures changes in NADH fluoresence caused by coupling oxidation of NADH to ADP production in the cells. Skinned gizzard cells in relaxing solution showed a low level of ATPase activity which was less than 5% of the maximum ATPase activity. Upon activation with Ca^{2+}, force and ATPase activity increased in parallel. When the cells were relaxed in low Ca^{2+} the force and ATPase decreased in parallel. Maximum Ca^{2+}-activated force was associated with 0.2 moles phosphate per mole myosin light chain. Additional phosphorylation of myosin light chains to 0.6 moles per mole with addition of calmodulin did not increase force or ATPase activity. Furthermore, thiophosphorylation of myosin light chains to 0.8 moles phosphate per mole light chain did not result in increased tension or ATPase activity. Maximum force and ATPase activity in the absence of Ca^{2+}, resulting from maximally thiophosphorylated myosin light chains, was not changed by high Ca^{2+}. These data suggest that ATPase activity in skinned gizzard cells correlates with tension development and not necessarily with the level of myosin light chain phosphorylation. Support: NIH AR37447-01A1, Muscular Dystrophy Assoc., American Heart Assoc. (National and Florida Affiliate).

M-Pos336 **PHOSPHORYLATION OF THE 20,000 DALTON LIGHT CHAIN OF MYOSIN IN GLYCERINATED PORCINE CAROTID ARTERY BY PURIFIED PROTEIN KINASE C.** Timothy A. Sutton and Joe R. Haeberle, Departments of Physiology/Biophysics and Medicine, Krannert Institute of Cardiology, Indiana University School Medicine, Indianapolis, IN 46202.

Phosphorylation of the 20,000-Da light chain (LC_{20}) of purified, smooth muscle heavy meromyosin by protein kinase C (PKC) alters the kinetics of LC_{20} phosphorylation by myosin light chain kinase (MLCK) as well as the phosphorylation-dependent stimulation of actin-activated myosin MgATPase activity (Nishikawa et al., J.Biol.Chem. 258:14069 & 259:8808). Using a glycerinated porcine carotid artery smooth muscle preparation and purified PKC, we investigated the effect of PKC phosphorylation on both endogenous MLCK activity and contraction. Muscles were contracted in the presence of 20 uM Ca^{2+} with and without PKC (1.6 uM), diolein (5 ug/ml), and phosphatidylserine (50 ug/ml) at 21oC. Incubation of a relaxed muscle with Ca^{2+} and PKC resulted in isometric force development to a peak value at 30 min which was 115% of that obtained in a previous control contraction with Ca^{2+} alone. Tryptic phosphopeptide maps of LC_{20} isolated from ^{32}P-labeled skinned muscles were compared to phosphopeptide maps of purified chicken gizzard (CG) LC_{20} phosphorylated either with purified MLCK or PKC. Muscles incubated for 30 min with Ca^{2+} plus PKC contained a single phosphopeptide which co-migrated with one of the two PKC-dependent phosphopeptides from CG LC_{20}. Muscles incubated for 30 min with Ca^{2+} minus PKC contained a single phosphopeptide which co-migrated with the MLCK-dependent phosphopeptide from CG LC_{20}. These findings suggest that phosphorylation of LC_{20} by PKC antagonizes LC_{20} phosphorylation by endogenous MLCK. The observation that skinned muscles maintain full isometric force in the absence of MLCK-dependent phosphorylation, suggests that phosphorylation by PKC of LC_{20} and/or other regulatory proteins may regulate force maintenance in smooth muscle. Supported by the NIH (AR 38834) and the American Heart Association.

M-Pos337 EVIDENCE FOR MULTIPLE KINETIC FORMS OF MYOSIN IN RELAXED SMOOTH MUSCLE. T.M. Butler, D.S. Pacifico and M.J. Siegman, Dept. of Physiol., Jefferson Med. Coll., Phila.,PA 19107

Permeabilized rabbit portal veins in rigor were incubated for 10 min in a relaxing soln containing ^{3}HATP, an ATP regenerating system, and a ^{14}C mannitol volume marker. The muscles were either frozen then or at various times after transfer to a similar soln containing unlabelled ATP. In the ^{3}HATP soln, there was a 60-70 μM excess of ^{3}HADP in the muscle over the nondetectable amount in the soln. Even though 96 ± 1% of the ^{3}HATP was removed after 1 min in the chase soln, the [^{3}HADP] in the muscle was 19 ± 2 μM after 4 min. This suggests that the ADP is bound to a site which is not accessible to CPK and is only very slowly replaced with ADP from ATP splitting. Thiophosphorylation of the myosin light chain (MLC) had no significant effect on the [^{3}HADP] in the muscle, but there was a more rapid release of ^{3}HADP into the chase soln. Following one min in ^{3}HATP, the difference in washout of label into the chase soln between relaxed and thiophosphorylated muscles was best described by two components containing 44 and 22 μM nucleotide with rate constants of 0.51 and 0.08 min^{-1}, respectively. The [myosin S_1] was 67 ± 7 μM from measurement of ^{35}S incorporation into the protein fraction following 100% thiophosphorylation of the MLC with ATPγ^{35}S. Thus, myosin seems to exist primarily in a complex with ADP under both relaxed and thiophosphorylated conditions, and thiophosphorylation of the MLC appears to cause an increase in the rate of release of ADP from all of the myosin. The multiple rates of ADP release might reflect different isoforms of myosin or the presence of a regulatory system which is affecting some of the myosin under relaxing conditions. The multiple kinetic forms present in relaxed muscle might persist under phosphorylated conditions, and there may be a 5-10 fold difference in cycling rates for different phosphorylated crossbridges in smooth muscle. (Sup. by HL 15835 to the PA Muscle Inst.).

M-Pos338 PHOSPHOCREATINE IS NOT DEPLETED IN URINARY BLADDERS FROM βGPA FED GUINEA PIGS. P.F. Dillon, R.A. Meyer, M-X He, and G.D. Romig, Departments of Physiology and Radiology, Michigan State University, East Lansing, MI 48824.

Guinea pigs were fed a diet of 2% β-guanidinopropionic acid (βGPA) for three months. During that time, the total creatine content of skeletal muscle was greatly reduced. In the smooth muscle dominated urinary bladder, however, there was no significant change in the ratio of phosphocreatine to ATP NMR resonances when compared with controls. There was a large variability in the βGPA phosphate peak, indicating independence of creatine and βGPA entry. The replacement of creatine with βGPA has been used as evidence for a creatine carrier in striated muscle, and the absence of competition may indicate the absence of a creatine carrier in smooth muscle. The additional phosphogen in smooth muscle enhances the maintenance of pH during after 2 hours of ischemia: 6.48±0.07 (SE) in βGPA bladders and 6.21±0.03 in controls. There were no differences in wet weight, dry weight, initial pH, initial or ischemic free Mg^{++}, or initial PCr to ATP ratio between the control and βGPA bladders. Supported by USPHS grants 34885, 24232, and 38235.

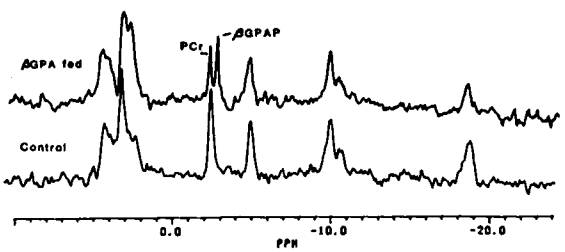

M-Pos339 31P-NMR MEASUREMENT OF ADP AND CALCULATION OF CREATINE KINASE EQUILIBRIUM CONSTANT. M.J. Fisher & P.F. Dillon, Depts. Physiol. & Radiol., MI State U., E. Lansing, MI

Saturation transfer studies of unidirectional reaction rates indicate that creatine kinase (CK) functions near equilibrium in skeletal and cardiac muscle. Smooth muscle CK activity is less well-defined. Nevertheless, assumed CK equilibrium constants (Kobs) are used in calculations of important respiratory regulators (viz., [ADP] and cytosolic phosphorylation potential). This study was designed to calculate Kobs in porcine carotid arteries after directly measuring all Lohman reaction components using 31P-NMR and enzymatic analyses. Segments of arteries were placed in a 10 mm NMR tube and superfused with low phosphate (Pi=0.12mM), high K+ (80mM), substrate-free PSS at room temperature (n=5). The superfusate was oxygenated (CONTROL), equilibrated with N2 gas (HYPOXIA), and finally re-oxygenated (POST-CONTROL) for 1.5 hrs/period. 31P-NMR measurements (Bruker AM-400 WB spectrometer) of intracellular pH and free Mg++, and relative areas (T1-corr.) of phosphorylated metabolites were made at 30 min intervals (1800 scans, TR=1 sec). An ADP peak area was directly defineable after 1 hr of hypoxia. In addition, a group of arteries were rapidly frozen with liquid N2 after CONTROL (n=5), extracted with ethanol-perchloric acid, and analyzed using the Lowry-Passonneau method. CONTROL [Creatine], [ATP], and [phosphocreatine (PCr)] were 1.4±0.07, 0.70±0.10 and 0.68±0.11 μmol/gm wet wt, (n=5). After 1.5 hrs of HYPOXIA, ATP and PCr had decreased by 15% (0.60±0.01mM) and 60% (0.22±0.02mM), resp., and [ADP]=0.20±0.02mM. The HYPOXIA Kobs=26.1±4.9, for pH=6.89±0.01 and Mg++=0.53±0.05. Using pH-corrected Kobs, [ADP]=0.11±0.01mM and 0.07±0.004mM for CONTROL and POST-CONTROL periods. These data show that in metabolically stressed smooth muscle, Kobs can be determined with few assumptions using ^{31}P-NMR, and, in turn, used to calculate [ADP] in healthy tissue. (Supp. by NIH AM34885)

M-Pos340 PHOSPHORYLATION OF MYOSIN HEAVY AND LIGHT CHAINS IN CULTURED RAT AORTA CELLS. Sachiyo Kawamoto and Robert S. Adelstein, NHLBI, NIH, Bethesda, MD 20892.

Rat aorta cells were cultured using conditions described in J. Biol. Chem. (1987) 262:7282. Postconfluent primary cultures of these cells were equilibrated with $^{32}P_i$ and smooth muscle myosin was purified by immunoprecipitation using polyclonal antibodies raised against mammalian smooth muscle myosin. Autoradiography of SDS-polyacrylamide gels revealed that the 204kDa myosin heavy chain (MHC) and myosin light chains (MLCs) were phosphorylated. Using two-dimensional gel electrophoresis (IEF/SDS) we were able to identify five different isoforms of the phosphorylatable MLC, including two with M.W. = 22,000 and three with M.W. = 20,000. Each of the isoforms was found to be partially monophosphorylated and diphosphorylated at sites known to be phosphorylated by MLC kinase. The average content of phosphate was 0.9 mol P/mol MLC. MHC was found to contain 0.7 mol P/mol MHC. Two-dimensional tryptic peptide maps of the MHC showed that the phosphate was confined to two peptides, one containing phosphoserine and the other both phosphoserine and phosphothreonine. The peptide containing phosphoserine alone was also found to be the single major phosphopeptide in the 204kDa MHC prepared from strips of rat aorta. Treating cultured cells with dibutyryl cAMP or forskolin resulted in a decrease in MLC phosphorylation and an increase in MHC phosphorylation. These observations raise the possibility of an additional regulatory mechanism in smooth muscle operating via MHC phosphorylation.

M-Pos341 Mg^{2+} CONTRACTIONS OF DETERGENT SKINNED SWINE CAROTID MEDIA. Robert S. Moreland and Suzanne Moreland. Bockus Research Institute, Graduate Hospital, Philadelphia, PA and The Department of Pharmacology, The Squibb Institute for Medical Research, Princeton, NJ.

Ca^{2+}-calmodulin dependent phosphorylation of the 20,000 M_r smooth muscle myosin light chain (MLC) results in high rates of shortening velocity and the rapid development of stress which has been hypothesized to be maintained by a separate Ca^{2+} dependent system characterized by low levels of MLC phosphorylation (MLC-P) and shortening velocity. This Ca^{2+} dependent stress without proportional MLC-P has been termed "latch" and the slowly cycling, stress maintaining crossbridges are called "latchbridges". The divalent cation Mg^{2+} has been shown to modulate contractions of smooth muscle and, in high concentrations, to elicit contractions that are MLC-P independent. The purpose of this study was to test the hypothesis that high concentrations of Mg^{2+} directly activate the regulatory process responsible for latchbridge formation. This was accomplished by comparing Mg^{2+} induced contractions of Triton X-100 skinned swine carotid media with the characteristics of the Ca^{2+} dependent latch state. The following results were obtained: 1) In the absence of Ca^{2+}, free Mg^{2+} (3 - 20 mM) caused an increase in shortening velocity and a concentration dependent increase in stress that was completely independent of MLC-P; 2) Mg^{2+} induced contractions could be supported by the ATP analog, CTP, which is a substrate for actomyosin ATPase but not the MLC kinase; 3) Stress development in response to Mg^{2+} was abolished at long tissue lengths which also inhibit the expression of latchbridges; 4) The calmodulin antagonist, trifluoperazine (TFP), inhibited the MLC-P independent contractions elicited by Mg^{2+}. TFP also inhibits the latch state. The results of this study are consistent with the interpretation that a MLC-P independent regulatory system may be present in vascular smooth muscle which can be directly activated by pharmacological levels of Mg^{2+}. This study was supported, in part, by NIH: HL 06532 and HL 37956.

M-Pos342 MYOSIN LIGHT CHAIN PHOSPHORYLATION IN CANINE CRANIAL TIBIAL ARTERIES *IN SITU*.
S.Moreland, L.M.Antes, and G.J.Grover. Department of Pharmacology, The Squibb Institute, Princeton, NJ.

Two regulatory systems are believed to control the contractile state of vascular smooth muscle *in vitro*. In one, crossbridges are phosphorylated by myosin light chain (MLC) kinase; in the other the crossbridges are unphosphorylated (latchbridges). The role of these systems in the control of vascular resistance *in vivo* is unknown. This study compared MLC phosphorylation (MLC-P_i) with vascular tone in an artery *in situ*. Cranial tibial arteries of pentobarbital anesthetized dogs were frozen in liquid N_2 cooled clamps. At rest, MLC-P_i was 0.52 ± 0.05 mol P_i/mol MLC. By 30-60 sec after initiation of norepinephrine (NE) infusion directly into the artery, blood flow (measured at the ipsilateral femoral artery) decreased to 46 ± 10% of control and MLC-P_i declined to 0.24 ± 0.03. *In vitro*, MLC-P_i in this artery was low at rest (0.09 ± 0.03) and increased transiently with NE stimulation (0.47 ± 0.01 at 1 min, 0.33 ± 0.1 at 10 min) while stress rose monotonically. The apparent contradiction between the *in situ* and *in vitro* results may be due to the increase in sympathetic nerve activity associated with pentobarbital anesthesia. At rest, the intermittent release of NE *in vivo* may stimulate the cells in a pulsatile manner resulting in continuous activation of MLC kinase and high levels of MLC-P_i similar to those measured at early times of NE stimulation *in vitro*. During the NE infusion *in vivo*, NE was present continuously rather than intermittently resulting in an eventual decrease in MLC-P_i analogous to the steady state situation *in vitro* when phosphorylated crossbridges were dephosphorylated and latchbridges apparently supported a greater percentage of tone. In other dogs, dosed with hexamethonium to block sympathetic ganglia, resting MLC-P_i was 0.18 ± 0.04. By 30-60 sec after initiation of NE infusion, MLC-P_i increased to 0.77 ± 0.06 and blood flow fell to 53 ± 22% of control. These data support the hypothesis that the high resting MLC-P_i in intact anesthetized dogs was due to a pentobarbital induced increase in sympathetic activity. The results of this study suggest that vascular tone can be maintained *in vivo* either by phosphorylated crossbridges or by latchbridges depending on dynamic changes in [NE] at its site of action on the vascular smooth muscle cells.

M-Pos343 REGULATION OF SHORTENING VELOCITY BY CROSSBRIDGE PHOSPHORYLATION IN SMOOTH MUSCLE.
Chi-Ming Hai and Richard A. Murphy. Department of Physiology, University of Virginia, Charlottesville, VA 22908.

We have proposed a model which incorporates a dephosphorylated "latchbridge" to explain the mechanics and energetics of smooth muscle (Am. J. Physiol., 1988, in press). Features of the model are: (i) myosin kinase and phosphatase can act on both free and attached crossbridges, and (ii) dephosphorylation of an attached phosphorylated crossbridge produces a non-cycling "latchbridge" with a slow detachment rate. This model predicts the latch state: stress maintenance with reduced phosphorylation, crossbridge cycling rates and ATP consumption. In this study, we adapted A.F. Huxley's formulation of crossbridge cycling (Progr. Biophys. Mol. Biol. 7: 255, 1957) to the latchbridge model to predict the relationship between isotonic shortening velocity and phosphorylation. The model successfully predicted the linear dependence of maximum shortening velocity at zero external load (V_o) on phosphorylation, as well as the family of stress-velocity curves determined at different times during a contraction when phosphorylation levels varied. Because phosphorylated cycling crossbridges and latchbridges interchange continuously through phosphorylation and dephosphorylation, the apparent attachment and detachment rates of the crossbridge population were a weighted average of the two crossbridge cycles. The result was a linear dependence of V_o on phosphorylation with no need to invoke an internal load or multiple regulatory mechanisms. (Supported by 5-P01-HL19242)

M-Pos344 PREGNANCY-INDUCED INCREASES IN STRESS OF OVINE UTERINE ARTERIES (UA) ARE NOT ASSOCIATED WITH ALTERATIONS IN ACTIN OR MYOSIN CONTENT OR MYOSIN HEAVY CHAIN (MHC) RATIO.
D.J.Annibale, C.R.Rosenfeld, K.E.Kamm, Depts. of Pediatrics and Physiology, Univ. Tx. Hlth. Sci. Cntr., Dallas, Tx., 75235.

We have shown that UA isolated from pregnant (P) ewes develop greater stress than those from nonpregnant (NP) animals (Fed. Proc. 46:652. 1987). In contrast, pregnancy did not alter the stress of carotid (CA) and renal (RA) arteries. Therefore, we investigated the hypotheses that the increased stress in UA is associated with alterations in MHC or actin contents or in MHC isoform. CA, UA and RA were dissected from NP and term P ewes. SDS homogenates of CA, UA and RA were subjected to 4% SDS-PAGE; MHC ratios were calculated from relative densities of MHC1 and MHC2. Additionally, UA samples were subjected to 3-20% gradient SDS-PAGE. Scans of these gels were used to calculate the relative proportion of actin and MHC as compared to total staining protein. No significant percent changes (mean±SD) in MHC (10±3 v. 10±2) or actin (34±7 v. 36±4) content were seen in UA isolated from NP or P ewes. The MHC ratio also was not significantly different for CA, UA nor RA isolated from P or NP ewes. The range of this ratio for UA was broad, 0.9-2.2, as compared to 1.1-1.6 for CA and 1.1-1.4 for RA (1.5±0.4 [n=17]; 1.3±0.2 [15]; and 1.2±0.1 [9] respectively). Alterations in MHC content, MHC isoform, or actin content do not explain increased stress observed in UA isolated from pregnant ewes. (Supported by HL32607, HD07308, and HD08783.)

M-Pos345 MECHANICS OF INTACT SINGLE SMOOTH MUSCLE CELLS STUDIED BY TENSION TRANSIENT ANALYSIS. M.Yamakawa, D.Harris*, and D.Warshaw, Physiol. & Biophys., U. of Vermont, Burlington, VT 05405.

To access the crossbridge cycle in smooth muscle, we measured tension transients in response to a rapid change in length in single smooth muscle cells isolated from the gastric muscularis of the toad, Bufo marinus. Cells, in amphibian physiological saline, were tied between an ultrasensitive force transducer and piezoelectric length driver (J. Gen. Physiol. 82: 157, 1983). Small, rapid step stretches and releases of cell length (< = 2%, complete in 3.6 ms) were applied to relaxed and electrically stimulated isometrically contracting cells. Minimal tension responses were observed in relaxed cells. However, in activated cells, tension increased during the stretch and decreased during the release. Upon completion of the length step, tension recovered fully with a time course best fit by two exponentials (40-100 and 1-5s^{-1}). For 2% length steps, both rate constants for the fast and slow recovery processes were faster for stretches than for releases. To correlate tension recovery to structures associated with force production, we measured cell stiffness ($\Delta F/\Delta L$) during tension transients by superimposing sinusoidal length perturbations (200 Hz, ΔL=0.5% cell length) on the length steps and recording the resultant sinusoidal force response (ΔF). Significant changes in stiffness amplitude were observed during tension transients, which in some cases dissociated from the tension time course. Since negligible phase shift between ΔF and ΔL occurred during the transients, the changes in stiffness amplitude represent changes in pure elastic stiffness without significant viscosity changes. Rate constants for tension recovery and their dependence on the amplitude of the length step along with stiffness changes in single smooth muscle cells suggest that significant differences in the crossbridge cycle kinetics exist relative to fast skeletal muscle. (Supported by: NIH AR34872, HL35684)

M-Pos346 STRESS AND SHORTENING VELOCITY IN RABBIT RENAL ARTERY. P. H. Ratz. Department of Pharmacology, Eastern Virginia Medical School, Norfolk, VA 23501.

Release of intracellular calcium (Ca_i) is primarily responsible for the rapid increase in stress and crossbridge phosphorylation and cycling rates that occur upon agonist-activation in swine carotid media (SCM). Rabbit renal artery (RRA) was investigated since contractions in this artery are thought to be largely dependent on release of Ca_i. Length-tension curves showed that in the intact RRA, the ratio of passive to active force at optimal length (L_o) was 0.11 +/- 0.02 (n=7), a value nearly identical to that reported for SCM. As in SCM, passive force was zero below 0.8 L_o. However, passive force at 1.2 L_o was only 0.40 +/-0.09 F_o (n=6) in the RRA, whereas the value reported for SCM is greater than 1.6 F_o. The active length-tension curve (109.6 mM KCl) in RRA was broader than that reported for SCM; force at 0.5 L_o and 1.2 L_o was 0.56 +/- 0.08 F_o (n=5) and 0.82 +/- 0.04 F_o (n=6), respectively. F_o was 2.46 x 10^5 N/m^2 (n=7). Estimates of muscle shortening rates were obtained at 1 and 10 min of phenylephrine-induced (1 uM) contractions by measuring the half-time for force re-development ($t_{1/2}$) after quick releases from 1.1 L_o to 1.0 L_o and by measuring isotonic shortening following quick releases to different loads and extrapolating to zero load (V_o). As in SCM, muscle shortening in RRA declined from 1 to 10 min of activation ($t_{1/2}$ at 1 min: 6.26 sec +/- 0.67 (n=5); 10 min: 10.9 +/- 0.46 (n=4); V_o at 1 min: 0.081 L_o/sec (n=1); 10 min: 0.055 L_o (n=1)). At comparable times of muscle activation, the rate of muscle shortening in RRA appeared to be almost 2-fold faster than reported for SCM. Whether this is a direct result of comparably higher levels of myosin phosphorylation due to mobilization of Ca_i is under investigation.

M-Pos347 CHARACTERIZATION OF LAMB TRACHEAL SMOOTH MUSCLE (LTSM) FIBER BUNDLES. Kazuo Obara, Johann Caspar Rüegg* and Primal de Lanerolle, Dept. of Physiology and Biophysics, Univ. of Illinois, Chicago, IL and *II. Physiologisches Institut, Univ. of Heidelberg, F.R.G.

Studies on the role of myosin phosphorylation in regulating the contractile properties of tracheal smooth muscle have shown conflicting results, perhaps due to the presence of diffusional barriers in these relatively thick (0.5 mm) tracheal preparations. We have microdissected fiber bundles that are 0.1-0.2 mm in diameter from LTSM and characterized the contractile properties of these fibers. We find that they contract rapidly and generate maximal force ($2-5x10^5 N/m^2$) in 30-40 secs following the addition of methacholine (MC). The unloaded velocity of shortening (V_{us}) also peaks at 15 secs and declines to about 45% of maximal V_{us} by 5 mins. Myosin phosphorylation increases from a resting level of 0.24 mol PO_4/mol LC_{20} to a peak of 0.49 mol PO_4/mol LC_{20} at 15 secs and then plateaus at 0.40 mol PO_4/LC_{20} at 2 mins following the addition of 10^{-6} M MC (which generates about 85% of maximal force). Isoproterenol pretreatment attenuates the contractile response and causes a rightward, non-parallel shift in the MC dose-response curves for active tension and suprabasal myosin phosphorylation. These data demonstrate that LTSM fiber bundles are a useful model for studying the regulation of smooth muscle contraction.

M-Pos348 THE EFFECT OF OKADAIC ACID (OA), A PHOSPHATASE INHIBITOR, ON THE CONTRACTILE PROPERTIES OF LAMB TRACHEAL SMOOTH MUSCLE (LTSM). Akira Takai, Kazuo Obara*, Johann Caspar Rüegg and Primal de Lanerolle*, II. Physiologisches Institut, Univ. of Heidelberg, F.R.G. and *Dept. of Physiology, Univ. of Illinois, Chicago, IL.

OA is a toxin purified from the marine black sponge. It is a potent phosphoprotein phosphatase inhibitor (Takai et al., FEBS Lett. 217:81-84,1987) that contracts both skinned and intact smooth muscles (Shibata et al., JPET 223:135-143, 1982). We have compared the effects of OA (50 μM) with those of 10^{-6}M methacholine (MC; which generates about 85% of maximal force) on LTSM fiber bundles (0.1-0.3 X 4-6 mm). OA slowly contracts LTSM (T_{50}=621 secs compared to 14 secs for MC) and this contractions occurs in the presence or absence of external calcium. OA induced about 20% more force than 10^{-6}M MC and myosin phosphorylation also increased at maximal force generation. The unloaded velocity of shortening (V_{us}), determined by releasing the muscle to 80% of L_o, increased as force increased in fibers treated with OA but V_{us} remained lower than V_{us} measured in the MC precontraction. However, the addition of 10^{-6}M MC to fibers maximally contracted with OA increases V_{us} to a level comparable to the MC precontraction. These data demonstrate that inhibition of phosphoprotein phosphatase activity leads to force generation and increases in V_{us} and in myosin phosphorylation, apparently in the absence of an increase in intracellular calcium.

M-Pos349 **AN IMPROVED TISSUE PREPARATION FOR SMOOTH MUSCLE EM IMMUNOCYTOCHEMISTRY**

L.J. McGuffee, S.A. Little and R.M. Bagby*, Department of Pharmacology, University of New Mexico, Albuquerque, NM, 87131 and *Department of Zoology, University of Tennessee, Knoxville, TN 37996. (Intro. by J.A. Trotter)

A major limitation to the use of electron microscopic (EM) immunocytochemistry is the loss and/or translocation of antigenicity during tissue preparation. We have previously shown that EM immunolocalization of calcium binding proteins in cardiac tissue can be improved by quick freezing, freeze–drying and embedding tissue at low temperature (Jorgensen and McGuffee, J. Histochem. Cytochem. 35:723–732, 1987). In the present study, we examined the loss and relocation of myosin label in freeze–dried and in chemically fixed rat mesenteric artery. Labeling in the cytoplasm is about five times higher in freeze–dried compared to chemically fixed cells. Labeling over organelles is essentially zero in freeze–dried cells. These results show that both loss and translocation of myosin antigenicity can be avoided by freeze–drying the tissue followed by embedding at low temperature. We anticipate that this preparation will be useful for EM immunocytochemistry of other less prevalent proteins in muscle. Supported in part by NIH GM30003 and an Established Investigatorship of the American Heart Association.

M-Pos350 ANALYSIS OF DENSE BODY MOTION IN CONTRACTING SMOOTH MUSCLE CELLS. G.J. Kargacin, P.H. Cooke, S.B. Abramson, L.M. Isenstein, K.E. Fogarty and F.S. Fay., Dept. of Physiology, Biomedical Imaging Group, U.Mass. Med. Ctr., Worcester, MA 01655

Saponin permeabilization of isolated smooth muscle cells altered their optical properties so that contractile structures became visible under the phase contrast microscope. The cells were able to shorten in response to Ca^{++} and ATP and thus provided us with an opportunity to study the movement of contractile elements during shortening. In particular, we identified individual dense bodies within the cells, collected digital images at fixed time intervals during shortening to follow the movement of these bodies and plotted their positions on a reference frame oriented along the cell. Cluster analysis and analysis of the relative motion of bodies indicated that some bodies remained at more or less fixed distances from one another during shortening. These bodies fell into laterally oriented groups that, in most cases, were found at intervals along the long axis of the cell. The most rapid shortening in the cells appeared to occur between bodies in separate groups. Computer reconstructions of optically sectioned fixed cells stained with an antibody to alpha-actinin revealed the existence of areas along the cell where the number of dense bodies was relatively high interspersed between areas with fewer bodies. The axial spacing of the high density areas was approximately the same as that of the semi-rigid groups found in the motion analysis. Although further experiments will be necessary to correlate the findings of the two approaches, our results suggest that force may be generated primarily between groups of bodies indicating that smooth muscle may be more ordered than previously thought. The methods we have used in this study should also be applicable to the analysis, in other cells, of the motion of subcellular particles and the forces acting upon them. Supported by NIH grants HL14523 and AM07341.

M-Pos351 INTERMEDIATE Pi $\rightleftharpoons$ HOH EXCHANGE DURING ACTIN-ACTIVATED ATP HYDROLYSIS BY HMM. John A. Evans, Laboratory of Cell Biology, NHLBI, NIH, Bethesda, MD 20892.

The consensus that myosin S-1 shows a single pathway of O^{18} exchange, both in the presence and absence of actin, does not hold for HMM. Shukla and Levy have suggested that both myosin and tryptic HMM, but not chymotryptic HMM, show two pathways of O^{18} exchange. In the case of myosin, this is not surprising since the presence of myosin filaments could lead to heterogeneous interaction of the myosin heads with actin, but it is surprising that there are two pathways with HMM, which in other respects has proven to be similar to S-1. In the present study we have reinvestigated the question of whether the actin-activated ATPase activity of HMM shows two pathways of exchange, using tryptic HMM as well as two different kinds of chymotryptic HMM. We made certain that the HMM preparations were free of myosin contamination and used a very low ionic strength (μ = 12 mM) so that we could work over a wide range of actin-activated ATPase activity. Our results for all three types of HMM could be fit assuming that, from 2 to 5 μM actin concentration, 80-90% of the HMM shows the same actin activated ATPase activity and the same single pathway of O^{18} exchange as does S-1, while 10-20% of the ATPase activity proceeds without any exchange. Above 5 μM actin the data could be fit either by making the above assumption or by simply assuming a single pathway of exchange. It is likely that the 10-20% of the HMM which does not show normal O^{18} exchange at low actin concentration is denatured in some way, either by SH oxidation which has been shown to affect the level of O^{18} exchange or possibly by proteolysis occurring during the preparation of the HMM. Therefore, we think it very unlikely that the two pathways of O^{18} exchange we observe at low actin concentration are a normal feature of the actin-activated HMM ATPase activity.

M-Pos352 DOES ACTIN RELEASE ATP FROM MYOSIN BOUND ATP ? T. Barman & F. Travers, INSERM U 128, CNRS, B.P. 5051, 34033 MONTPELLIER Cedex,France

The binding of ATP to S1 (M + ATP $\rightleftarrows$ M.ATP $\xrightarrow{k2}$ M*.ATP) was studied by the ATP chase method. Such experiments give a rapid rise of Pi of amplitude Pi/M = kcat /(kcat + k-2) followed by kcat. The amplitude is sensitive to kcat/k-2 ; with S1 k-2 < kcat and Pi/M = 1 i.e. Pi gives [active site]. Sleep & Hutton (Biochemistry 17, 5423 : 1978) propose that actin interacts with M*.ATP resulting in k-2 > kcat. We tested this proposal by carrying out ATP chase experiments in water or 40 % ethylene glycol : (1) with [actin] $\backsim$ Km for actin, at 15°C, 5mMKCl, 50mMTris, pH8 ; (2) with [actin] > Km, at -15°C, 5mMKCl, 5mMTris, pH8 and (3) with crosslinked acto S1. In all cases Pi/M was high and equal to the amplitude with S1 alone from which k-2 < 0.2kcat. These apparently contradictory results can be explained by the absence of M*.ATP on the acto-S1 pathway : the S1 released from acto-S1 by ATP has a different conformation (M+.ATP) which may not interact with actin. Thus, when ATP is mixed with acto S1, k-2 remains < kcat but when actin is added to M*.ATP, k-2 could become > kcat. Another explanation could be due to the presence of a type of S1 which binds ATP reversibly without hydrolysis.

Biosca, Barman & Travers (1984) Biochemistry 23, 2428.
Biosca, Travers, Barman, Bertrand, Audemard & Kassab (1985) Biochemistry 24, 3814.

M-Pos353 THE ACTIN DEPENDENCE OF THE TWO PATHWAYS FOR OXYGEN EXCHANGE BY HEAVY MEROMYOSIN. Kamal K. Shukla, James F. Marecek and Harvey M. Levy, Department of Physiology and Biophysics, School of Medicine, SUNY at Stony Brook, Stony Brook, N.Y. 11794.

There is now good evidence for two pathways in the hydrolysis of MgATP by actomyosin. One pathway (P1) shows a low level of intermediate oxygen exchange; the other (P2) shows a high level of exchange. We have used chymotryptic heavy meromyosin (HMM) to determine the actin dependence of the fluxes along the two pathways. The exchange is analyzed by using [γ-^{18}O]MgATP as substrate and measuring the distribution of ^{18}O in the product P_i. The experimental distributions are fit to theoretical distributions based on the kinetics of actomyosin MgATPase. The analysis gives the relative flux along P1 and P2; the absolute flux is given by the product of the relative flux times the measured total flux, k_{cat}. A plot of the flux (sec^{-1}) of P1 (on the ordinate) vs the actin concentration is sigmoid whereas the same plot for P2 is biphasic rising relatively rapidly to a peak. Thus over low levels of actin, the sigmoid curve of P1 lags below the curve of P2; at an intermediate level of actin the curves cross, i.e. the fluxes are equal, and with increasing actin the flux of P1 rises above P2. The maximum apparent flux of P1 was about 7 sec^{-1} near 100 μM actin (23°C, pH 7.4, no added KCl); for P2 it was about 2.5 s^{-1} at a significantly lower actin level, about 25 μM actin. The findings suggest that P2 involves the interaction of HMM with one actin unit whereas P1 involves the interaction of HMM with two actin units. (Supported by NIH Grant AR 36701.)

M-Pos354 ISOMETRIC CONTRACTION INDUCED BY PHOTOLYSIS OF CAGED ATP - AN EPR STUDY.
P.G. Fajer, E.A.Fajer, and D.D. Thomas, Department of Biochemistry, University of Minnesota, Minneapolis, MN 55455.

In order to avoid the problem of a rigor core (regions in the center of perfused muscle fiber bundles that do not receive saturating ATP during isometric contraction), we have used the photolabile precursor of ATP, caged ATP. Glycerinated rabbit psoas fibers were labeled on the fast-reacting thiol SH1 with maleimide spin label modifying at least 50% of the myosin heads. The fibers were incubated for 30 minutes in a 5 mM solution of caged ATP prior to the photolysing UV laser flash. The flash liberated 2-3 mM ATP (and a minimum of 0.2 mM throughout the fiber bundle). The tension generated during the EPR measurement was at least 90% of the maximum tension produced with 5 mM ATP using an unlabeled single muscle fiber. Doubling the intensity of light, or providing an ATP backup system, had no effect on the EPR results. Before, during and after the flash, the spectral position was monitored at a position corresponding to the highly oriented probe in rigor. In the absence of Ca++ the intensity dropped quickly to a steady-state value identical to that obtained in relaxation using ATP. In the presence of Ca++ the steady-state level reached was that observed in relaxation but the spectrum recovered much more quickly towards the rigor value reflecting the increased ATPase. We conclude that in isometric contraction the fraction of spin labels (and presumably heads) with rigor-like orientation is similar to that observed in relaxation.

M-Pos355 Resolution of Myosin Conformational States During Contraction of Glycerinated Fibers
Kiandokht Beyzavi, Vincent A. Barnett, & David D. Thomas, University of Minnesota Medical school, Mpls, MN 55455.

We have used conventional electron paramagnetic resonance (EPR) spectroscopy on iodoacetamide spin labeled (IASL) myosin in glycerinated psoas fibers to study the conformational dynamics of myosin during isometric contraction. The rigor spectrum showed that all probes were strongly immobilized (no nsec motion) and highly oriented relative to the fiber axis. In relaxation, all of the probes became disordered. These disordered probes were resolved into two components, both of which showed mobility in the nsec range, but one was more weakly immobilized than the other. (Barnett, et al.1987 Biophys meeting). Digital analysis of the contracting fiber spectrum showed that it was a linear combination of 30% rigor and 70% relaxing fiber spectra. Thus we have resolved contracting fibers spectrum into 3 components: (1) 30% rigidly oriented as in rigor, (2) 29.1% disordered and exhibiting moderate rotational freedom (3) 41.2% disordered and weakly immobilized. These studies correspond qualitatively with previous studies with MSL (Cook, et al.1982 Nature), but MSL does not become weakly immobilized by ATPand it only shows a single mobile population present during the relaxed state. Therefore both probes report a small percentage of rigor-like myosin heads during isometric contraction but they perturb this fraction to a different extent (MSL 20%, IASL 30%).

M-Pos356 KINETICS RELATING CALCIUM AND FORCE IN SKELETAL MUSCLE (Intr. by M.J. Poznansky)
Stein, R.B.[1,2], J. Bobet[1], M.N. Oguztoreli[2], and M.W. Fryer[3], Departments of Physiology[1] and Mathematics[2], University of Alberta, Edmonton, Alberta, Canada and School of Physiology and Pharmacology[3], University of New South Wales, Sydney, N.S.W., Australia.

Different models for predicting the time course of muscle tension from that of intracellular calcium ion concentration were compared. Calcium and force transients from rat and frog skeletal muscle were obtained for a variety of stimulation patterns. Mathematical descriptions of several possible mechanisms relating force and calcium were developed. These were fitted to the data using a nonlinear fitting algorithm, and the goodness of fit of each model was evaluated. The scheme proposed by Ashley and Moisescu (Nature New Biol. 237:208-211, 1972) in which the kinetics of calcium binding by troponin are rate limiting for force generation did not generally produce a good fit. A scheme in which the crossbridge cycle was rate-limiting and the rate constant for crossbridge detachment increased abruptly at the onset of relaxation produced good fits for all records, and could account for both the nonlinearities observed in twitch summation and the sigmoid shape of the steady-state force-p Ca^{2+} relation.

Supported by the Musacular Dystrophy Association of Canada and the Natural Sciences and Engineering Research Council of Canada.

M-Pos357 PROBES UNIQUELY ATTACHED TO THE LIGHT CHAINS OF MYOSIN. B.D. Hambly, K. Franks and R. Cooke (introduced by S. Koons) Dept. of Biochem./CVRI, Univ. of California, San Francisco, CA
Spectroscopic probes bound to the SH-1 and ATPase sites of the myosin crossbridge have produced data, albeit controversial, concerning changes in orientation of, and proportion of, bound cross-bridges during contraction. Due to their location close to the thin filament, these sites are not sensitive to changes in crossbridge orientation in regions closer to the thick filament. It is desirable to find appropriate probe label sites closer to the thick filament. The myosin light chains (LC's), located in this proximal region of the crossbridge, may be labelled in vitro, then exchanged into either isolated myosin or glycerinated muscle fibers. Labelling experiments have been conducted on the most readily exchangeable LC, the regulatory LC2. Three sites on rabbit skeletal muscle LC2 have been labelled. (1) A succinimidyl paramagnetic probe has been attached to a reactive Lys/s. Approximately one mole/mole of LC2 appears to preferentially bind to LC2 under defined conditions. We are currently defining the location of this probe. This probe incorporates readily onto the myosin heavy chain. (2) A chromophoric probe specific for Trp residues has been used to specifically label the single Trp located in the C-terminal domain of LC2. (3) The two Tyr of LC2, also located in the C-terminal domain, have been uniquely labelled with an imidazole paramagnetic probe. This probe appears to impair the binding of LC2 to the myosin heavy chain. The benzyl ring of each of the two Tyr's has been nitrated to produce strongly chromophoric residues. We are currently optimizing conditions for exchange of LC2 onto the myosin heavy chain in various preparations. Synthesis of probes based on those described and capable of suitable immobilization is proceeding. Supported by the NH&MRC of Australia and USPHS AM30686.

M-Pos358 THE KINETICS OF MYOSIN SUBFRAGMENT-1 INTERACTION WITH ACTIN IN THE ABSENCE OF NUCLEOTIDE. Shwu-Hwa Lin and Herbert C. Cheung, Graduate Program in Biophysical Sciences and Department of Biochemistry, University of Alabama at Birmingham, Birmingham, AL 35294

We previously showed that the interaction of actin with myosin subfragment-1 labeled at SH_1 with 5-iodoacetamidofluorescein (S-1•AF) was accompanied by a two-fold increase in the emission intensity of the attached fluorescein moiety (Aguirre, et al., (1986) Biochemistry 25:6827). The kinetics of this interaction has been studied in stopped-flow experiments in 60 mM KCl, 30 mM TES, pH 7.5, and 18 °C. The S-1•AF intensity increased by ca. 50% upon mixing, followed by a slower increase before it reached a constant level. The initial increase was too rapid to be resolved. The kinetic traces of the slow fluorescence change could not be fitted with a single exponential. Most of the traces could be fitted to a biexponential function yielding two observed rate constants. At [S-1] = 2.7 μM and [actin] = 18 μM, $k_1 \sim 34\ s^{-1}$ and $k_2 \sim 4\ s^{-1}$. Thus about 50% of the total fluorescence increase that was previously observed for the formation of acto•(S-1•AF) resulted from formation of an initial enounter complex. The remaining fluorescence increase was due to structural changes that occurred in two steps under our experimental conditions. The results are compatible with a model in which acto•S-1 exists in two states. Work supported in part by NIH grant AR 31239.

M-Pos359 DIFFERENT CROSSBRIDGE DISSOCIATION RATES IN SKINNED MUSCLE FIBERS OF RABBIT SOLEUS AND PSOAS MUSCLE. G.J.M. Stienen and M.C.M. Roosemalen. Laboratory for Physiology, Free University, van der Boechorststraat 7, NL-1081 BT Amsterdam, The Netherlands.

Force (P) -velocity (V) relationships were determined at different ATP concentrations in chemically skinned fiber segments of rabbit soleus muscle and, for comparison under identical conditions, in fast fiber segments of rabbit psoas muscle. The activating solutions contained 60 mM Imidazole (pH=7.1), 20 mM CaEGTA (pCa=4.4), 26 mM PCr, 200 U/ml CPK, 1 mM free Mg_o, MgATP varied between 10 uM and 5 mM, ionic strength 200 mM (adjusted with KCl), temperature 15 °C. Shortening velocity was determined from the initial slope of a single exponential fitted, over a period of 100 ms, to the early part of the displacement signal during steady shortening. The maximum shortening velocity (Vmax) was obtained from a hyperbola of the form $(P+a)(V+b)=b(Po+a)$, fitted to the data. At 5 mM MgATP, the slow soleus muscle fibers had a maximum shortening velocity (Vmax) of 0.51±0.05 Lo/s (mean±s.e.m.); Lo: segment length at a sarcomere length of 2.4 um, and a curvature (a/Po) of 0.12±0.01. The corresponding values for psoas fibers were 3.05±0.21 Lo/s and 0.17±0.03. Vmax as a function of the ATP concentration followed in both cases the hyperbolic Michaelis-Menten relation. The Km (±S.D.) for ATP of Vmax for the soleus fibers was 0.12±0.03 mM. For the psoas fibers a Km value of 0.15±0.03 mM was obtained. From the Vmax and Km values, the apparent dissociation rate (K1k2) for the actomyosin complex can be calculated (c.f. Ferenczi et. al., J. Physiol. 1984, 350:519-543). For soleus fibers, this results in a K1k2 value of about $5.10^5\ M^{-1}s^{-1}$, which is considerably smaller than the value of $2.10^6\ M^{-1}s^{-1}$ obtained for psoas fibers.

M-Pos360 DIFFERENTIAL BEHAVIOR OF TWO CYSTEINE RESIDUES ON THE MYOSIN HEAD IN MUSCLE FIBERS. T. Miyanishi & J. Borejdo. Cardiovascular Research Institute, University of California, San Francisco, CA 94143, U.S.A.

We have previously shown that the orientation of iodoacetoamido tetramethylrhodamine (IAR) labels on SH_1 thiol of S-1 moieties changes upon adding MgADP to the fibers in rigor (Borejdo et al., 1982; Burghardt et al., 1983). Here we report the results of experiments in which the SH_2 of S-1 was labeled. This was accomplished using maleimidorhodamine (MLR) in the presence of MgADP, having initially blocked SH_1 with iodoacetoamide (IAA) or with fluorodinitrobenzene (FDNB). FDNB could later be removed to restore SH_1. The specificity of modification of thiols was checked by measuring the stoichiometry of attached dye, by determining the extent of the decrease in EDTA(K^+)- and CA^{++}-ATPase activities and by the localization of the dyes on peptides containing SH_1 and/or SH_2. Labeled S-1 was diffused into single glycerinated fibers of rabbit psoas muscle and the orientation of chromophores was measured by fluorescence detected dichroism. The dye attached to SH_1 was oriented at about 63° with respect to the fiber axis in rigor and about 50° in the presence of MgADP, regardless of whether SH_2 was modified or not. The dye on SH_2 was oriented near 46° both in the presence and in the absence of ADP, regardless of whether SH_1 was modified or not. Our results show that rhodamine oriented differently when attached to SH_2 compared with when attached to SH_1, and that in the former placement it was not sensitive to MgADP. We think this indicates that the SH_2-containing region has a different mobility to that of the SH_1-containing region, i.e. that this is evidence for internal flexibility of S-1. Supported by Amer. Heart Assn. CI-8 and USPHS HL16683.

M-Pos361 RATE OF ATP RELEASE DURING ATP HYDROLYSIS BY GLYCERINATED FLIGHT MUSCLE FIBRES OF THE GIANT WATER BUG, Lethocerus collosicus. Martin R. Webb*, John Lund+, J.L. Hunter* and David C.S. White+ *National Institute for Medical Research, Mill Hill, London NW7 1AA, U.K. and +Department of Biology, University of York, York YO1 5DD, U.K.

We have used oxygen exchange techniques to measure the rate of ATP release from insect flight fibers for a variety of different activations. When fibers are bathed in a solution containing ATP in $H_2{}^{18}O$, phosphate-water oxygen exchange occurs during ATP hydrolysis. The P_i product contains a distribution of ^{18}O atoms (Lund, Webb and White, (1987) J. Biol. Chem. 262, 8584-8590). During this hydrolysis, some ATP is released (by reversal of the ATP binding step). This ATP must necessarily have also experienced oxygen exchange, to the same extent as P_i formed on the same kinetic pathway. By measuring both the rate of this ATP:$H_2{}^{18}O$ exchange and the distribution of ^{18}O in ATP, concurrently with the exchange in P_i, we have obtained the rate constant for ATP release. This is 0.5 s^{-1} (22°C, I = 200 mM) for either maximally oscillation- or strain-activated fibers, 1 s^{-1} for Ca^{2+}-activated, slack fibers and 1-2 s^{-1} for relaxed fibers. These values assume a single kinetic pathway operates within the fiber. This is the situation for mechanically-activated fibers, but an oversimplification for the non-mechanically-activated state for which the ATP exchange distribution supports a model with multiple pathways of hydrolysis. Supported by the Medical Research Council (UK).

M-Pos362 THE DIPROTONATED FORMS OF INORGANIC PHOSPHATE (Pi) AND ITS ANALOG ARSENATE (Ars) DEPRESS FORCE IN SKINNED CARDIAC MUSCLE FIBERS. T.M. Nosek, M.P. McLaughlin, & R.E. Godt, Dept. of Physiol. & Endo., Medical College of Georgia, Augusta, GA 30912.

The depression of force with fatigue of skeletal muscle and hypoxia of cardiac muscle is attributed, at least in part, to an increase in intracellular [Pi]. In skeletal muscle, maximum Ca^{2+} activated force (Fmax) appears to be inhibited by the $H_2PO_4^-$ form of Pi (Nosek et al. Science 236:191, 1987) and by the structurally similar analogs Ars and vanadate (Van) (Nosek et al. Biophy. J.51:5a, 1987). The purpose of this study was to determine whether Fmax of chemically skinned (Triton X-100) rabbit papillary muscle is affected similarly by Pi, Ars (both at 30 mM total), and Van (0.1 mM total). The concentrations of the diprotonated forms of Pi (pK 6.78) and Ars (pK 6.8) were increased by changing the pH from 7.4 to 6.2. The pK of Van (8.23) precluded changing its protonation significantly over this pH range. All three compounds depressed Fmax, with the effect of Van >> Ars > Pi, compared to the pH-matched control. The decrease in Fmax by Van was not significantly affected by the change in pH. However, the depressant effects of Pi and Ars were significantly greater at pH 6.2. Thus, we conclude that Fmax of both cardiac and skeletal muscle appears to be inhibited by the diprotonated forms of Pi and Ars. (Support: Dean's Res. Fellow. and NIH HL/AR 37022 & AR 31636).

M-Pos363 CHARACTERIZATION OF *IN VITRO* MOVEMENT OF ACTIN FILAMENTS DIRECTED BY MYOSIN FRAGMENTS BOUND TO A NITROCELLULOSE SURFACE. S.J. Kron, Y.Y. Toyoshima and J.A. Spudich (Intr. by T.G. Wensel) Cell Biology, Stanford University School of Medicine, Stanford, CA 94305

By replacing the glass surface with a nitrocellulose film, we have modified the *in vitro* motility assay to observe actin sliding movement directed by the soluble fragments of myosin, HMM and S1 (Toyoshima *et al.*, *Nature* 328:536-539, 1987). We have characterized this assay with respect to the effects of various chemical and physical parameters. The ionic strength, pH and ATP dependence of actin sliding movement on an HMM surface were similar to that of movement on myosin filaments. We studied the dependence of movement on the length of the actin filaments and the density of HMM on the nitrocellulose surface. Over the range of actin lengths from 0.5 to 20 μm, there was no significant difference in the rate of actin sliding movement. When actin affinity purified HMM was used to examine the effect of HMM density, actin sliding movement could only occur at densities greater than 300 HMM molecules per μm^2, and above this density, the rate of movement was nearly constant. In contrast, the dependence on density of unpurified HMM showed a gradual increase in sliding speed above a limiting threshold density. NEM inactivated HMM when mixed at a 1 to 10 ratio with unmodified HMM inhibited the rate of movement by 50%. These results suggest that this assay is applicable to a wide range of experimental conditions but is very sensitive to the quality of the protein preparation.

M-Pos364 VISUALIZATION BY ELECTRON MICROSCOPY OF THE INTERMEDIATES IN THE ACTOMYOSIN CYCLE PREPARED BY A RAPID-FREEZING/STOPPED-FLOW METHOD. T.D. Pollard, D.G. Bhandari, P. Maupin, J. Sinard. Dept. of Cell Biology and Anatomy, Johns Hopkins Med.Sch.,Baltimore, MD 21205.

We have constructed a device to mix 2 samples rapidly and then rapidly freeze the reaction products at millisecond time intervals. The frozen samples can then be freeze-fractured, etched and coated in preparation for electron microscopy. We have used this method to study the structure of the weakly bound intermediates in the actomyosin ATPase cycle. High concentrations of actin filaments and myosin subfragment-1 were used to achieve a substantial population of these intermediates attached to actin in the presence of ATP without chemical crosslinking. Individual myosin heads are easily resolved in these replicas and those attached at different azimuthal angle around the actin helix can be identified in comparison with published 3-D reconstructions of fully decorated filaments. The structure of the bound myosin heads was evaluated by blinded observers who measured the angle that the bulk of each head made with the long axis of the filament. Rigor complexes are bound at an average angle of 40-50°. Most of the weakly bound intermediates (a mixture of A·M·ATP and A·M·ADP·P_i) are also bound at about 45°, but there is reproducibly a minor population of myosin heads at about 90°. This indicates that the main mass of the head is bound to actin at approximately the same orientation in rigor (with no nucleotide in active site) and in the weakly attached states (with ATP or products at the active site). Thus the motion-producing structural changes that occur when the products dissociate must be within the myosin head or near the head-tail junction. (Supported by NIH grant GM26132, a grant from MDA and a postdoctoral fellowship from the American Heart Association.)

M-Pos365 STRUCTURE-ACTIVITY RELATIONSHIPS OF CHLORIDE-SENSITIVE FLUORESCENT INDICATORS FOR BIOLOGICAL APPLICATIONS. R. Krapf, N.P. Illsley, H.C. Tseng and A.S. Verkman (spon. by P.-Y. Chen). Cardiovascular Research Institute, Univ. of California, San Francisco, CA 94143.

The quinoline compound 6-methoxy-N-(3-sulfopropyl) quinolinium (SPQ) has been applied to measure membrane transport of chloride in biological systems. To understand the structure-activity relationships of compounds with chloride-sensitive fluorescence properties, 25 structural analogues of SPQ with 2 and 3 rings having a single nitrogen heteroatom quarternized with a sulfoalkyl group were synthesized and characterized. The effect of variations in ring structure, length of sulfoalkyl chain, position of ring substituent and nature of ring substituent were examined. For each compound, the water solubility, octanol:water partition coefficient, absorbance and fluorescence spectra, fluorescence lifetime and Stern-Volmer constants (K_q) for quenching by a series of anions were measured. All compounds were quenched by chloride, bromide, iodide and thiocyanate, but not by cations, sulfate, phosphate, nitrate or by pH (5-8); several compounds were quenched slightly by bicarbonate (K_q=8-12 M^{-1}). High chloride sensitivity (K_q>50 M^{-1}) required the presence of a quinoline backbone substituted with electron donating groups such as methyl and methoxy, but did not depend on length of the sulfoalkyl chain or on the position of ring substituents, except that substitution at the 8-position resulted in a marked decrease for the Cl K_q. All compounds with high chloride sensitivity had fluorescence excitation spectra in the ultraviolet (excitation maximum <350 nm) and fluorescence lifetimes >15 ns. These results establish a set of guidelines for synthesis of chloride-sensitive fluorescent indicators tailored for specific biological applications, including cell trappable indicators with ester substituents and "ratiometric" indicators with quinoline conjugated to a Cl-insensitive chromophore.

M-Pos366 MEMBRANE BOUND OPTICAL INDICATOR FOR AQUEOUS SODIUM AND POTASSIUM CONCENTRATIONS. J. Roe, F.C. Szoka and A.S. Verkman. Depts. of Bioengineering, Pharmaceutical Chemistry and Cardiovascular Research Institute, University of California, San Francisco, CA 94143.

The lipophilic compound 7-(n-decyl)-2-methyl-4-(3',5'-dichlorophen-4'-one)-indonapthl-1-ol (MDPIN) was evaluated as an absorbance and fluorescence indicator of solution Na and K. When MDPIN and a cation-specific chelator (crown ether - Na, valinomycin - K) are condensed in a lipid phase (membrane or nonpolar solvent), presentation of an aqueous monovalent cation causes a phase transfer ion exchange reaction, resulting in an immediate change in the spectral properties of MDPIN. Specificity of the interaction is conferred by the chelator, and sensitivity by the chelator:MDPIN mole ratio. In octanol, the molar absorptivity (ε) of 1:1 MDPIN:valinomycin (in $M^{-1}cm^{-1}$) is 5900 (488 nm) and 480 (610 nm). ε increases by 5% (488 nm) and 230% (610 nm) upon addition of 10 mM K to an aqueous phase in contact with the octanol. MDPIN is fluorescent with excitation peaks at 295 and 340 nm and emission peaks at 381 and 402 nm; addition of K/valinomycin causes a spectral shift with progressive and complete loss of the 381 nm emission peak. These effects were absent with tetradecane replacing octanol, suggesting importance of a MDPIN interaction with a polar solvent moiety. MDPIN was incorporated into sonicated phosphatidylcholine vesicles from an acetone stock solution to a MDPIN:val:PC ratio of 1:1:50. Addition of 25 mM K resulted in an increase in ε (22% at 575 nm), and a spectral peak shift from 610 to 575 nm; no change in ε was observed with 25 mM Na, or with 25 mM K in the absence of valinomycin. These results provide a strategy for optical measurement of monovalent cations with potential application for development of fiberoptic Na/K sensors and intracellular Na/K indicators.

M-Pos367 APPLICATIONS OF FOURIER-TRANSFORM RAMAN SPECTROSCOPY TO BIOPHYSICAL SYSTEMS. E. Neil Lewis, Victor F. Kalasinsky and Ira W. Levin, Laboratory of Chemical Physics, NIDDK, National Institutes of Health, Bethesda, MD 20892

For biological samples conventional Raman spectroscopy, an inelastic light scattering technique using visible laser excitation sources, often suffers from the appearance of a dominant fluorescent signal originating from either the intrinsic nature of the preparation or the presence of tenacious sample impurities. A potentially promising method for avoiding the pernicious fluorescent and decomposition properties accompanying materials which absorb in the visible spectral region involves a new approach coupling the multiplex, throughput and precise frequency measurement advantages of a Michelson interferometer with a near-infrared laser source and a high sensitivity detector. A discussion will be presented of the adaptation of our high performance Fourier transform (FT) infrared interferometer for use as an FT Raman spectrometer. A CW Nd:YAG laser operating at 1064 nm, Rayleigh line rejection filters, and a liquid nitrogen cooled InGaAs detector provide the basic accessories for performing Fourier transform Raman spectroscopy. A variety of membrane and related samples will illustrate the advantages and disadvantages of this vibrational spectroscopic technique.

M-Pos368 RAPID SCANNING EXCITATION MICROFLUOROMETRY USING AN ACOUSTO-OPTIC TUNABLE FILTER.

I. Kurtz and P. Katzka. Department of Medicine, UCLA School of Medicine, Los Angeles, California.

We have recently described a new technique for rapidly acquiring spectral information from optical pH or Ca^{2+} probes using an acousto-optic tunable filter (AOTF) (Biophys J 51:287a, 1987). For the present study, a microfluorometer was designed using a tellurium oxide AOTF which was coupled between a 75-watt xenon arc lamp and the excitation port of an Olympus BH-2 microscope. The device was interfaced to an IBM PC computer for data acquisition and analysis. The instrument is capable of rapid excitation wavelength ratioing and excitation spectral scanning of optical probes in living cells. The device can also be coupled to a low light level television camera for spectral imaging of single cells. The AOTF can be alternated between two excitation wavelengths at ~150 KHZ and excitation spectra can be acquired in ~20 msec. By spectrally apodizing the filter, the sidelobe structure has been improved and the peak/1st sidelobe ratio increased from 13DB to ~30DB.

M-Pos369 SEMINAPHTHO-FLUORESCEINS AND -RHODAFLUORS: DUAL FLUORESCENCE pH INDICATORS

J.E. Whitaker, R.P. Haugland, F.G. Prendergast**; Molecular Probes, Inc, 4849 Pitchford Ave., Eugene, OR 97402; **Mayo Clinic, Dept. of Pharmacology, 200 SW 1st St., Rochester, MN 55905.

A new class of fluorescent benzo[c]xanthene pH indicators has been developed. These dyes exhibit distinct, long wavelength emissions in acidic and basic media with well defined isosbestic points and pK_a's within the physiological range. These properties facilitate intracellular ratio imaging and flow cytometric pH measurements in single cells which are less dependent than other indicators on dye concentration, leakage and photobleaching. The pH of a system may be obtained by determining the ratios of the acidic and basic intensities with respect to each other or the isosbestic point or by direct measurement of the intensities of one or both forms independently. These measurements may be performed with absorption, excitation or emission methods. Membrane permeant derivatives of these dyes have been prepared which are hydrolysed by intracellular esterases to yield the free fluorophores which are retained by cells. The excited state and biological properties of these indicators will be presented.

M-Pos370 NADH FLUORESCENCE SPECTROSCOPY AND IMAGING OF SINGLE CARDIAC MYOCYTES.

John Eng*, Ron M. Lynch and Robert S. Balaban NIH, NHLBI Bethesda MD 20892. *Howard Hughes Research Scholar.

NADH plays a critical role in oxidative phosphorylation as the primary source of reducing equivalents to the respiratory chain. Recently, the NADH redox state has been implicated as a regulatory site of oxidative metabolism in the heart. Using a modified fluorescence microscope we have detected and imaged the NADH fluorescence signal from single rat myocytes. Myocytes were prepared using standard procedures. The cells were placed in a chamber mounted on a microscope stage and constantly superfused with incubation medium. The microscope consisted of a modified inverted scope which permitted the rapid acquisition of fluorescence emission spectra (390-595 nm) or digital video images. NADH was excited using the 366 line of a mercury light source. The NADH fluorescence from the myocytes in the presence of glucose alone was 447 nm $\pm$ 0.2 (n=25), not corrected for the microscope transmission characteristics. The peak to peak signal to noise for 560 msec of spectral data acquisition was better than 50:1 without any spectral smoothing of the data. Addition of KCN doubled the NADH fluorescence signal without changing its spectral characteristics. Using an intensified video camera, NADH images were collected as single video frames with a S/N of greater than 5:1. This "background" NADH fluorescence signal from these myocytes should provide useful insights into the regulation of myocardial respiration at the single cell level.

M-Pos371 PHOTOACTIVABLE FLUOROPHORES FOR FLUORESCENCE PHOTOACTIVATION AND DISSIPATION MEASUREMENTS. Grant A. Krafft, Jose Luis Arauz-Lara, Richard T. Cummings, W. Randall Sutton, and Bennie R. Ware. Department of Chemistry, Syracuse University, Syracuse, New York 13244-1200.

Fluorescence photoactivation and dissipation (FPD) is a tracer transport experiment analogous to fluorescence photobleaching recovery (FPR), except that a positive signal is created by photoactivation of molecules, called photoactivable fluorophores (PAFs), that undergo irreversible photochemistry from an initial non-fluorescent state to become fluorophores. Two types of PAF probes are described here. An example of the first type is 2-aminoanthracene, coupled to 3,4-dimethoxy-2-nitrobenzyl alcohol via a carbamate linkage. An acetic acid group is attached to the carbamate nitrogen, permitting linkage to amino residues on the poly-L-lysine. The nitrobenzyl group quenches virtually all emission by 2-aminoanthracene until photoactivation (362 nm) releases the quencher group from the fluorescent aminoanthracene. The second type of PAF is an O,O-di-ether functionalized derivative of 5-chloroacetamidofluorescein. One of the ether groups is a six-carbon carboxylic acid that imparts aqueous solubility and permits covalent attachment to amino residues. The other ether group is the photocleavable 4,5-dimethoxy-2-nitrobenzyl group. The chloroacetamide can be used to label nucleophilic protein residues, and also can be converted to the more reactive iodoacetamide derivative. The O,O-di-ether PAFs are completely non-fluorescent, but convert efficiently to high fluorescent fluorescein mono-ethers upon photoactivation (362 nm) in neutral or slightly basic solution. Both of these PAFs have been used to make FPD measurements using the modulation detection methodology developed for FPR.

M-Pos372 ESTIMATION OF LIGHT SCATTERING INTENSITIES IN THE PRESENCE OF DUST. David A. Knoll and Victor A. Bloomfield, Department of Biochemistry, University of Minnesota, St. Paul MN 55108

Light scattering intensities are widely used to measure the molecular weights of biological macromolecules. The major sources of large intensity fluctuations are photon counting error (or shot noise if photocurrent is measured) and the presence of dust. Counting error can be reduced by averaging for longer times, but error introduced by dust cannot. Although the amount of dust in a sample can be greatly reduced by filtration or centrifugation, any which remains can greatly degrade the accuracy of results. This is especially true in samples of low concentration or at low scattering angle. The effect of residual dust particles, few in number but high in scattering power, is to introduce positive skewness into the distribution of measured intensities. We are developing statistical methods to estimate the true intensity of samples containing small amounts of dust. Using the technique of kernel estimation with gaussian or log-normal kernels, we can obtain an estimate of the most probably intensity, or mode of the intensity distribution. We have found the mode to be a more robust estimator of the true intensity than either the median or mean intensity. In one typical case, the mode is affected only about 1/4 as much as the mean, and about 1/3 as much as the median, by the presence of dust. Experimentally, the mode of the light scattering intensity distribution may be obtained using the probability density function of contemporary digital correlators.

M-Pos373 NITROXIDES AS PROBES OF METABOLISM IN A MODEL OF TUMOR TISSUE--AN ESR IMAGING STUDY. J. W. Dobrucki, T. Walczak, H. M. Swartz, University of Illinois, College of Medicine, Urbana, IL 61801.

Nitroxides are widely used as probes of the physical-chemical environment of cells and more recently as probes of cellular metabolism. They have also been used for visualizing and quantifying the areas of viable and nonviable cells in multicellular spheroids using ESR imaging. The use of nitroxides as metabolic probes is based on the sensitivity of their spectral line shapes to the concentration of oxygen and the increased rates of reduction of some nitroxides in hypoxic cells. A key to the use of nitroxides in biological systems is a knowledge of their distribution and reactions. We report here a study of the distribution and reduction of Tempone and 5-doxyl-stearic acid (5DS) in multicellular spheroids using ESR spectroscopy and imaging techniques. Spheroids are spherical clusters of cells containing an outer zone of viable, well-oxygenated cells, an intermediate zone and a hypoxic, central region with damaged and dead cells. Spheroids are considered a relevant *in vitro* model of poorly vascularized areas of solid tumors. ^{15}N-perdeuterated Tempone (^{15}N-PDT) was found to distribute throughout spheroids (1,200 μm diameter) grown from Chinese hamster ovary cells. ^{15}N-PDT was reduced in all regions of the spheroid at a rapid rate independent of the concentration of oxygen. 5DS also distributed throughout the spheroid but its rate of reduction increased twenty-fold when the spheroid was put in hypoxic medium. We conclude that it will be feasible to study nitroxide metabolism and oxygen concentration in single intact spheroids using ESR spectroscopy and imaging.

Supported in part by NIH Grants RR 01811, GM 35534, and GM 34250.

M-Pos374 3-AMINOPROPYLPHOSPHONIC ACID AS AN INDICATOR OF pHin VIA 31P-NMR Okerlund, L.S. (Intr. by Dr. R.J. Gillies), Department of Biochemistry, Colorado State University, Fort Collins, CO 80523.

Conventionally, intracellular pH (pHin) is monitored with 31P-NMR using the chemical shift of inorganic phosphate. This technique suffers a number of drawbacks (1). Because of these problems, we are investigating the use of alternative 31P-based indicators of pHin. 3-aminopropylphosphonic acid (3-APP) is nontoxic to cells at concentrations of 20 mM and does not effect cell culture doubling time or the proliferative response to serum. 3-APP has a pK of 6.9. The protonated and deprotonated forms are in fast exchange and resonate between 22 and 29 ppm, relative to 85% phosphoric acid. Therefore, it will not be obscured by phosphorous-containing metabolites. To be appropriate for cellular studies, exogenous indicators must be relatively impermeable to the plasma membrane. To test for 3-APP permeability, resonances from NMR spectra were collected from perchloric acid extracts of cells incubated in the presence of 20 mM 3-APP for varying amounts of time. Our data suggests that equilibration of 3-APP into cells takes longer than 24 hours and that 3-APP is relatively impermeable. At pH 7.4, the majority of 3-APP exists as a highly polar zwitterion and should not readily cross the plasma membrane. We therefore feel that this compound may be appropriate for the observation of pH changes in mammalian cells.

(1) DeFronzo, M. and Gillies, R.J., Characterization of methylphosphonate as a 31P NMR pH indicator. J. Biol. Chem., 262, 11032

M-Pos375 HIGH-FIELD PROTON NMR STUDIES OF CELLULAR WATER IN NORMAL, CANCEROUS AND EGF-TREATED HAMSTER CELLS. D.E. Callahan, T.L. Trapane, S.F. Deamond, S.A. Bruce, P.OP. Ts'o & L.-S. Kan Division of Biophysics, The Johns Hopkins University, Baltimore, MD 21205

Proton T1 and T2 values of the cellular water in normal (FC13) and tumorigenic (BP6T) Syrian hamster fetal fibroblasts have been compared at 300 Mhz (7.0 Tesla) (Xin, W. et. al Cell Biophys, 8, 213). T2 values were found to be reduced for BP6T cells relative to those of FC13 cells, while T1 values were similar. We have now obtained T1, T2 and Da (apparent self-diffusion coefficient) at 100 Mhz (2.4 T). For both cell types, 100 Mhz T2 values were higher than 300 Mhz T2 values. However, T2 for FC13 and BP6T was the same at 100 Mhz, in contrast to the measurements made at 300 Mhz where the T2 of BP6T cells was lower. Da indicates that water mobility is higher in BP6T cells than in FC13 cells. This high-field behavior of T2 for normal versus transformed cells is opposite of that which is usually observed at lower fields (Beall, P.T., et. al Cancer Res, 42, 4124). In an attempt to reproduce the BP6T T2 and Da behavior, FC13 were treated with EGF which makes them similar to BP6T cells in morphology and rate of proliferation. In these studies, T1 and T2 at 100 Mhz and T1 at 300 Mhz detected no significant differences in EGF-treated cells 6-72 hours post-treatment. A time-dependent effect was observed, however, in the 300 Mhz T2 and Da values of these treated cells. Both parameters were higher at 6 hours for treated cells. A heterogeneity in this EGF response was observed depending on the FC13 cell preparation used. Since the Da behavior relative to the 300 Mhz T2 behavior is different in BP6T cells and EGF-treated FC13 cells, it is postulated that different relaxation processes produce the reduced 300 Mhz T2 values in these two cell types. (Supported in part by DOE contract DE-AC02-76EV03280 & NIH training grant 2 T32 CA09110.)

M-Pos376 ASSESSMENT OF HMPS ACTIVITY IN NEOPLASTIC CELLS BY H-1 NMR SPECTROSCOPY
S.Mitchell,A.Johnson,B.D.Ross,*J.A.Willis,M.Garwood. (Intr. by W.H.Gallagher). University of Minnesota, *Houston Biotechnology Incorporated.

A proton (^{1}H) nuclear magnetic resonance technique for assessing the relative contribution of the hexose monophosphate shunt (HMPS) to glucose metabolism in cultured malignant cells is demonstrated. This technique requires the incubation of surface-anchored cells in Krebs Ringer Bicarbonate buffer containing 5.5mM 1-^{13}C-glucose. The lactate produced from metabolism of 1-^{13}C-glucose via the HMPS will lack the ^{13}C label in the C-3 methyl position, whereas lactate produced by glycolysis retains the ^{13}C label at the C-3 position. The ratio of the sum of the areas of the lactate ^{13}C satellite proton resonance signals to the ^{12}C proton resonance signals in ^{1}H spectra of aliquots of collected media allows calculation of HMPS activity in terms of percentage glucose catabolism. This technique was used to study rat C6 glioma cells incubated with 1-^{13}C-glucose to compare the ^{1}H signal areas of 3-^{13}C-lactate to 3-^{12}C-lactate. Control cells were found to have an HMPS activity of 9.0 $\pm$ 0.5%. Cells incubated with .001mM phenazine methosulfate (a chemical oxidant of NADPH) for 2 hours, had an activity of 35.2 $\pm$ 1.8% which decreased to 13.4 $\pm$ 2.8% after 12 hours of incubation. In contrast, cells incubated with 1.0mM KCN were found to have only 5.0% HMPS activity after 12 hours incubation and had increased lactate production of 218% that of controls. These results demonstrate a technique which can be used for sequential monitoring of HMPS activity under normal and modified conditions in malignant cells. Since the HMPS provides pentose sugars and NADPH, necessary for nucleic acid and lipid biosynthesis, this technique provides potential for monitoring perturbations in HMPS activity brought about by antineoplastic agents.

M-Pos377 31P NMR LIPID ANALYSIS FROM BIOLOGICAL SOURCES. Patricio Meneses and Thomas Glonek. Intr. by Thomas O. Henderson. Chicago College of Osteopathic Medicine, Chicago, Illinois.

Phospholipids from biological sources may be quantitated to more than 2 significant figures using 31P NMR spectroscopy in conjunction with an analytical reagent composed of two parts: (1) 2 ml reagent chloroform, containing 0.01-100 mg crude tissue lipid obtained by the Folch, Lees and Sloane procedure; and (2) 1 ml of an aqueous methanol reagent composed of one part 0.2M EDTA in D2O titrated from the free acid to pH=6 with CsOH and four parts of Methanol. [KOH and (Me)4NOH may be substituted for CsOH; however, while useable, these reagent changes result in reagents of limited stability (KOH) and phospholipid chemical-shift changes (KOH and (Me)4NOH).] Using a 500 MHz 31P NMR spectrophotometer (magnetic field=11.75 T), the extracted phospholipids yield narrow Lorentzian signals (1.8 - 3.2 Hz at half-height) with widths at half-height equal to their $1/\pi T2$ values. The chemical shifts (δ) at 24 °C, following the IUPAC shift convention, and relative to 85% phosphoric acid were determined as follows: PC=-0.84;LPC=-0.28;PC plas=-0.78;LPC plas=-0.20; PE=-0.01;LPE=0.44;PE plas=0.07;LPE plas=0.56;PS=-0.12;SPH=-0.08;PI=-0.37;PG=0.47;CL=0.17;PA=0.27; DiMePE=-0.18;LPI=0.10;LPA=0.83;LPG=1.09;DAG-AEP=21.19. The reagent permits assays of high precision and accuracy using little spectrometer time (ca. 15 min/assay) and is useful for routine analysis of phospholipids.

M-Pos378 **MAGNETIC RESONANCE IMAGING (MRI) OF HUMAN AORTO-CORONARY BYPASS GRAFTS.**
K. Taber, W.-F. Wong, M. Jerosch-Herold, N. Bryan, M. DeBakey, G. Lawrie, M. Nava, J. Guyton and J. Morrisett. The Methodist Hospital, Baylor College of Medicine, Houston, TX 77030.

Occluded grafts resected at reoperation typically display varying proportions of proliferated intima, atherosclerotic core lesion, thrombus, non-intimal fibrotic material, and residual lumen. Our objective was to determine the capacity of MRI to discriminate between these features and serve as a basis for their quantitation. After resection, grafts were marked with a line of India ink to retain slice radial orientation information, then imaged with a Bruker MedSpec 24/40 imager/spectrometer operating at a proton frequency of 100 MHz and equipped with 3 cm transmitter/receiver coil. A multi-slice, single echo (variable echo delay) sequence, 0.705 G/cm gradient, and 2 mm slice thickness was used. The areas of well delineated image features were determined with a pixel-counting procedure in the TomikonN software. After imaging, grafts were cut transversely into exactly 4 mm segments and the distal end of each segment inked to retain its correct end-end orientation. After the graft segments were photographed, they were fixed in 10% formalin/PBS overnight, then cast in paraffin, sectioned, and stained with hematoxylin/eosin, Van Giessen, or Trichrome reagents, and mounted. When delay times Tr=3000 ms and Te=30 ms were used (spin density weighted), it was possible to distinguish adventitia (light) from media (dark) from acellular fibrosis (dark) from old thrombus containing cholesterol (light). Residual lumen could be visualized either when filled with saline (light) or left empty (dark). Atheromatus gruel could be distinguished readily from a new clot (varying shades of gray). We conclude that MRI is capable of distinguishing patent from occluded grafts, and of discriminating between most of the morphological features seen in diseased vessels, ex vivo. (Supported by NIH grants HL-27341 and HL-32971).

M-Pos379 IN VIVO GLUCOSE METABOLISM OF A RAT GLIOMA: A ^{13}C NMR SPECTROSCOPY STUDY

B.D. Ross, *R.J.Higgins, *J.E. Boggan, +J.A. Willis, *B. Knittel and *S.W. Unger. Univ. of Minnesota, Navarre, MN 55392, *University of CA at Davis 95616, +Houston Biotechnology Inc., The Woodlands, TX 77381, *University of CA at Berkeley 94720.
(Int. by M.D. Rosenberg)

Since abnormally high rates of glucose utilization and aerobic glycolysis have been associated with the maintenance of brain tumor energy supply, the ability to noninvasively monitor glucose metabolism may provide insights into the biochemical alterations associated with brain tumor metabolism. Surface coil ^{13}C nuclear magnetic resonance (NMR) spectroscopy was used to follow the metabolism of 1-^{13}C-glucose in an intracerebrally located C6 glioma in the rat. C6 glioma cells (1×10^6) stereotactically inoculated in the rat brain resulted in a single mass lesion detectable by ^1H magnetic resonance imaging (MRI) at between 15 and 20 days post inoculation. Only rats with tumors cortically located and at least 5 mm in diameter were selected from ^1H MRI examinations. Three control rats and 3 rats harboring brain tumors were infused through a cannulated femoral vein with 1-^{13}C-glucose (250 mg/ml) at a constant rate of 0.025 ml/min for 2 hours. In vivo ^{13}C NMR spectra were acquired on a 4.7 Tesla Nicolet spectrometer system with gated bilevel ^1H decoupling. Control rats infused with 1-^{13}C-glucose revealed only the presence of the α,β-anomers of 1-^{13}C-glucose and glutamate/glutamine resonances. In contrast, in vivo ^{13}C NMR spectra of glioma tumors revealed the direct production of 3-^{13}C-lactic acid and 1-^{13}C-glycogen, during infusion with 1-^{13}C-glucose. Results from this study demonstrate the capability of NMR for monitoring in vivo glucose metabolism of a rodent brain tumor.

M-Pos380 P-31 NMR: WORKSTATE AND EXOGENOUS SUBSTRATE DEPENDENCE OF CREATINE KINASE FORWARD FLUX

A.Johnson,P.Mohanakrishnan,B.Lew,A.H.L.From,K.Ugurbil,Univ.of Minnesota,Navarre,MN 55392

We have applied the technique of P-31 NMR saturation transfer to study creatine kinase catalyzed forward flux (CK-Ff, CP→ATP) in Langendorff perfused rat hearts as a function of (1) myocardial oxygen consumption rate (MVO_2), and (2) the type of exogenous carbon source in the perfusion medium. Rat hearts were perfused with either 11mM glucose as the sole carbon substrate (G-hearts) or 10mM pyruvate plus 11mM glucose (PG-hearts) and studied at six rigorously defined workstates designed to achieve widely varying levels of energy utilization. The workstates, set by manipulating heart rate, end-diastolic pressure, and in some cases by adding an inotrope, allowed us to study CK activity over an extended range of MVO_2 (10 to 90μmol/min/gdw). We found that at comparable levels of MVO_2, NMR measured CK-Ff in G-hearts was consistently higher than in PG-hearts by a factor of up to 2.5, demonstrating lack of simple one to one coupling between CK-Ff and MVO_2. The behavior of the reaction with increasing MVO_2 also showed dependence on the type of exogenous substrate; CK-Ff first increased and then decreased in G-perfused hearts, but remained relatively constant in the PG -perfused hearts over most of the MVO_2 range examined. Simulated flux using the CK rate equation, measured and calculated reactant concentrations, and published values for the relevant kinetic constants, closely matched NMR measured CK-Ff at all but the highest levels of MVO_2 for the G-perfused hearts. However, simulated flux did not parallel measured flux for the PG-hearts and predicted an increase in flux with MVO_2 which was not experimentally observed. Hanes-Woolf analysis of the data from both G- and PG-perfused hearts yielded a reasonably good fit for calculated [ADP] which is consistent with the general supposition that CK-Ff is primarily regulated by free cytosolic [ADP]. The apparent kinetic constants were Km(ADP) = 20μM and Vmax(CP→ATP) = 10mM/sec.

M-Pos381 EFFECTS OF TEMPERATURE AND Mg^{2+} ON pH DETERMINATIONS FROM THE CHEMICAL SHIFT OF INORGANIC PHOSPHATE USING ^{31}PNMR SPECTROSCOPY.

*A.C. Elliot and +M.J. Dawson, *Dept. of Physiology, University of Manchester, U.K., +Dept. of Physiology & Biophysics, University of Illinois, Urbana, IL 61801.

^{31}P NMR is now a well established method for the measurement of intracellular pH (pH_i). Such measurements are usually based upon the effect of pH on the chemical shift of inorganic phosphate (Pi). In addition to the effects of differences in chemical composition between the calibration solution and the cytosol, inaccuracies may be introduced to the estimate of pH_i if the calibration curve is determined at a temperature different to that used experimentally. A variety of physiological and medical problems now being studied by ^{31}P NMR involve exposure of tissues to hypo or hyperthermia and it is therefore necessary to calibrate the pH_i measurement at several temperatures. We have obtained pH calibration curves for Pi at 4, 21 and 37°C in model cytosolic solutions. Because divalent cation effects are likely to be the major source of error in NMR determinations of pH_i, and because free intracellular [Mg^{2+}] is both variable and uncertain, we obtained titration curves in the presence of 0-5mM free [Mg^{2+}]. We observed a higher apparent pK at 4°C (6.83) than at 21 or 37°C (6.75 & 6.77 respectively; all values for zero-Mg titrations) and the lower pK at higher temperature was also apparent in solutions containing up to 5mM free [Mg^{2+}]. There was a significant effect of Mg^{2+} on the basic region of the titration curves and on the basic endpoint. We conclude that the size of the error in the measurement of absolute values of pH_i as a result of uncertainties in free [Mg^{2+}] depends on the range in which pH_i lies, and is generally less than 0.1 pH units.

M-Pos382 THREE DIMENSIONAL ELECTRON SPIN RESONANCE IMAGING, *Ronald K. Woods; *Goran Bacic; *Harold M. Swartz; +Paul C. Lauterbur, University of Illinois at Urbana-Champaign, College of Medicine, * ESR Center, 506 S. Mathews, Urbana, IL 61801, +Biomedical Magnetic Resonance Laboratory, 1307 W. Park St., Urbana, IL 61801.

Three dimensional ESR imaging is being developed to achieve precise spatial resolution of the unique information that can be provided by naturally occuring paramagnetic species or specifically introduced spin labels. The symmetry constraints placed on samples studied by 2D techniques are completely removed, thus increasing the degree of morphological sophistication of the sample that can be studied. Spatially resolved data are obtained with a set of rectangular transverse gradient coils, mounted on circular z gradient coils, and rotated about the z axis to produce any desired gradient. The system includes a Zenith Z100 interfaced with an X-band E112 spectrometer. Reconstruction of either 33*3 or 65*3 arrays employs a three point second difference filter followed by a two-stage back projection. Images have been made of samples with various degrees of complexity: a plexiglas cube containing 0.55 and 2.2mm^3 cavities filled with DPPH; a conically-hollowed cylinder of gamma-irradiated quartz; and a segment of rat femur soaked with ^{15}N-PDT. Discrete objects are accurately located, but the inherent line width, especially for DPPH, reduces the resolution of the image. Plans are underway to sharpen the images by convolution difference techniques, to correct for nonuniform cavity sensitivity, to carry out the data acquisition and reconstruction on an IBM computer and to construct a high-gradient stationary three coil system. Partially supported by NIH Grant #RR01811.

M-Pos383 MODELLING SICKLE CELL VASO-OCCLUSION IN THE RAT LEG BY TECHNETIUM AND MAGNETIC RESONANCE IMAGING: CORRELATION BETWEEN THE NUMBER OF TRAPPED CELLS AND H-1 RELAXATION TIMES. ME Fabry, V Rajanayagam, E Fine*, RL Nagel, S Holland#, JC Gore#, and DK Kaul, Depts of Medicine and Nuclear Medicine*, A Einstein Coll of Med, Bronx, NY, 10461, and Dept of Diagnostic Radiology#, Yale Univ School of Med, New Haven, Conn, 06510.

The red cells of sickle cell anemia patients exhibit a great heterogeneity of cell density. We have demonstrated that the densest of these cells (SS4) disappear during sickle cell painful crisis and that these cells are the least competent in the microcirculation. We therefore proposed an animal model for sickle cell painful crisis which consists of injecting technetium-99m-labelled (Tc), saline-washed normal (AA), homozygous sickle (SS), or density defined SS red cells (such as SS4) into the femoral artery of the rat and quantitatively performing both Tc imaging and H-1 magnetic resonance imaging (MRI) at 0.15 Tesla. The volume of cells trapped was determined by measuring the activity of a reference vial containing a known volume and hematocrit of the Tc-labelled cells used for injection. Activities in the leg were determined by outlining the area of interest on a computer acquired Tc image. Between 5 and 20 μl of SS4 cells were trapped in the capillary bed of the thigh which is served by the femoral artery; in contrast, fewer AA cells are trapped (less than 0.3 μl). If the MRI T_1 was plotted versus μl of cells trapped, an increase of T_1 over the control value of 415 $\pm$ 44 msec was found when the volume of trapped cells exceeded 5.9 μl. Below 5.9 μl no increase in T_1 occurred, and above 5.9 μl, T_1 increased as more cells were trapped to a maximum of 940 msec. This is consistent with a model in which minor trapping is not harmful, but more trapping leads to MRI detectable pathology.

M-Pos384 NMR VISIBILITY OF MITOCHONDRIAL MATRIX ATP AND PHOSPHATE. Susan M. Hutson*, Deborah Berkich*, Gerald K. Williams**, Peter T. Masiakos*, Richard Briggs**, Kathryn LaNoue**. Departments of Physiology* and Radiology**, Milton S. Hershey Medical Center, Pennsylvania State University, Hershey, Pennsylvania 17033.

Discrepancies between estimates of phosphate metabolites by NMR ^{31}P spectroscopy and estimates by enzymatic analysis have suggested the existence of NMR invisible pools within the cell. The purpose of this study was to determine the extent of visibility of the mitochondrial pools. The ratio of internal to external ATP was varied at 8°C from (0.1 to 2 by incubating mitochondria, which had been loaded with ATP, in the presence of 1.0 mM phosphate (Pi) with and without addition of oligomycin, carboxyatractyloside or ATP. The data suggest that the mitochondrial matrix ATP is completely visible. T_1 values for internal ATP were calculated from signal intensities using different delays during signal acquisition. The T_1 of the ß-phosphate of ATP appears to be very short. A mean T_1 of 0.2 sec was estimated from spectra obtained in four separate experiments with mitochondria oxidizing succinate and glutamate in the presence of phosphate. By including 20% fluorocarbons in the incubation buffer, it was possible to maintain the mitochondria at 25°C. Although the signal was broader than at 8°C, matrix nucleotides were visible. T_1's values for internal inorganic phosphate appeared to be dependent on the size of the matrix nucleotide pool. There were, however, some discrepancies between matrix Pi concentrations determined using NMR and biochemical assay. In situ, Ca^{2+} and Mn^{2+} may alter the observed spectra and generate invisible pools. However, addition of Ca^{2+} (5 or 30 nmol/mg) had little effect on the adenine nucleotide spectra while Mn^{2+} (5 nmol/mg) broadened the ^{31}P peaks dramatically. The physiological significance of these observations is under investigation.